THE UNIVERSITY OF ALBERTA

COLUMN EFFICIENCY IN GAS-LIQUID CHROMATOGRAPHY

A THESIS

SUBMITTED TO THE FACULTY OF GRADUATE STUDIES

IN PARTIAL FULFILMENT OF THE REQUIREMENTS FOR THE DEGREE

OF DOCTOR OF PHILOSOPHY

DEPARTMENT OF CHEMISTRY

by

G. D. LUTWICK, M. Sc.

Edmonton, Alberta

August, 1961

ABSTRACT

Column efficiency in gas-liquid chromatography has been studied as a function of linear carrier gas velocity at constant average pressures. This part of the study has experimentally confirmed that at least two terms must be added to the original van Deemter relation to account for band broadening in gas-liquid chromatography. It is proposed that the following simplified equation relating height equivalent to a theoretical plate, (H), to carrier gas velocity and pressure adequately accounts for the experimental data.

$$H = A + \frac{B}{\overline{P}u} + Cu + Eu + F'\overline{P}u$$

In this equation A is the eddy diffusion term and B, C, E and F' are coefficients of the terms involving band broadening resulting from longitudinal diffusion in the gas phase, resistance to mass transfer in the liquid phase, resistance to mass transfer at the gas-liquid interface and resistance to mass transfer in the gas phase, respectively. Evidence for the first three terms has been extensively discussed in the early literature on gas-liquid chromatography. Evidence for resistance to mass transfer in the gas phase has been obtained in this work from an interpretation of variations in resistance to mass transfer with pressure and carrier gas. Evidence for resistance to mass transfer at the gas-liquid interface consists of variations in a liquid phase dependent

resistance which is independent of pressure but markedly affected by the nature of the carrier gas. The experimental data obtained during the course of this investigation would indicate that the values of the coefficients in the usual analytical packed column would be about as follows:

A, 0.06 to 0.14 cm; B, 0.1 to 0.5 atm. cm^2/sec;
C, 0.001 to 0.020 sec; E, 0.003 to 0.08 sec;
F', 0.003 to 0.006 atm/sec.

The proposed equation has been applied to explain controversial results which have been reported by other workers. Thus the often quoted existence of a negative eddy diffusion term has been accounted for.

The proposed equation has also been examined for temperature effects. To include the effect of temperature these studies suggest the following equation:

$$H = A + \frac{B''T^{3/2}}{\bar{P}u} + \frac{C''u}{T} + \frac{E''u}{T} + \frac{F''\bar{P}u}{T^{3/2}} .$$

The apparatus normally used in gas-liquid chromatography was modified so that one could vary the carrier gas velocity and operate at a constant average pressure. This was possible by means of two cylinders of compressed gas, one at the inlet and one at the outlet of the column.

In an appendix the application of sulphuric and phosphoric acids as subtractive reagents in gas-liquid

chromatography has also been investigated. Sulphuric acid has been shown to separate alkenes and oxygenated compounds from alkanes. Phosphoric acid has been shown to separate alcohols and ketones from alkanes, alkenes and esters. The effect of reactor column length and temperature were also investigated.

ACKNOWLEDGEMENTS

The author wishes to express his sincere appreciation to Dr. W. E. Harris for his advice and guidance during the course of this research.

The author also thanks Dr. H. Habgood, Dr. G. Freeman, and Dr. F. Birss for helpful discussions during the preparation of this work.

The author is indebted to the National Research Council for financial assistance during the summer sessions.

TABLE OF CONTENTS

LIST OF TABLES

LIST OF FIGURES

NOMENCLATURE

Symbol	Dimensions	Description
A	cm	Velocity-independent constant reflecting random flow pattern in packed column.
a_2	cm^2	Area of cross-section of liquid phase
B	cm^2/sec	A coefficient reflecting the axial or longitudinal diffusion in the gas phase
B'	cm^2atm/sec	A coefficient reflecting the axial or longitudinal diffusion in the gas phase
C	sec	A coefficient of resistance to mass transfer in the liquid phase
C'	sec	A coefficient of resistance to mass transfer in the liquid phase
C_I		Coefficient in equation (vii)
C_2		Coefficient in equation (vii)
C_3		Coefficient in equation (vii)
D_g	cm^2/sec	Diffusivity of solute in the carrier gas
D_g^8	cm^2atm/sec	Diffusivity of solute in the carrier gas
D_1	cm^2/sec	Diffusivity of solute in the liquid phase

Symbol	Dimensions	Description
d		Diameter of a capillary tube
d_f	cm	Effective thickness of the liquid phase
d_g	cm	Effective thickness of the mobile gas phase
d_p	cm	Effective average support particle diameter
E	sec	Coefficient of resistance to mass transfer at the gas-liquid interface
F	sec	Coefficient of resistance to mass transfer in the mobile gas phase
F'	sec/atm	Coefficient of resistance to mass transfer in the mobile gas phase
F_l		Volume fractions of liquid in the column
F_g		Volume fraction of gas in the column
G	sec	Coefficient of a velocity distribution term
G'	sec/atm	Coefficient of a velocity distribution term
H	cm	Height equivalent to a theoretical plate
J	cm^2/sec	Coefficient of longitudinal diffusion in the liquid phase

Symbol	Dimensions	Description
K		Distribution coefficient
K'		A distribution coefficient
K		An absorption rate constant
L	cm	Length of column
M_1		Molecular weight of component 1
M_2		Molecular weight of component 2
N		Number of plates measured
P	atm	Average pressure across the column
P_o	atm	Pressure at outlet of column
P_i	atm	Pressure at inlet of column
Q		Electric field strength of permanent dipole of the liquid phase
R		Radius of a capillary tube
r		Distance from the axis of the capillary tube
T	degree	Temperature
Ta	sec	Retention time of air
u	cm/sec	Velocity of the carrier gas averaged over the column
u_0	cm/sec	Velocity of the carrier at the outlet of the column
V_1	cm^3	Molecular volume of component 1

Symbol	Dimensions	Description
V_2	cm^3	Molecular volume of component 2
V_R	ml	Retention volume of solute from time of injection
V_{R_n}	ml	Retention volume of solute measured from the air peak
W	ml or sec	Width of peak at the base line
α		Polarizability of the carrier gas
$\alpha_{1,2}$		Separation factor of constituents 1 and 2
β		A geometry constant
β'	cm^{-1}	A geometry constant
γ		Correction factor accounting for the tortuosity of the gas channels in a packed column
ϵ		Bonding force at the interface of the gas and liquid phases
η	micropoise	Viscosity of the carrier gas
λ		Constant characteristic of the packing
ρ		Correlation coefficient
σ	cm^2	Surface area per unit column length

I. INTRODUCTION

A. General

Chromatography is a physical method for separating materials from one another. Physical methods involve the distribution of materials between two phases with subsequent separation. In chromatography the operation can be repeated many times and as a consequence very efficient and effective separation results.

All chromatographic separations involve the transport through a column of the components of a mixture. The sample may consist of solids, liquids or gases. The column contains a stationary phase which may be either a solid or a liquid. The transport of the constituents of the sample through the column is effected by a moving phase; which is either a gas or a liquid. Owing to differences in the distribution coefficient of different sample components between the moving and stationary phases, selective retardation is exerted by the stationary phase. Thus the components of the mixture move through the column at different rates. They thus separate and move through the column as separate zones or bands.

Chromatographic separations can be divided into four types depending upon the combination of phases used. Thus it is possible to have the following four combinations in chromatographic processes

liquid - solid
liquid - liquid
gas - solid
gas - liquid

Liquid-solid chromatography was first applied by Tswett (1), in 1906. He applied chromatography to the separation of colored plant pigments using calcium carbonate as an adsorbent. Tswett's discovery was unnoticed for twenty-five years until Kuhn, Winterstein and Lederer (2) used the chromatographic technique to separate carotenes and xanthophylls. Gas-solid chromatography in which the gas phase is mobile was introduced by Turner (3) in 1943 and is used principally for the separation of gases with low boiling points. Liquid-liquid chromatography was introduced by Martin and Synge (4) in 1941. It has become particularly important in the separation of complex biochemical mixtures. Paper chromatography is a special form of liquid-liquid chromatography in which the support for the stationary liquid phase is paper. Gas-liquid chromatography was first employed by James and Martin (5) in 1951, ten years after being suggested by Martin and Synge (4). Their paper has been followed by intensive application of various solvents to the separation of a wide variety of organic compounds with appreciable vapor pressures. Recent research has also led to the extension of the upper temperature limit to 1000°C (6) and this in addition has introduced the possibility of using gas chromatography for inorganic analysis.

The foregoing classifications of chromatography can be further subdivided into elution development, frontal

analysis and displacement analysis. In gas-liquid chromatography elution development is used almost exclusively, hence only this technique will be considered. In elution development the mobile phase selectively transports the components of a mixture through a column. Each component is carried through the column independently of other substances present, hence there can be complete separation of the components.

The effectiveness of a column for carrying out a chromatographic separation can be conveniently described in terms of two factors, the number of theoretical plates N associated with the column and the separation factor . The separation factor for any two components is most simply expressed as the ratio of the retention volumes, i.e.,

$$\alpha_{12} = V'_{R_2}/V'_{R_1} \qquad \text{(i)}$$

where V'_{R_n} is the retention volume measured from the air peak of component n. The number of theoretical plates, N, associated with an elution peak is given by the expression

$$N = 16\left(V_R/W\right)^2 \qquad \text{(ii)}$$

In this expression V_R is the retention volume of the peak measured from the injection point; W, expressed in the same units as V_R, is a measure of the peak width, and is the distance between the points at which tangents drawn from the

inflection points of the elution curve intercept the base line. The broadening of the elution peak is proportional to $\sqrt{N}$.

Retention volume depends on the distribution coefficient and it is the differences in distribution coefficients which allows one to make chromatographic separations. The ratio of the concentrations of a substance between the phases at equilibrium is the distribution coefficient (K). In gas-liquid chromatography the concentrations are usually expressed as the amount of solute per unit volume of stationary and moving phase as in equation (iii).

$$K = \frac{\text{weight of solute per ml of solvent}}{\text{weight of solute per ml of gas}} \qquad \text{(iii)}$$

As can be seen by equation (iii) the distribution coefficient is a dimensionless quantity. The distribution coefficient may be independent of the concentration of dissolved material or it may vary with concentration. Hence there are linear and non-linear isotherms. Some schematic isotherms are shown in Figure 1. In case (a) a plot of the concentration of material in the moving phase against concentration in the stationary phase at a given temperature gives a straight line passing through the origin. This is a linear isotherm. Graphs (b) and (c) are non-linear isotherms and may be curved away or toward the horizontal axis. Corresponding to these types of

Figure 1

Schematic Representation of Linear and Non-linear Isotherms

(A) linear isotherm.

(B) non-linear isotherm in which K decreases with increase in concentration of solute.

(C) non-linear isotherm in which K increases with increasing concentration of solute.

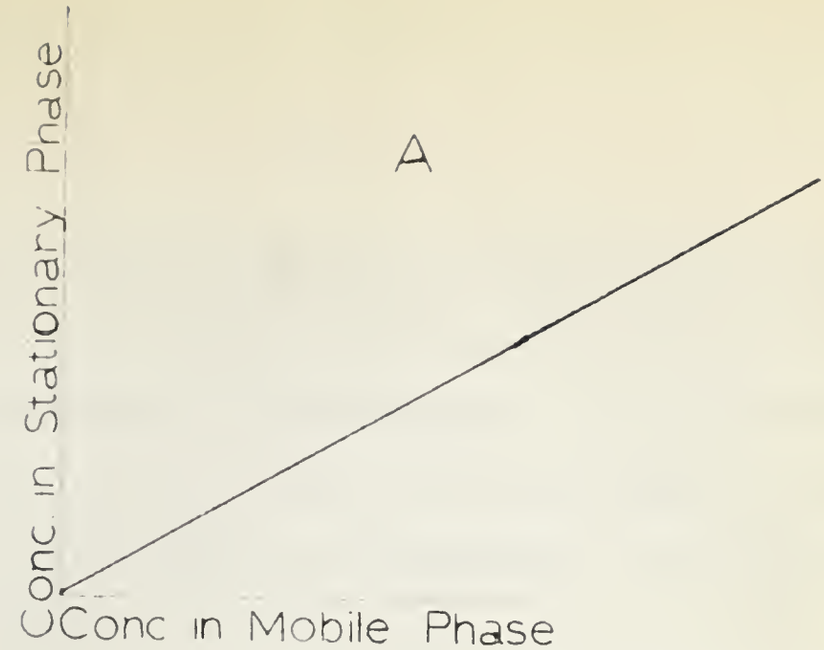
A
Conc. in Stationary Phase
Conc in Mobile Phase

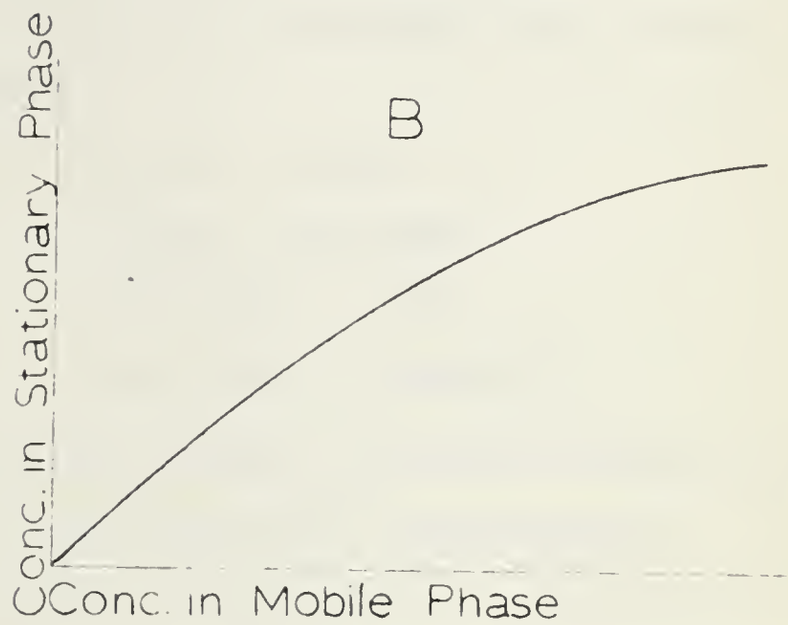
B
Conc. in Stationary Phase
Conc. in Mobile Phase

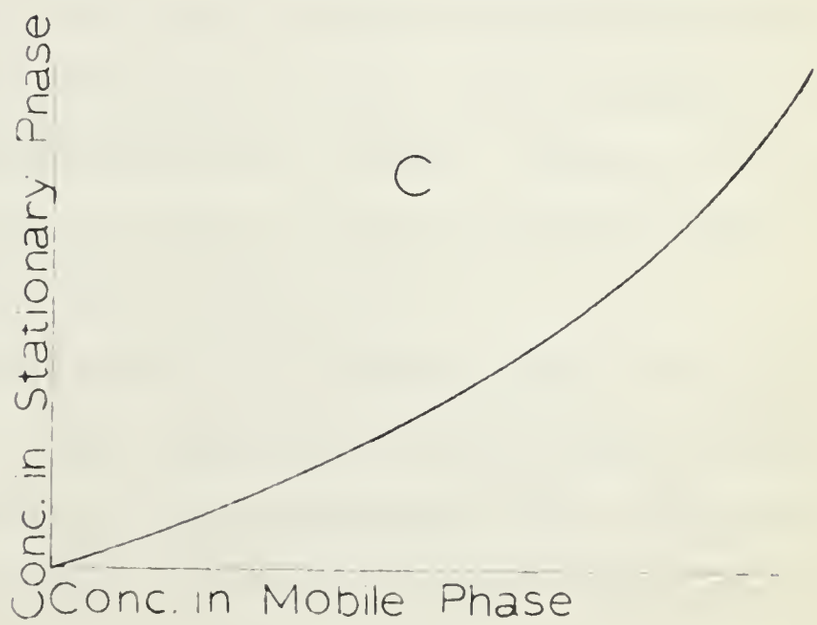
C
Conc. in Stationary Phase
Conc. in Mobile Phase

isotherms one can then have linear or non-linear chromatography.

Gas-liquid chromatography may be further classified into ideal or non-ideal chromatography. In ideal chromatography equilibrium between gas and liquid phase is established immediately. In non-ideal chromatography the establishment of equilibrium requires a finite time.

On this basis we therefore have another four types of chromatography.

linear - ideal

linear - non-ideal

non-linear - ideal

non-linear - non-ideal

In gas-liquid chromatography conditions are such that we need only consider linear-non-ideal chromatography. In linear-ideal chromatography band broadening does not occur, i.e. there is no increase in the carrier gas volume (corrected to a standard temperature and pressure) which contains the solute as it progresses through the column. Theories to account for band broadening in linear-non-ideal chromatography are considered in the following section.

This thesis is an investigation of the phenomena responsible for band broadening in gas-liquid chromatography. It was instigated by the appearance in the literature of experimental results inconsistent with theory (20). In the

sections which follow the original rate theory presented by van Deemter et al (12) is reviewed. Since this investigation was started some extensions of the original van Deemter theory have appeared (13, 14, 16). These extensions are also reviewed. The theoretical aspects are discussed in the following sections along with the experiment designed to elucidate the phenomena operative in band broadening. The results obtained are discussed in the light of theory and an equation accounting for the observed results is presented.

B THEORIES OF GAS-LIQUID CHROMATOGRAPHY

Two theories have been proposed to describe the broadening of a band in gas-liquid chromatography. These are the "Plate Theory" and the "Rate Theory".

The plate theory was proposed by Martin and Synge (4) in 1941 and applied by them to liquid-liquid chromatography. In the plate theory the column is conceived as consisting of a number of stages or plates and all non-ideality is included in lag of equilibrium between the moving phase and the stationary phase. For many plates a gaussian distribution results. The plate theory introduces the term "height equivalent to a theoretical plate" (HETP) defined as "the thickness of a layer such that the solution issuing from it is in equilibrium with the mean concentration of solute in the non-mobile phase throughout the layer" (4). The height equivalent to a theoretical plate for any column is obtained by dividing the length of the column by the number of plates as defined in equation (ii). A column is considered to be more effective the larger the number of plates.

The rate theory, proposed by van Deemter, Zuiderweg and Klinkenberg (12) in 1956, relates HETP to the physical phenomena occurring in the chromatographic column for continuous flow. Before presenting the result of their theory for linear-non-ideal chromatography,it is worthwhile to consider conditions for

linear-ideal chromatography. It is assumed in linear-ideal chromatography that:

(i) the proportion of the moving and stationary phases at all points of the column is constant.

(ii) the rate of flow of the moving phase is uniform throughout the column

(iii) molecular diffusion of the solute molecules in a longitudinal direction does not occur in either of the two phases.

(iv) distribution equilibrium between the two phases is attained instantaneously.

If we consider the macroscopic aspect of the column, conditions (i) and (ii) are usually fulfilled in gas-liquid chromatography. In the microscopic aspect, the condition of uniform flow does not prevail. Uniform flow is not obtained because there is a pressure gradient along the length of the column and as a consequence of this and the compressibility of gases the linear velocity of the carrier gas increases from the column inlet to the column outlet. This non-uniformity affects all solute molecules to the same extent and hence will not cause band broadening in the sense in which band broadening has been defined at the end of the introduction. Secondly, the condition of uniform flow does not prevail in a packed bed. As a result of the packing gas molecules travel through the column along many different paths. The various paths have somewhat

different lengths. Furthermore, the movement is not always axially directed and the gas velocity is dependent upon the width of the voids between the particles. These effects cause the residence time of the carrier and solute gas molecules in the different effective paths of the column to vary. The result of there being different effective paths is a reduction in peak height and broadening of the band as illustrated in Figure 2. The broadening depends on the shape and size of the particles constituting the packing and the regularity with which they have been packed. The band broadening occurring as a result of these effects is said to be caused by "eddy diffusion".

The third assumption involves molecular diffusion of the solute molecules. This diffusion is superimposed on the forced flow of the carrier gas, and its axial component tends to enhance or counteract the transport of the solute through the column. The corresponding effect in the liquid phase is considered small as compared to that in the gas phase and has been neglected. Molecular diffusion of this type is the second mechanism which results in band broadening.

The fourth assumption involves the distribution equilibrium between the phases. This would require an instantaneous attainment of equilibrium, i.e. an infinite rate of mass transfer of solute between the two phases. This condition is not realized at finite rates of flow. As a conse-

Figure 2

Schematic Representation of Band Broadening in Linear Gas-Liquid Chromatography

1. Ideal chromatographic peak

2, 3. Non-ideal chromatographic peaks with a linear isotherm.

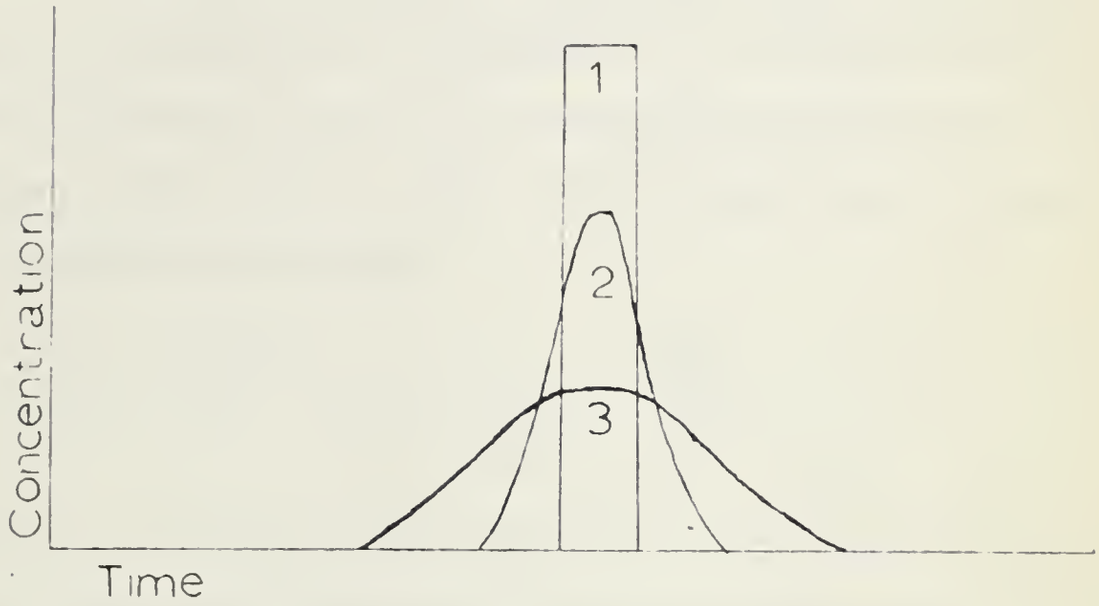
1
2
3
Concentration
Time

quence of the finite rate of mass transfer the solute molecules either fail to go into solution, and thus travel somewhat ahead of the average solute molecule or go into the liquid and fail to pass into the moving phase and thus lag behind the average solute molecules. The resistance to mass transfer is therefore the third important factor causing band broadening.

The three above mechanisms of band broadening led van Deemter, Zuiderweg and Klinkenberg (7) to derive equation (iv) from differential equations for material balance per unit cross sectional area relating HETP (H) and linear gas velocity (u) in gas-liquid chromatography.

$$H = 2\lambda d_p + \frac{2\gamma D_g}{u} + \frac{8}{\pi} \frac{K'}{(1+K')^2} \frac{d_f^2}{D_l} u \qquad \text{(iv)}$$

where is a constant characteristic of the packing, d_p is the average particle diameter of the solid support for the stationary phase, is a correction factor accounting for the tortuosity of the channels for the moving phase,

D_g, D_l are the diffusivities of solute in the gas and liquid phases respectively, d_f is the effective film thickness of liquid phase,

u is the linear gas velocity,

$K' = K \; {}^{F_l}/_{F_g}$ where

K is the distribution coefficient of solute and F_l, F_g are the fractions of the column cross section occupied by the liquid and gas phases respectively.

In the derivation of this formula van Deemter et al assumed that the resistance to mass transfer is associated only with the liquid phase and that longitudinal diffusion in the liquid plan is negligible. They also assumed that the thickness of the gas layer, d_g, through which the solute molecules must diffuse to reach the stationary phase was half the diameter of the fine pore structure of the packing, i.e. about 10 microns (12). Hence, since diffusivity in the liquid phase, D_l, is about 10^{-4} times the diffusivity in the gas phase, D_g, the resistance to mass transfer in the gas phase was considered negligible.

Jones (13), using a statistical approach, i.e. the random walk model (7), has pointed out that a sample molecule can diffuse to the walls of the channels through the packing more often than the number of times it has access to the liquid phase if the walls are only partially coated. He calculated that a liquid coating of 30% by weight which is 10 microns thick will cover only 1% of the available surface of a support with an area of 3 square meters per gram. This would mean that resistance to mass transfer in the gas phase is 100 times greater than it would be if all of the surface was coated with liquid. Therefore even though diffusivity is much greater in the gas phase than in the liquid phase, in view of this fact the resistance to mass transfer in the gas phase may not be negligible. The resistance to mass transfer in the gas phase term was given by Jones (13) as equation (v).

$$F = \frac{C_2 K'^2}{(1+K')^2} \frac{d_g^2}{D_g} u \qquad \text{(v)}$$

For high values of K', the gas phase mass transfer term becomes more significant. The gas phase mass transfer term is discussed further in the following section entitled "Scope of the Present Work".

Jones further modified the van Deemter equation by postulating a velocity distribution term shown in equation (vi) as

$$G = \frac{C_3 d_p^2 u}{D_g} \qquad \text{(vi)}$$

where C_3 is a constant dependent on shape of the support particles and the gas velocity distribution. The remaining factors have the meanings defined earlier. This band broadening term is similar to the gas phase term given by equation (v). A correlation term to account for the dependence of the velocity distribution term, G, on the mobile gas phase term, F, has been included by Jones. This results in equation (vii).

$$H = 2\lambda d_p + \frac{2\gamma D_g}{u} + \frac{C_1 K'}{(1+K')^2} \frac{d_1^2 u}{D_1} + \frac{C_2 K'^2}{(1+K')^2} \frac{d_g^2 u}{D_g} + \frac{C_3 d_p^2 u}{D_g}$$

$$+ \; 2\rho (C_2 C_3)^{\frac{1}{2}} \frac{K'^2}{(1+K')^2} \frac{d_p d_g}{D_g} u \qquad \text{(vii)}$$

In this equation ρ is a correlation coefficient and all other factors are the same as those previously defined.

The first three terms of equation (vii) are the same as those in the van Deemter equation (iv). The fourth term is for resistance to mass transfer in that portion of the gas which is mobile. The fifth term accounts for band broadening due to the velocity distribution within the gas phase. The sixth term accounts for the dependency of the fifth term on the fourth. This dependency arises from the dependency of the velocity profile of a fluid passing through a capillary on the velocity of the fluid along the axis of the capillary. This idea shall be expanded in the following section. This equation can be written in the simplified form:

$$H = A + \frac{B}{\bar{P}u} + Cu + F\bar{P}u + G\bar{P}u + 2\rho\,(FG)^{\frac{1}{2}}\,\bar{P}u \qquad \text{(viii)}$$

where A is $2\lambda d_p$, B is $2\gamma D_g\bar{P}$, C is $C_1\frac{K'}{(1\ K')^2}\ \frac{d_1}{D_1}$,

F is $\frac{C_2K'^2}{(1\ K')^2}\ \frac{d_g^2}{D_g\bar{P}}$ and G is $\frac{C_3d_p^2}{D_g\bar{P}}$.

Pressure, averaged over the length of column is introduced as a variable to account for the variation of gaseous diffusion with pressure as given by equation (xxxiv). Giddings (14) has suggested that the velocity distribution term, G, equation (vi), affects the eddy diffusion term. It is thought to arise due to the relatively stagnant gas in the pores of the packing. It is here that the gas velocity will vary greatly from the interparticle gas velocity. He has suggested the term shown in equation (ix) to express the effect of this factor on eddy diffusion

$$A' = \frac{2\lambda d_p}{1 + A\ D_g/\beta^2 d_p u} \qquad \text{(ix)}$$

In this equation β is a geometry constant related to the distance between adjacent paths and $2\lambda d_p$ is the eddy diffusion term of the Van Deemter relation. The terms in equation (ix) indicate that the eddy diffusion term is dependent on the nature of the carrier gas, linear gas velocity and pressure. This can be seen if it is written in a simplified form as

$$A' = \frac{2\lambda d_p}{1+\frac{\beta' D_g'}{\overline{P}u}} \qquad \text{(x)}$$

where $\beta' = \frac{4}{\beta^2 d_p}$

and $D_g' = \overline{P}D_g$

Rearranging equation (x) equation (xi) results

$$A' = \frac{2\lambda d_p \overline{P}u}{\overline{P}u + \beta' D_g} \qquad \text{(xi)}$$

Equation (xi) shows that as the velocity and/or pressure increases the eddy diffusion term approaches the limit $2\lambda d_p$ and at low flow rates and/or pressures the eddy diffusion term decreases. This decrease is significant when $\beta' D_g'$ is large compared with $\overline{P}u$. Inherent in expression (xi) is the dependence of $\beta' D_g'$ upon the carrier gas. As the carrier gas increases in molecular weight $\beta' D_g'$ decreases with a corresponding decrease in the value of $\overline{P}u$ at which $\beta' D_g'$ becomes unimportant. That is, the limit $2\lambda d_p$ is reached at lower flow rates and pres-

sures with heavier carrier gases.

In addition Giddings (15) has considered a number of models arising from proposed equations in gas-liquid chromatography. Written in simplified form these are

$$H = A + \frac{B}{P_o u_o} + Cu_o \qquad \text{(xii)}$$

$$H = \left(A + \frac{B}{P_o u_o}\right) f_1 + Cu_o f_2 \qquad \text{(xiii)}$$

$$H = \left(\frac{B}{P_o u_o} + EP_o u_o\right) f_1 + Cu_o f_2 \qquad \text{(xiv)}$$

$$H = \left(A + \frac{B}{P_o u_o} + EP_o u_o\right) f_1 + Cu_o f_2 \qquad \text{(xv)}$$

$$H = \frac{B}{P_o u_o} + Cu_o \qquad \text{(xvi)}$$

$$H = \frac{Bf_1}{P_o u_o} + Cu_o \qquad \text{(xvii)}$$

$$H = \frac{Bf_1}{P_o u_o} + Cu_o f_2 \qquad \text{(xviii)}$$

In these expressions f_1 and f_2 are averaging coefficients shown in equations (xix) and (xx) which are derived from the inlet and outlet pressures of the column.

$$f_1 = \frac{9}{8} \frac{\left[\left(P_i/P_o\right)^4 - 1\right]\left[\left(P_i/P_o\right)^2 - 1\right]}{\left[\left(P_i/P_o\right)^3 - 1\right]^2} \qquad \text{(xix)}$$

$$f_2 = \frac{3}{2} \frac{\left(P_i/P_o\right)^2 - 1}{\left(P_i/P_o\right)^3 - 1} \qquad \text{(xx)}$$

He determined the coefficient of these equations from experimental data for fractions of the total column by least mean squares. He concluded that none of these equations were completely satisfactory. His tentative conclusions were that

(1) the coefficient of resistance to mass transfer in the liquid phase, C, tends to a limit which is inversely proportional to the pressure.

(2) the eddy diffusion term, A, and resistance to mass transfer in the gas phase of the pores, E, can in many cases be neglected.

(3) the averaging coefficient f_2 is more consistent with the experimental data than is f_1.

The equation shown in (xxi) was not considered by Giddings (15)

$$H = A + \frac{B}{\overline{P}u} + Cu + E\overline{P}u \qquad \text{(xxi)}$$

on theoretical grounds. In equation (xx) he has pointed out that the eddy diffusion term (A) and the resistance to mass transfer in the gas in the pores (E) can be combined into a single term of the form $(\frac{1}{A} + \frac{1}{E\overline{P}u})$. This term suggests that at low velocities rapid diffusion in the gas phase makes $E\overline{P}u$ smaller than A. This over-all term then approaches $E\overline{P}u$ in value and equation (xxi)can be reduced to equation (xxii)

$$H = \frac{B}{\overline{P}u} + Cu + E\overline{P}u \qquad \text{(xxii)}$$

which is synonymous with equation (xiv). It should be pointed out that equations (xii), (xvi), and (xvii) are expressed only in terms of the column outlet conditions. When outlet velocity is used in the calculation of the mass transfer term the value will be different from that obtained when the average column velocity is used. This can be understood if one realizes there are two competing processes giving rise to the mass transfer term. These two processes are the transport of the solute molecules by the gas through the column, and the tendency for the movement of the solute molecules to be impeded by the liquid phase. The effect of the liquid phase is constant since we are considering a linear isotherm over the entire length of column. The linear velocity of the carrier gas increases from column inlet to column outlet. Hence the distance travelled by a solute molecule between reentries to the liquid phase increases from inlet to outlet, i.e. the number of reentries to the liquid per unit column length decreases with increasing gas velocity. Thus the use of outlet velocities gives incorrect values of HETP.

Khan (16), in 1960, proposed a non-equilibrium theory of gas-liquid chromatography. He divided the column into three phases. These phases consisted of gas, liquid and the interface between the two. The terms derived by Khan are given in equation (xxiv).

$$H = 2\lambda d_p + \frac{2\gamma D_g}{u} + \frac{2}{3}\frac{K}{(1+K)^2}\frac{d_f^2}{D_g}u + 2\frac{K^2}{(1+K)^2}\frac{a_2}{k_1}u$$

$$+ \frac{2}{3}\frac{K}{(1+K)^2}\frac{a_2}{k_1\sigma}u + \frac{2}{3}\frac{K}{(1+K)^2}\frac{d_f^2}{D_l}u + 2K\frac{D_l}{u} \qquad \text{(xxiv)}$$

where λ, d_p, γ, D_g, u, d_f, D_l have the same meaning as in the van Deemter equation, and σ is surface area per unit column length.

Khan's equation is the same as van Deemter's equation but with three extra terms to account for resistance to mass transfer in the gas phase, interfacial resistance to mass transfer and longitudinal diffusion in the liquid phase. In this equation the principal new band broadening phenomena suggested occurs at the interface. The interface can be considered as an energy barrier. This energy barrier is formed by the attractive forces between the dipole of the liquid phase and the induced dipole of the carrier gas. Hence the magnitude of the interface term is a function of the carrier gas and the liquid phase. Khan made no allowance for the variation in these forces with varying gas, i.e. his interface term is independent of the carrier gas. It shall be pointed in "Scope of the Present Work" why the interface term should be carrier gas dependent.

C. SCOPE OF THE PRESENT WORK

It has been shown in the preceding section that a variety of equations have been proposed to account for band broadening in gas-liquid chromatography. These equations have not been thoroughly tested and, as has been pointed out by Brandt (17) as recently as July of 1961, ... "the area is in great need of a good deal of definitive experimentation".

If all possible terms suggested by van Deemter, Jones, and Khan, which contribute to band broadening are combined into a single equation, an equation of the form shown in (xxv) is obtained.

$$H = A + \frac{B}{\overline{P}u} + \frac{J}{u} + Cu + Eu + F'\overline{P}u + G'\overline{P}u + 2\rho\,(F'G')^{\frac{1}{2}}\overline{P}u \qquad \text{(xxv)}$$

In equation (xxv) average column pressure, $\overline{P}$, is an independent variable to account for the variation of gaseous diffusion with pressure as given by equation (xxxiv). u is linear velocity of the carrier gas, A is the eddy diffusion term, B is the coefficient of longitudinal diffusion in the gas phase, C is the coefficient of resistance to mass transfer in the liquid phase, E is the coefficient of resistance to mass transfer at the gas-liquid interface, F' is the coefficient of resistance to mass transfer in the mobile gas phase, G' is the coefficient of resistance to mass transfer in the relatively stagnant gas phase, J is the coefficient of longitudinal diffusion in the liquid phase. In this equation the pressure dependence of the A term suggested by Giddings is not included for reasons which are stated later where the generalized equation is examined term by term.

If the average pressure across the column is constant, equation (xxv) can be reduced to the following form

$$H = A + \frac{B'}{u} + C'u \qquad \text{(xxvi)}$$

where $$B' = \frac{B}{\bar{P}} + J \qquad \text{(xxvii)}$$

and $$C' = C + E + F\bar{P} + G\bar{P} + 2\rho\,(FG)^{\frac{1}{2}}\,\bar{P}. \qquad \text{(xxviii)}$$

B' is a combined longitudinal diffusion coefficient and C' is a combined resistance to mass transfer coefficient. Equation (xxvi) thus allows one to calculate the combined resistance to mass transfer coefficient (C') and the eddy diffusion term (A) from experimental data relating HETP and gas velocities.

Evaluation of the resistance to mass transfer in the gas phase only can be made from values of C' at various average pressures. Thus it is convenient to define a term (F') for the variation of C' with average pressure. Such a term would include all gas terms as given in equation (xxix).

$$F' = \frac{dC'}{d\bar{P}} = F + G + 2\rho\,(FG)^{\frac{1}{2}} \qquad \text{(xxix)}$$

The term, F', is hereafter referred to as the combined resistance to mass transfer in the gas phase coefficient. In equation (xxix), G accounts for the effect of velocity distribution in the mobile gas phase on the resistance to mass transfer. It also includes the effect of stagnant gas in the pores of the support particles. The stagnant gas portion of G should be a function of the per cent liquid phase in the column. Hence G and F' are functions of per cent liquid phase if the stagnant

gas resistance to mass transfer is appreciable. If there is no dependence of the combined resistance to mass transfer in the gas phase coefficient, F', on prt vrny liquid, this still does not completely rule out the velocity distribution term as a cause of band broadening. It is noted that C_3 in equation (vi), accounts for the effect of shape of the support particles and the effect of velocity distribution of carrier gas on G. Poiseuille's law (18) states that the rate of flow

$$\frac{dV}{dt} = \frac{\pi (P_i^2 - P_o^2) R^4}{16\, L\eta\, P_o} \qquad \text{(xxx)}$$

of a fluid in a capillary tube is inversely proportional to its viscosity according to equation (xxx). The mathematical expression of Poiseuille's law is given in equation (xxx) where $\frac{dv}{dt}$ is the volume rate of flow, P_i and P_o are the inlet and outlet pressures, respectively, L is the length of the capillary, R is the radius of the capillary and is the viscosity of the fluid flowing through the capillary tube. In laminar flow the velocity is distributed parabolically over the cross-section of a circular tube. The velocity at any one radial point is related to the average velocity $\overline{W}$ by equation (xxxi).

$$W = 2\overline{W}\left(1 - \frac{4r^2}{d^2}\right) \qquad \text{(xxxi)}$$

In equation (xxxi) W is the flow rate at a distance r from the axis and d is the diameter of the tube. Since C_3 of equation (vi) depends on velocity distribution then G' is a function of

viscosity η of the carrier gas. Also since there is a velocity profile in the mobile phase, F would be expected to be dependent on carrier gas viscosity. Thus, the combined resistance to mass transfer in the gas phase coefficient F' is a function of carrier gas viscosity and will be given as

$$F' = F + G + 2\rho(FG)^{\frac{1}{2}} \qquad \text{(xxxii)}$$

Since all gas terms are related to diffusivity and viscosity there is no direct method of determining each individually.

The interface term, E, of equation (xxv), will be carrier gas dependent since the character of this boundary will vary with the nature of the carrier gas. At the interface the carrier gas molecules are held by forces of attraction to the dipole of the liquid. This bonding force, ϵ, for any one liquid phase will be a function, therefore, of the polarizability of the carrier gas molecules (19). This function is given in equation (xxxiii)

$$\epsilon = \frac{-\alpha Q^2}{2} \qquad \text{(xxxiii)}$$

where Q is the electric field strength of the permanent dipole of the liquid phase, α is the polarizability of the carrier gas. The dependence of the interface term on carrier gas can be obtained by relating the intercept of the combined resistance to mass transfer, C', and average pressure, $\bar{P}$, to the polarizability of the carrier gas.

The variation of the intercept of the C' vs F relation with per cent liquid can be of little value in determining the magnitude of C and E since they both are functions of per cent liquid. To obtain C directly it is therefore necessary to relate C' with a property of the carrier gases common to E, F and G. The most promising would seem to be the molecular weight-molecular volume coefficients found in the Gilliland equation (xxxiv) (20) for diffusivity of one gas in another.

$$D_{12} = \frac{0.0043T^{3/2}\left(\frac{1}{M_1} + \frac{1}{M_2}\right)^{\frac{1}{2}}}{P\left(V_1^{1/3} + V_2^{1/3}\right)^2} \qquad \text{(xxxiv)}$$

In equation (xxxiv) D_{12} is the diffusivity of gas 1 in gas 2 where M_1, M_2 and V_1, V_2 are the molecular weights and molecular volumes at their boiling points, P is the prevailing pressure in atmospheres and T is the absolute temperature. Since D_g appears in the denominator of the gas phase resistance terms a plot of the reciprocal of the molecular weight-molecular volume portion of equation (xxxiv) vs C' would approach a limit as the molecular weight-molecular volume coefficient decreases to zero. This limit would be C, the resistance to mass transfer in the liquid phase since the carrier gas and its various effects have been removed, effectively leaving only the liquid phase resistance to mass transfer.

The longitudinal diffusion term, B', can be evaluated in either of the following ways: by plotting HETP against the reciprocal of the linear velocity at constant average pressure

or by plotting HETP against the reciprocal of the product of average pressure and linear velocity. The coefficient B' is given by the slope of either plot for very low velocities. Once B' has been evaluated for a number of gases then the existence of longitudinal diffusion in the liquid phase can be tested. If J is significant then a plot of B' against the diffusivity of solute in carrier gas, as given by equation (xxxiv), will intercept the B' coordinate at some positive value.

Eddy diffusion, the A term of equation (xxv), is considered as a multiple path term of the mobile gas phase. Hence, A should be independent of pressure and nature of the carrier gas. Giddings (14) has suggested that stagnant gas in the pores of the support particles influences the value of the diffusion term. The effect of the stagnant gas would seem to act as a resistance to the solute molecules in going from the stationary phase to the mobile phase. Furthermore, the stagnant gas would affect the column residence time of the solute molecules but not the path lengths of the mobile gas phase. Hence, the effects of stagnant gas should be considered as a term independent of eddy diffusion as in equation (xxv). The validity of this assumption shall be considered by investigating the variation of A values with pressure and nature of the carrier gases.

Bohemen and Purnell (21) have raised the question as to the existence of eddy diffusion by reporting negative values

for the A term in the original van Deemter equation. Their values of A were determined from plots of HETP against velocity without considering the effect of pressure variations with velocity and resistance to mass transfer in the gas phase. When average pressure ($\overline{P}$) is kept constant then equation (xxv) can be applied. Thus, H vs u and H vs $1/\overline{P}u$ relations should have a common intercept invariant with $\overline{P}$. An agreement in intercepts would indicate the existence of the van Deemter A term, i.e. eddy diffusion, and the necessity of including it in any proposed rate equation.

II. EXPERIMENTAL

The instrument used in this work was a modified Burrell Kromo-Tog K2 gas chromatograph with a thermal conductivity detector thermostated at 150°C. The columns were ¼-inch O.D. copper tubing. The ends of the columns were attached to tee joints as shown in Figure 3. One arm of the tee lead to the detector cell(TC) and the other to the mercury reservoir (Hg) of the outlet or inlet manometer (M). The manometers consisted of ¼-inch O.D. tygon tubing with a short piece of ¼-inch O.D. glass tubing leading into the mercury reservoirs through a rubber stopper. The tygon tubing was fastened to the glass tubing by first spreading it over one end of the glass tubing and sealing with "Plastiglo" two component polyurethane plastic coating.

The columns were immersed in a 1-litre Dewar flask (D) containing arochlor. Column temperatures were controlled by a 250-watt knife heater (H) regulated by a rheostat and stirrer (S). A thermometer (T) also dipped into the arochlor. The flow rate of the carrier gas was regulated by regulating the tank pressure at the inlet (CI). The first measurements of each run were at the highest velocity. The additional measurements were at successively lower velocities. A constant average pressure was maintained by adjusting the pressure of the gas entering the flow system on the exit side of the column (BPI). Thus as the pressure at CI was decreased there was a corresponding decrease in the flow rate and average pressure. The pressure at BPI was therefore increased and this increased the

Figure 3

Schematic Diagram of Gas-Liquid Chromatographic Apparatus

BPI - back pressure gas inlet

C - capillaries

CI - carrier gas inlet

D - 1 litre Dewar flask

E - electrical connections leading to recorder

G - gas storage bottle gauge

H - 250-watt knife heater

Hg - mercury reservoirs

I - sample inlet

M - mercury manometers

O - outlet

S - stirrer

T - thermometer

TC - thermal conductivity cell

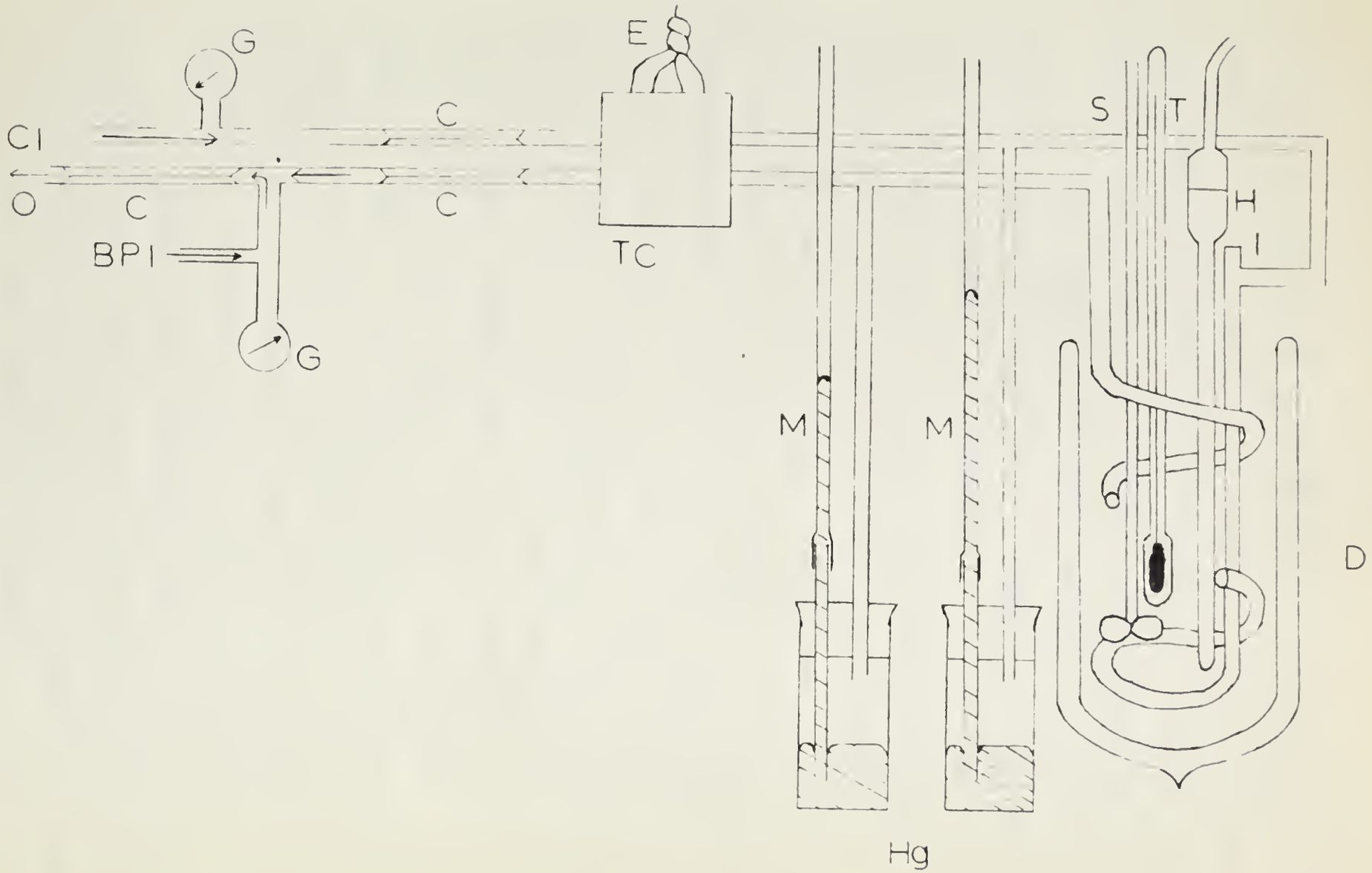
G
E
C
S
T
CI
O
C
C
H
I
BPI
TC
G
M
M
D
Hg

average pressure. By adjustments of this sort the average pressure was maintained at a constant value with varying flow rate. Control of pressure and flow rate was made easier by means of capillaries (C) between the detector and gas supplies.

The column packing was prepared by combining a weighed amount of support with a weighed amount of di-n-decylphthalate dissolved in chloroform. The chloroform was then removed under reduced pressure in a rotary evaporator. A weighed portion of the packing was poured by means of a small funnel into the copper tubing. A Vibratool was used to adjitate the column to ensure a maximum packing density. When the columns were filled the ends were plugged with a small piece of glass wool. The tubing was then coiled around a piece of pipe of such size that the coiled column fitted into the Dewar flask. The columns were conditioned until a steady baseline of ½-hour duration resulted at highest detector sensitivity. The physical characteristics of the columns used are given in Table I. The density of the di-n-decylphthalate was determined by means of a Westphal balance. The density of the firebrick was calculated by measuring the volume of methanol displaced by a weighed sample in a calibrated flask.

Samples were introduced with a 10 μl Hamilton syringe directly onto the top of the column packing through a silicone rubber puncture seal (I). It should be mentioned that as long as the samples are within the range of 0.5 - 1.5

TABLE 1

Physical Characteristics of Columns for HETP Measurementas. The Columns were Di-n-decyl-phthalate (Density of 0.957 at 26°C) on 30-60 Mesh Fisher Columnpax (Density 2.46 at 25°C) in $\frac{1}{4}$-inch O. D. Copper Tubing

% Liquid on column	4.1	6.7	11	11	14	20	25	30
Vol. of empty column V_{col}, cm^3	18.1	18.2	18.2	18.1	18.3	18.3	18.1	18.0
Wt. of support + Substrate, gm	8.46	9.63	7.22	11.9	9.94	10.5	13.6	13.7
Wt. of support, gm	8.11	8.99	6.44	10.56	8.55	8.44	10.2	9.57
Vol. of support, V_{sup}, cm^3	3.34	3.70	2.66	4.35	3.52	3.48	4.20	3.94
Wt. of substrate, gm	0.35	0.64	0.78	1.3	1.39	2.1	3.4	4.1
Vol. of substrate at 26°C V_{sub}, cm^3	0.37	0.67	0.81	1.36	1.45	2.2	3.6	4.3
Vol. of Gas, V_g, cm^3 $V_g = V_{col} - V_{sub} - V_{sup}$	14.4	13.8	14.7	12.4	13.3	12.6	10.3	9.8
Mass Ratio $= \frac{\text{Substrate}}{\text{Support}}$	0.043	0.072	0.12	0.11	0.16	0.25	0.34	0.43
Gas Cross Section, cm^2	0.056	0.054	0.057	0.048	0.052	0.049	0.040	0.038
Substrate Cross Section, cm^2	0.0014	0.0026	0.0032	0.0053	0.0056	0.0085	0.014	0.016
Column Length, cm	256	257	257	256	258	259	256	255

μl, sample size effects on HETP (H) are insignificant as depicted in Figure 4.

The characteristics of the carrier gases and solute used in this investigation are presented in Table 2. In this table are listed the molecular weights, molecular volumes, viscosity, polarizability of the carrier gases and the factor of the Gilliland relation dependent on the molecular characteristics.

Peak widths were obtained from the chromatograms by measuring the distance along the base line between the tangents drawn at the points of inflection of the peaks. The retention times (d) were measured from the points of injection to the junction of the two tangents. Linear velocity (u) of the carrier gases was determined from the air peak retention time and the length of column. The column lengths were determined before coiling the columns by measuring the length of copper wire equivalent to the length of the column. The lengths reported in Table I are averages of three measurements. The values of HETP (H) recorded in Tables 6 and 11 to 33 of the Appendix were determined by means of formula (xxxv).

$$H = \frac{L}{16} \left(\frac{W}{d}\right)^2 \qquad \text{(xxxv)}$$

Pressures were determined from the differential manometers (M) and a barometer. Average pressures in which the ratio of inlet (P_i) to outlet pressures (P_o) were greater than 1.5 were

Figure 4

Effect of Sample Size on HETP Using n-Pentane as Solute with Hydrogen Carrier Gas and Varying Amounts of di-n-Decylphthalate as Liquid Phase on 30-60 Mesh Firebrick.

1. 30% liquid at 32°C average carrier velocity 15 cm/sec
2. 25% liquid at 44°C average carrier velocity 32 cm/sec
3. 14% liquid at 32°C average carrier velocity 18 cm/sec
4. 11% liquid at 32°C average carrier velocity 15 cm/sec
5. 6.7% liquid at 44°C average carrier velocity 24 cm/sec
6. 4.3% liquid at 32°C average carrier velocity 18 cm/sec

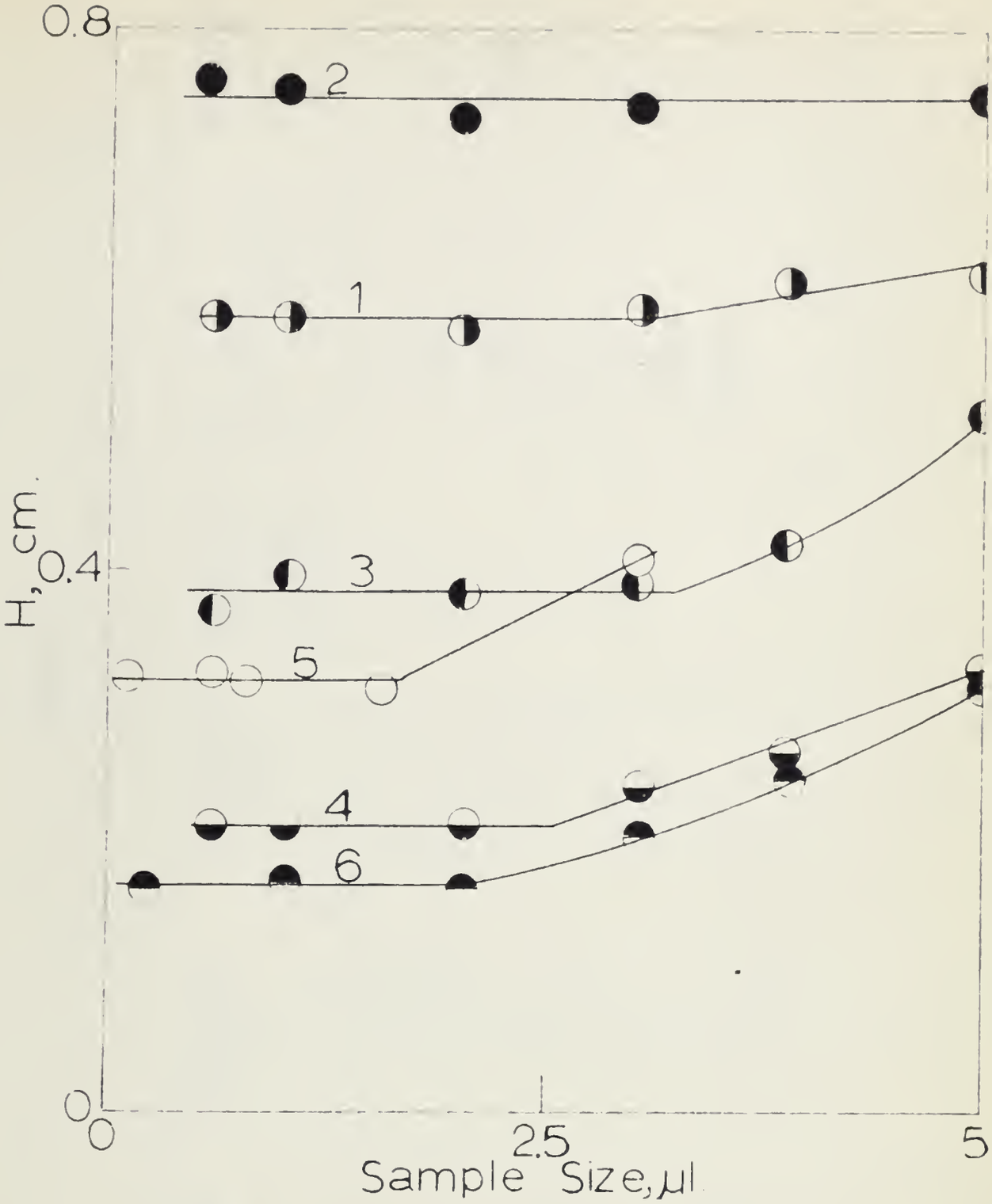
0.8
0.4
0
H, cm.
2
1
3
5
4
6
0
2.5
5
Sample Size, µl

TABLE 2

Carrier Gas and Solute Characteristics

Compound	Molecular Weight	Molecular Volume at b.p.	Viscosity at 44°C in micro-poise(26)	$\frac{\left(\frac{1}{M_1}+\frac{1}{M_2}\right)^{\frac{1}{2}}}{\left(V_1^{1/3}+V_2^{1/3}\right)^2}$	Polarizability X 10^{25}
H_2	2.01	14.3 (33)	89.5	0.0131	8.2 (24)
He	4.003	32.9 (34)	208	0.00772	2.04 (24)
CH_4	16.04	33.0 (33)	117	0.00415	25.8 (24)
N_2	28.01	31.2 (33)	185	0.00341	17.4 (24)
CO_2	44.01	34.0 (33)	158	0.00292	26.5 (27)
$CBrF_3$	148.9	40.6		0.00205	
$C_2Cl_2F_4$	170.9	69.2		0.00173	
C_5H_{12}	72.12	121			

He, CH_4, N_2, CO_2 are not retained by 2.55 meter 25% di-n-decylphthalate column at 44°C, i.e. their solubility is negligible.

determined by the method of James and Martin (5) given in equation (xxxvi).

$$\overline{P} = \frac{2}{3} P_o \frac{\left(P_i/P_o\right)^3 - 1}{\left(P_i/P_o\right)^2 - 1} \qquad \text{(xxxvi)}$$

When the ratio of inlet to outlet pressures were 1.5 or less an average was taken using formula (xxxvii).

$$\overline{P} = \tfrac{1}{2}(P_i + P_o) \qquad \text{(xxxvii)}$$

The error introduced in $\overline{P}$ by using equation (xxxvii) is 1.5% of P_o when the ratio of P_i to P_o is 1.5. The error decreases with a decrease in ratio.

The measured data obtained in this investigation is presented in Tables 5, and 10 to 32 inclusive, of Appendix I and III. The data covers the effect of carrier gas variation, liquid loading (4% to 30%), pressure variation (0.8 to 4 atmospheres) and temperature (25°C to 126°C).

III. RESULTS AND DISCUSSION

A. General

In Figures 5 and 6 are presented classical HETP (H) vs velocity (u) relations for an n-pentane - 30% di-n-decyl-phthalate system. The experimental data for these figures is given in Tables 11 to 17 inclusive of the Appendix. The carrier gases used varied in molecular weight from 2 for hydrogen to 171 for freon 114. The curves in Figures 5 and 6 have four noteworthy characteristics which are listed below.

1. The rate of decrease in efficiency increases with an increase in molecular weight of carrier gas at high carrier gas velocities.
2. The velocity at maximum efficiency decreases with an increase in carrier gas molecular weight and also there is an increase in sharpness of the minimum.
3. The value of HETP at the velocity of maximum efficiency decreases as the molecular weight of carrier gas increases.
4. For all carrier gases there is an increase in slope of the H vs u curves as u increases. This can be observed in the data of other workers (16, 23), although they have not drawn attention to this phenomenon. Any theory proposed to relate HETP with carrier gas velocity must account for all these observations. To explain these observations one must relate H to $\bar{P}u$ and to the nature of the carrier gas.

Figure 5

Relation Between HETP and Carrier Gas Velocity with a 30% di-n-Decylphthalate Column at 126°C Using n-Pentane as Solute at a Constant Outlet Pressure of 0.93 Atm.

1. ○ Helium
2. ● Nitrogen
3. ◒ Carbon dioxide
4. ◑ Freon 114

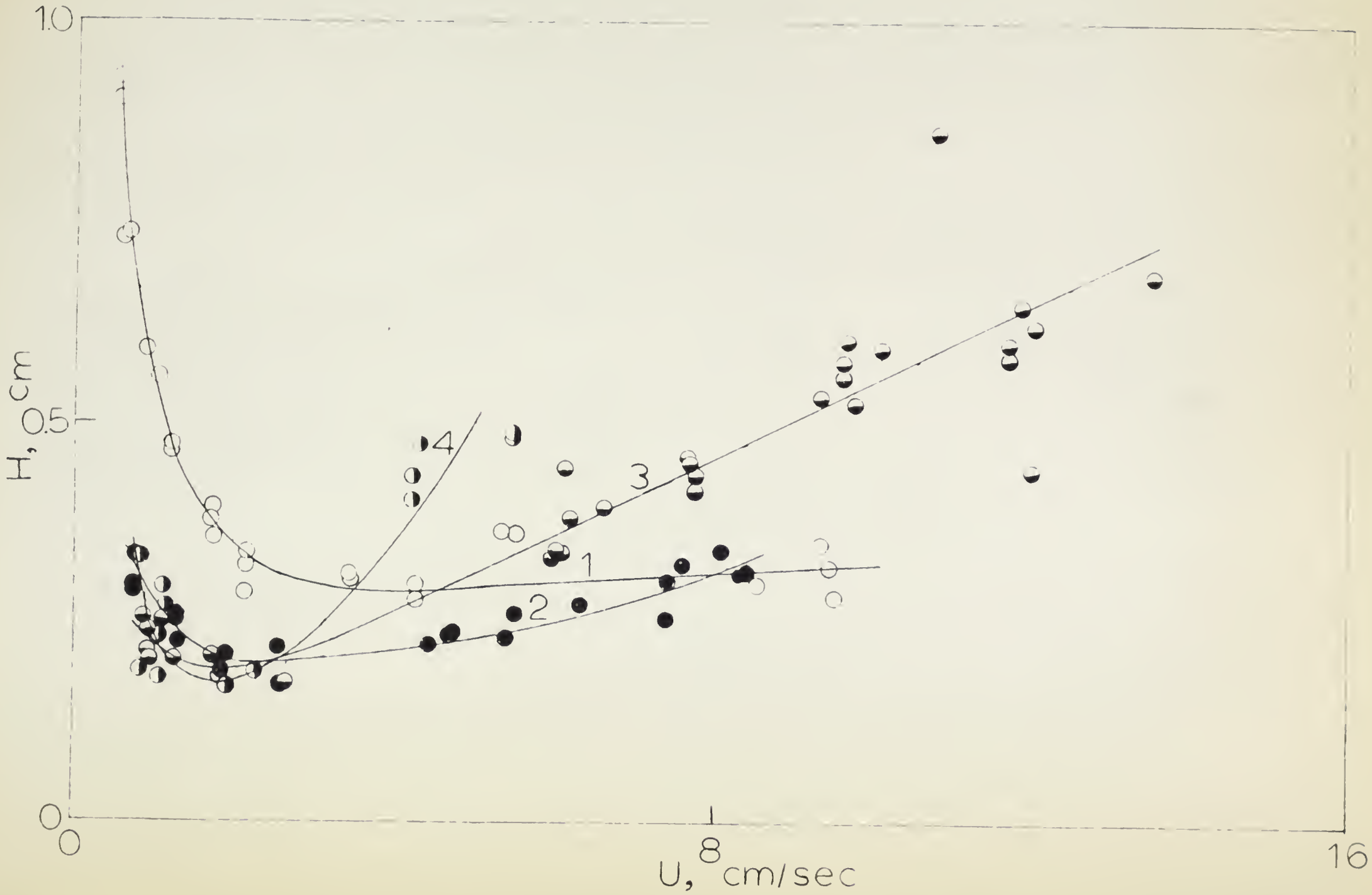
1.0
0.5
0
H, cm
0
8
16
U, cm/sec
1
2
3
4

Figure 6

Relation Between HETP and Carrier Gas Velocity with a 30% di-n-Decylphthalate Column at 126°C Using n-Pentane as Solute at a Constant Outlet Pressure of 0.93 Atmospheres.

1. ● Hydrogen
2. ○ Methane
3. ◒ Freon 13B1

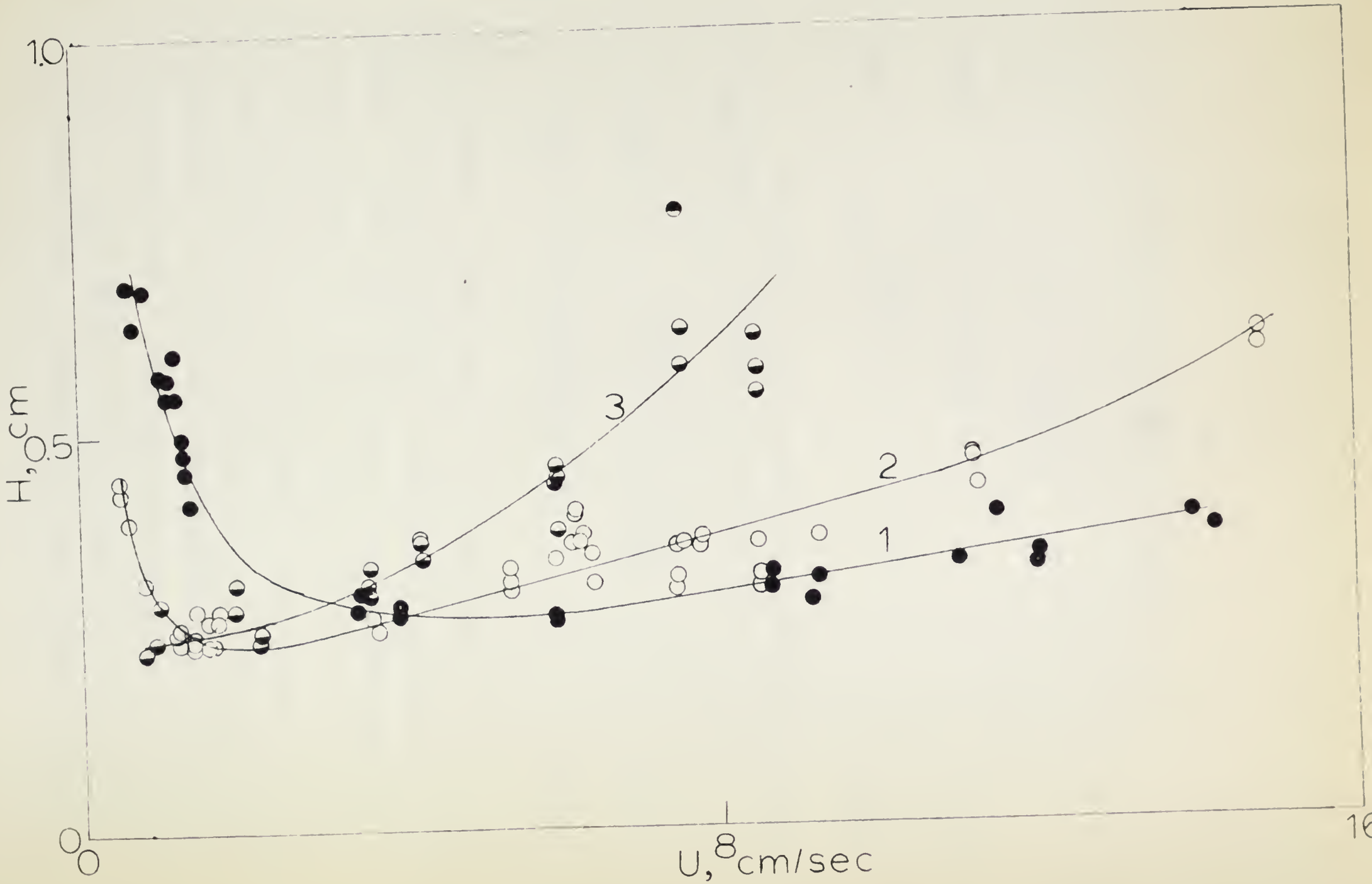
1.0
0.5
0
H, cm
0
8
16
U, cm/sec
1
2
3

The simple van Deemter equation

$$H = A + \frac{B}{\bar{P}u} + Cu$$

gives $$H_{min} = A + 2\sqrt{BC} \qquad \text{(xxxviii)}$$

and $$u_{min} = \sqrt{\frac{B}{C}} \qquad \text{(xxxix)}$$

In terms of equation (xxv) the corresponding values of H_{min} and u_{min} are shown in equation (xL) and (xLi).

$$H_{min} = A + 2\sqrt{B(C+E+F\bar{P}+G\bar{P}+2\rho(FG)^{\frac{1}{2}}P} \qquad \text{(xL)}$$

$$u_{min} = \sqrt{B/(C+E+F\bar{P}+G\bar{P}+2\rho(FG)^{\frac{1}{2}}P} \qquad \text{(xLi)}$$

It is assumed in equation (xxv) that resistance to mass transfer in the liquid phase (C) is independent of carrier gas and pressure. Thus, since the terms F, G and $2\rho(FG)^{1/2}$ increase with increasing molecular weight as well as pressure of the carrier gas, characteristics 1, 2 and 4 can be explained on this basis. The third characteristic is not as obviously explained since B decreases as $(C + E + F\bar{P} + G\bar{P} + 2\rho(FG)^{\frac{1}{2}}P)$ increases with increasing molecular weight. As a first approximation the decrease in value of H_{min} with an increase in molecular weight of the carrier gas is due to a difference in the relative rates of

change of B and $(C + E + F\overline{P} + G\overline{P} + 2\rho(FG)^{\frac{1}{2}}\overline{P})$. That is, B decreases at a faster rate than $(C + E + F\overline{P} + G\overline{P} + 2\rho(FG)^{\frac{1}{2}}\overline{P})$. increases. Thus it is necessary to include at least one term for resistance to mass transfer in the gas phase in an expression relating HETP and carrier gas velocity.

The values of the combined resistance to mass transfer shown in Figure 7 are derived from the data of Tables 6 and 18 to 23, inclusive. Figure 7 shows the variation of the combined resistance to mass transfer term, C', with average column pressure, $\overline{P}$, as the per cent liquid phase is varied. The slopes of these plots, $\frac{dC'}{d\overline{P}}$, that is the combined gas phase resistance to mass transfer, F', is shown in Figure 8 as a function of the ratio of the weight of di-n-decylphthalate to the weight of firebrick. Figure 8 shows that resistance to mass transfer in the gas phase is independent of the per cent liquid phase over the range of 4.3 to 30 per cent. Failure to detect a dependence of resistance to mass transfer in the gas phase on per cent liquid is evidence that stagnant gases in the pores of the parking do not affect HETP in packed chromatographic columns. This conclusion is based on the assumption that the liquid phase accumulates in the pores of the packing, and therefore as the per cent liquid phase increases the volume of stagnant gas must decrease. Hence, with an increase in per cent liquid there would be a decrease in the stagnant gas term with a corresponding decrease in the combined resis-

Figure 7

Relation Between the Mass Transfer Coefficient (C') and Average Carrier Gas Pressure ($\overline{P}$) with Varying Amounts of di-n-Decylphthalate as Column Liquid and Hydrogen Carrier Gas at 44°C.

1. ◓ 30%
2. ◐ 25%
3. ◒ 14%
4. ○ 11%
5. ● 11%
6. ◑ 6.7%
7. ◔ 4.3%

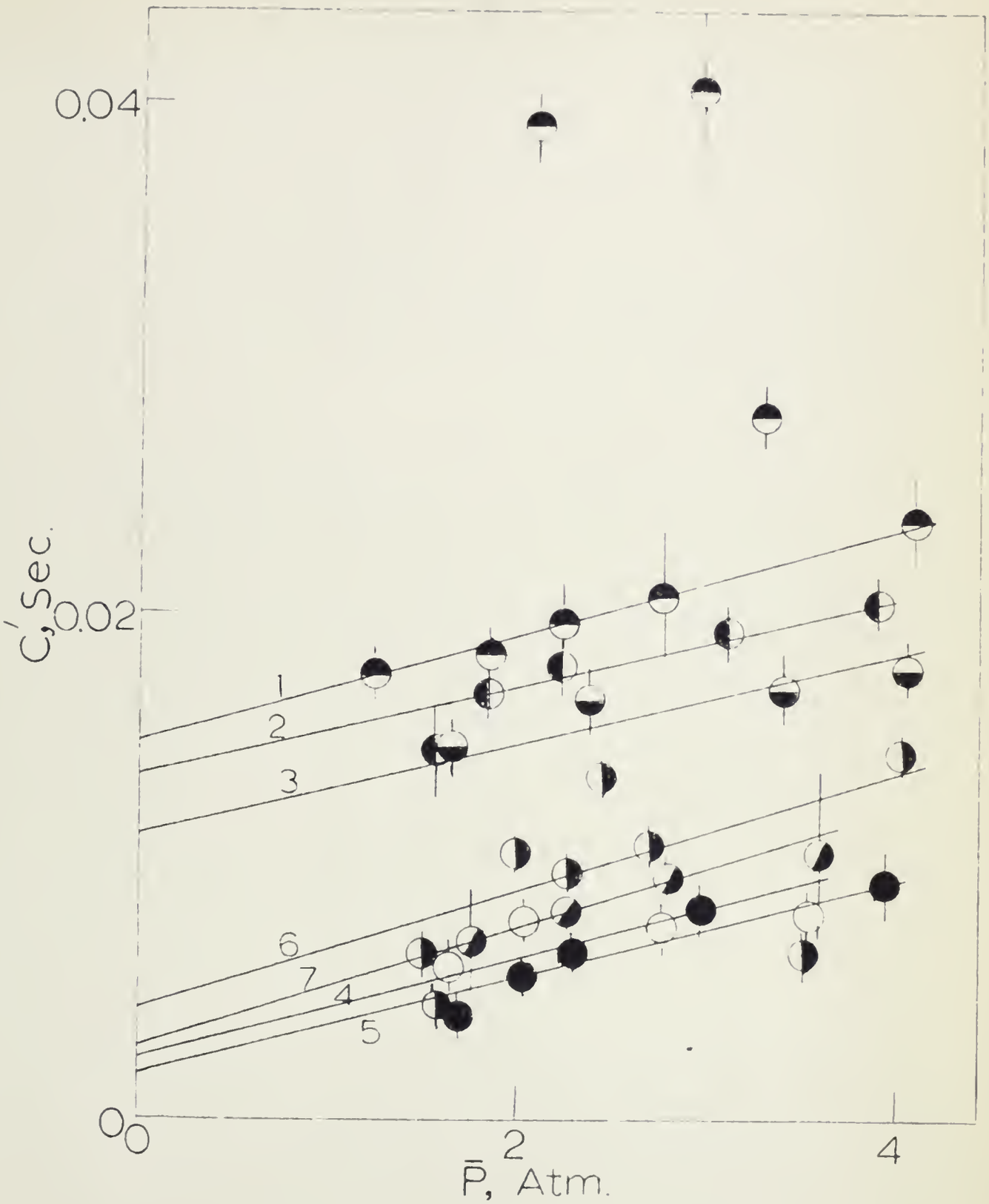
0.04
0.02
0
C', Sec.
1
2
3
6
7
4
5
0
2
4
P̄, Atm.

Figure 8

Relation Between Resistance to Mass Transfer in the Gas Phase (F') and the Ratio of the Amount of di-n-Decylphthalate to Firebrick. Hydrogen Carrier at 44°C.

s - weight of di-n-decylphthalate

f - weight of firebrick

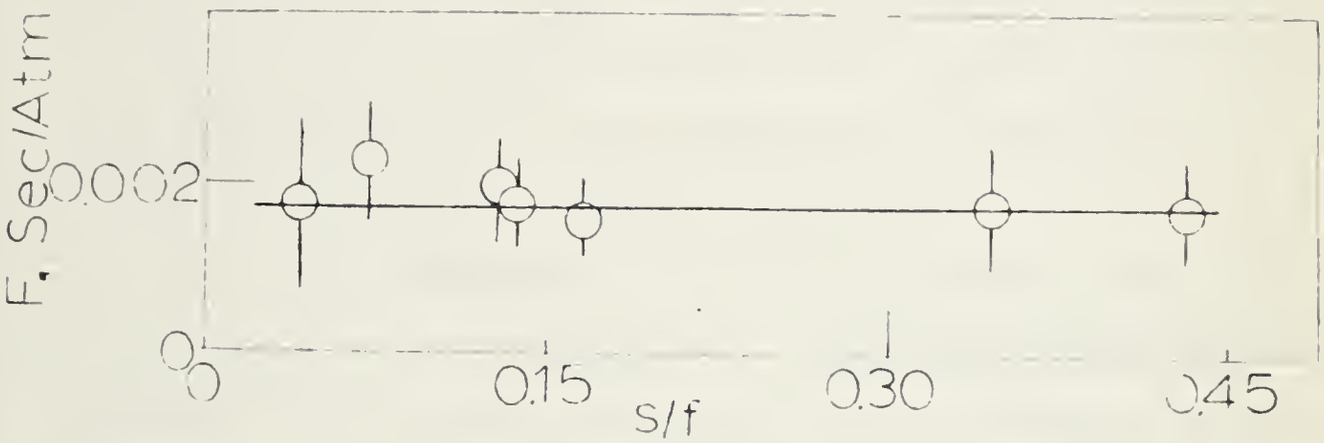
F, Sec/Atm
0.002
0
0
0.15
0.30
0.45
S/f

tance to mass transfer in the gas phase term F'.

The combined resistance to mass transfer terms, C', derived from Tables 22, 24, 25 and 26 are shown in Figure 9. In Figure 9 it is seen that the slopes of C' versus average column pressure, $\overline{P}$, relations, i.e. resistance to mass transfer in the gas phase, F', varies with nature of the carrier gas. This variation in slope is due to a variation in the diffusivity of solute in the carrier gas when the carrier gas is changed. The relationship of F' and diffusivity is discussed in a latter section and is shown in Figure 17.

The intercept of the C' vs $\overline{P}$ relations vary with per cent liquid as seen in Figure 7. From these data it could be assumed that this is a variation of the resistance to mass transfer in the liquid phase with a variation in per cent liquid. However, there is another possibility and that is a variation in resistance to mass transfer due to a variation in area of the interface. That the nature of the interface influences the efficiency of a chromatographic column is seen from the variation in intercept of the C' vs $\overline{P}$ relations with variations in carrier gas as depicted in Figure 9. Thus it is necessary to include a term to account for these variations. The nature of this term shall be presented later, but it suffices to state that C', i.e. the combined resistance to mass transfer, is composed of the three terms listed below.

Figure 9

Relation Between the Mass Transfer Coefficient (C') and Average Carrier Gas Pressure ($\overline{P}$) with Different Carrier Gases with a 6.7% di-n-Decylphthalate Column at 44°C.

1. ◐ carbon dioxide
2. ○ methane
3. ● nitrogen
4. ◒ hydrogen

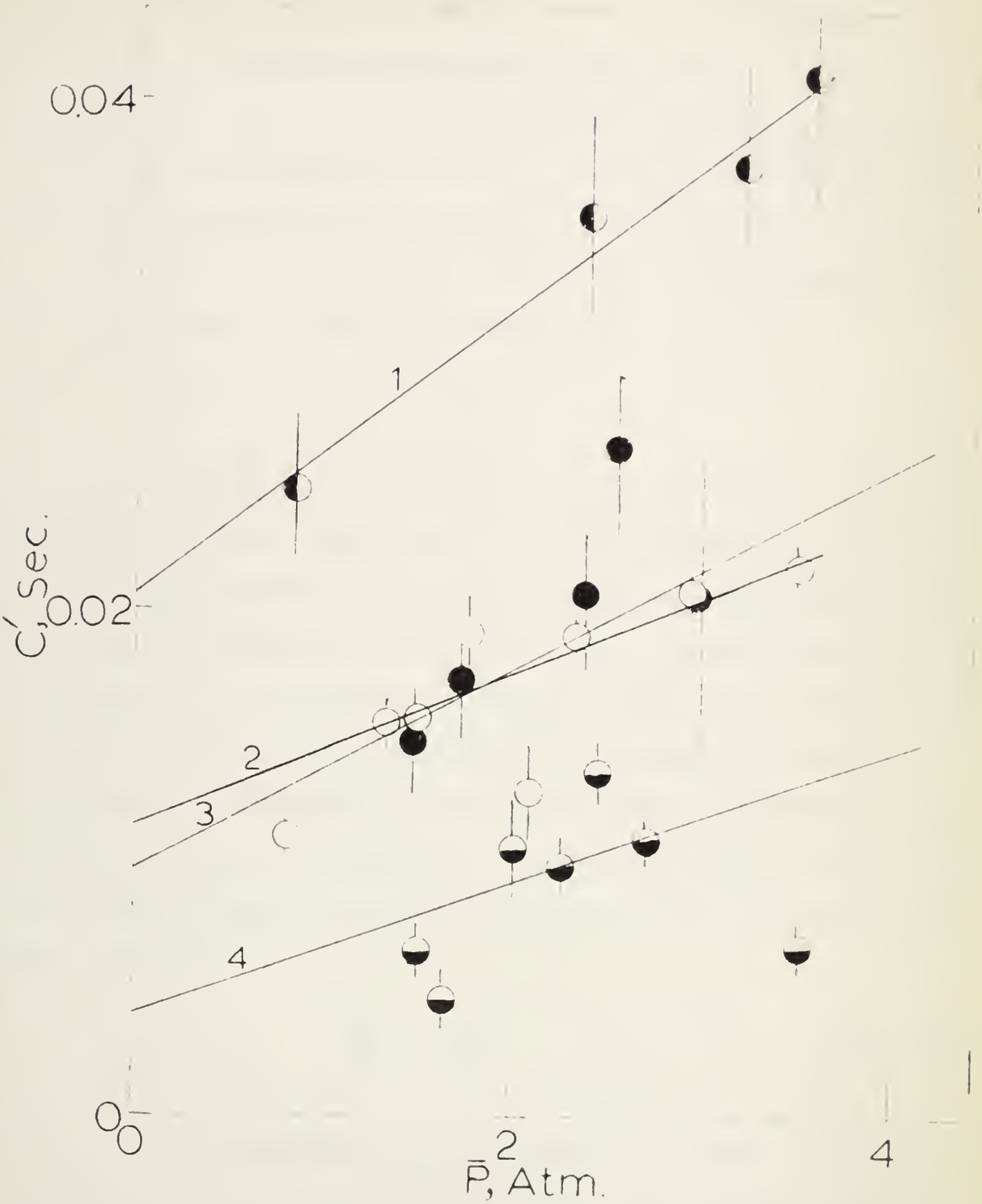
0.04
0.02
0
C', Sec.
1
2
3
4
0
2
4
P̄, Atm.

1. A resistance to mass transfer in the liquid phase C, which is dependent on the per cent liquid.
2. A resistance to mass transfer in the mobile gas phase, F', which is dependent on the nature of the carrier gas.
3. A resistance to mass transfer at the interface, E, which is dependent on the per cent liquid and upon the carrier gas. Thus C' can be expressed as

$$C' = C + E + F' \overline{P} \qquad \text{(xxxvi)}$$

Figure 10 is evidence for the absence of longitudinal diffusion in the liquid phase. In this figure, the values of B, i.e. the slopes of H vs $1/\overline{P}u$ relations, were obtained from the data in Tables 11 to 17, inclusive. These values of B are related to D_g', the factor of the Gilliland (15) diffusivity equation containing the gas molecule dependent factors. If longitudinal diffusion in the liquid phase is present such a relation would have a positive intercept on the B coordinate. This reduces the longitudinal diffusion terms given by equation (xxvi) to

$$\frac{B'}{\overline{P}u} = \frac{B}{\overline{P}u} \qquad \text{(xxxvii)}$$

To determine the existence of the eddy diffusion term, A, in the rate theory it is necessary to examine the intercepts of H vs $1/\overline{P}u$ and H vs u relations at constant

Figure 10

Variation of the Coefficient of the Longitudinal Diffusion Term with Carrier Gas with 30% di-n-Decylphthalate Column at 126°C.

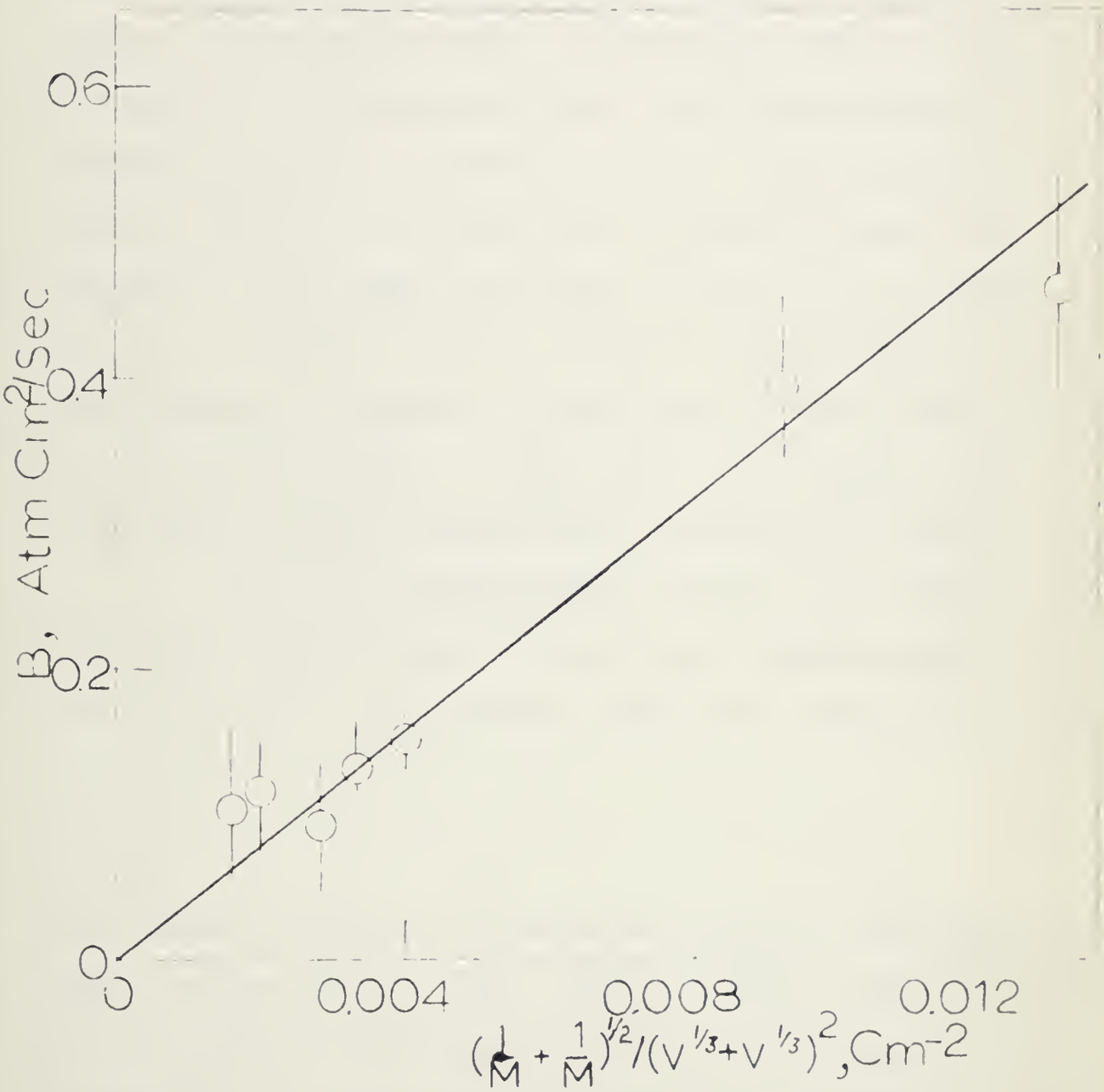
0.6
0.4
0.2
0
B, Atm Cm²/Sec
0
0.004
0.008
0.012
$(\frac{1}{M} + \frac{1}{M})^{1/2}/(V^{1/3}+V^{1/3})^2$, Cm⁻²

average pressure. Equation (xxv) states that these relations should have a common intercept at A on the H coordinate. The value of the intercept should also be independent of average pressure, temperature and the carrier gas. These characteristics of the eddy diffusion term are shown in Figures 11, 12 and 13, respectively, for a 2.55 meter, 30% di-n-decylphthalate column and n-pentane as solute. The data from which they are derived are given in Tables 11 to 17. The agreement of A values from H vs $1/\bar{P}u$ and H vs u plots are seen from a comparison of the values of Figure 12 with those of Figures 11 and 13. In Figure 12 the A values were determined from H vs u plots, while in Figures 11 and 13 the A values were determined from H vs $1/\bar{P}u$ plots. These data leave little doubt as to existence of eddy diffusion band broadening in packed columns.

From this experimental analysis of equation (xxv) in which all proposed terms contributing significantly to HETP are considered, the following simplified equation is suggested.

$$H = A + \frac{B}{\bar{P}u} + Cu + Eu + F\,\overline{Pu} \qquad \text{(xLiii)}$$

This equation agrees in form to the equation theoretically proposed by Khan (16) in 1960. The individual terms in equation (xLiii) shall be discussed in the following sections with reference to pertinent results which have appeared in the literature in addition to those gathered in this study.

Figure 11

The Relation of the Eddy Diffusion Term, A, to Temperature Using n-Pentane as Solute and a 2.55 Meter, 30% di-n-Decylphthalate Column and Helium as Carrier Gas.

Figure 12

The Relation of the Eddy Diffusion Term, A, to Pressure Using n-Pentane as Solute on a 2.55 Meter, 30% di-n-Decylphthalate Column at 44°C and Hydrogen as Carrier Gas.

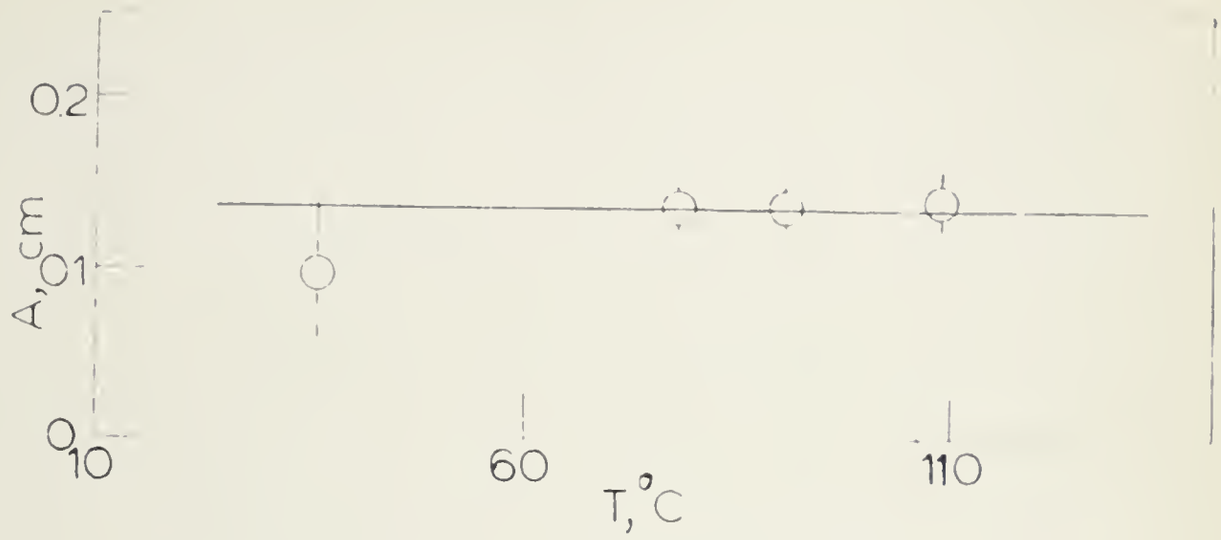
0.2
A, cm
0.1
0
10
60
110
T, °C

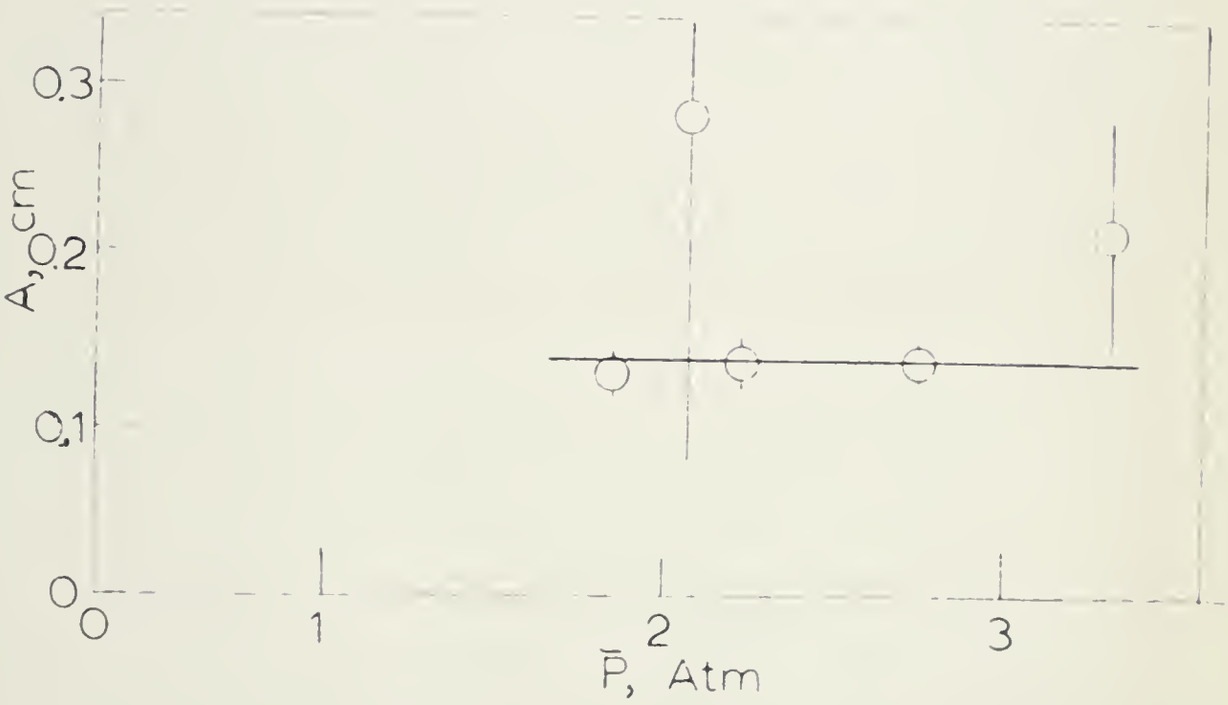
0.3
A, cm
0.2
0.1
0
0
1
2
3
P̄, Atm

Figure 13

Relation of the Eddy Diffusion Term, A, to Carrier Gas Using n-Pentane as Solute on a 2.55 Meter, 30% di-n-Decylphthalate Column at 126°C. at an Outlet Pressure of 0.93 Atmospheres.

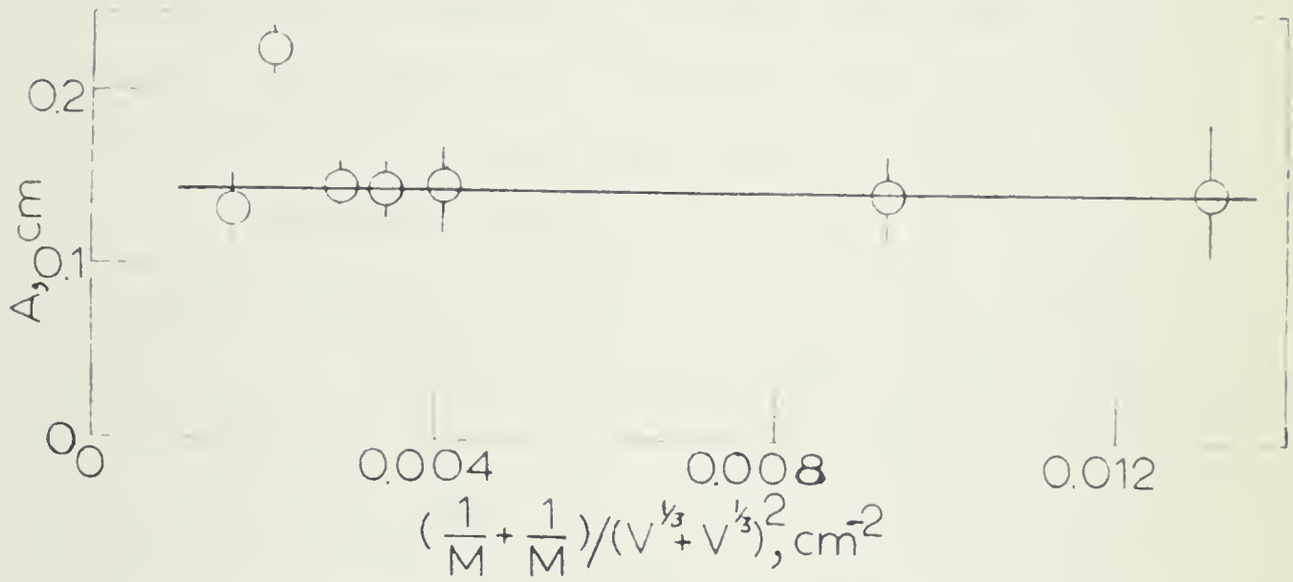
0.2
0.1
0
A, cm
0
0.004
0.008
0.012
$(\frac{1}{M}+\frac{1}{M})/(V^{1/3}+V^{1/3})^2$, cm^{-2}

B. Eddy Diffusion: The A Term

The eddy diffusion or A term reflects the nonuniformity in length of the various flow paths within the column packing. This has been expressed as a function of the particle diameters as given in equation (vii). As the diameter of the solid support, d_p, decreases the eddy diffusion factor, λ, increases. The value of A therefore depends upon the relative rates of change of d_p and λ with particle size.

Bohemen and Purnell (21) obtained A values by plotting HETP against the linear gas velocity u. They obtained negative values of A for packings in which d_p was small. These results can be explained by means of equation (xxxii). The finer the solid support the higher the pressure required to produce a given flow rate. This increase in pressure produces an increase in resistance to mass transfer in the gas phase. Hence, the combined resistence to mass transfer term, C', increases with a consequent decrease of the intercept of the asymptote with the HETP coordinate, which represented the value of the eddy diffusion term in the van Deemter equation. Therefore, the method of Bohemen and Purnell is not a valid procedure for obtaining A. When average pressure is kept constant with a variation in linear velocity the eddy diffusion term is constant as has been shown in Figure 12.

Giddings (14) has derived a term corresponding to

the van Deemter A term which is dependent on velocity of the carrier gas and nature of the carrier gas. This term is given by equation (ix). This equation states that with an increase in size of the carrier gas molecules the value of A should decrease. Figure 13 shows the relation of A to diffusivity of solute in the carrier. This figure shows that A is independent of the nature of the carrier gas. It is also inherent in Gidding's equation for A, that A should vary with column temperature and average pressure. A as functions of temperature and pressure are given in Figures 11 and 12. It is shown by these three figures that eddy diffusion does not depend upon temperature, pressure and nature of the carrier gas. The invariance of the A term with diffusivity points out that resistance to mass transfer in the gas phase in the pores does not affect the eddy diffusion term measurably. It thus appears that the original van Deemter expression for A is adequate.

Longitudinal Gaseous Diffusion: The B Term

Longitudinal diffusion of solute molecules in the gas phase is reflected in the B term of the general equation (x xv). In this equation $B/\bar{P}$ is identical with the B factor of the original van Deemter equation. That is, $B = 2\gamma D_g$ where D_g is the diffusivity of the solute in the carrier and γ is a factor accounting for the tortuous flow path around the packing particles.

For a given packed column the variables of the B term are included in the diffusivity factor D_g. The equations of Gilliland and Hirschfelder (20) indicate that D_g varies with temperature to the three halves power. Hence the value of B should also vary with temperature to the three halves power. It has been reported by Dewet and Pretorius (17), with no obvious theoretical foundation, that B is a function of temperature to the first power. It would seem, however, that from the large amount of data used by Gilliland in the development of his equation, that the B term probably depends upon temperature to the three halves power. In an attempt to obtain the correct form of the dependence of B on temperature, the data in Figure 14 and 15 have been plotted. The values of B have been obtained from Tables 12, 27, 28, 29 and 30 of the Appendix. In Figure 14, B is in terms of temperature to the first power and in Figure 15 as a function of temperature to the three-halves power. It is interesting that both relations agree about equally well with the experimental results and it is not apparent which function of temperature is correct. The experimental data are therefore not conclusive.

Bohemen and Purnell (21) have pointed out that according to the van Deemter equation, different carrier gases affect only the B term, i.e. longitudinal diffusion. Hence, they have derived equation (xliv)

Figure 14

The Relation of the Longitudinal Diffusion Coefficient, B, to Temperature Using n-Pentane as Solute with 30% di-n-Decylphthalate Column and Helium as Carrier Gas.

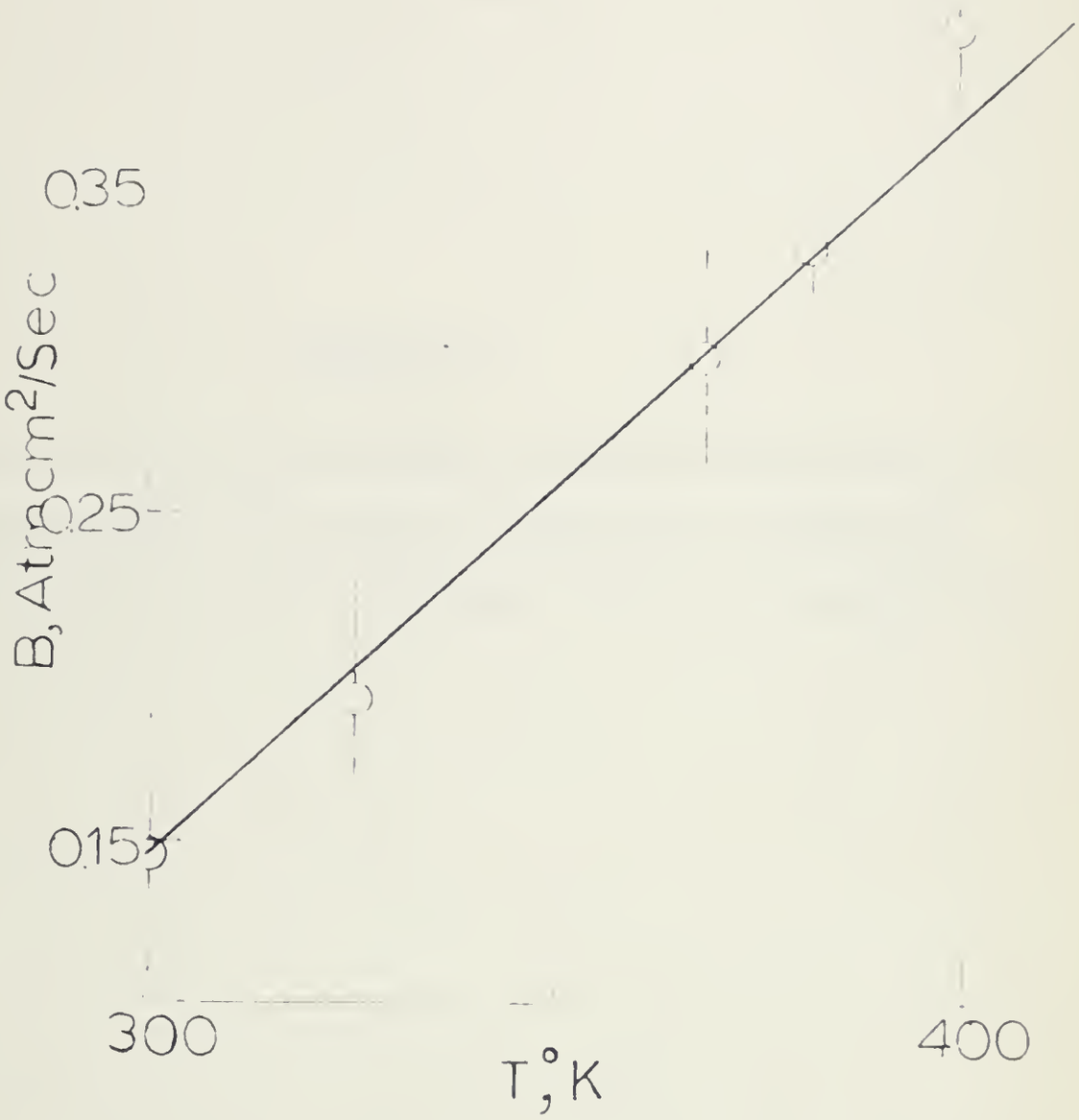
0.35
0.25
0.15
B, Atm cm²/Sec
300
400
T, °K

Figure 15

The Relation of the Longitudinal Diffusion Coefficient to Temperature to the Three-Halves Power with n-Pentane as Solute with 30% di-n-Decylphthalate Column as Carrier Gas.

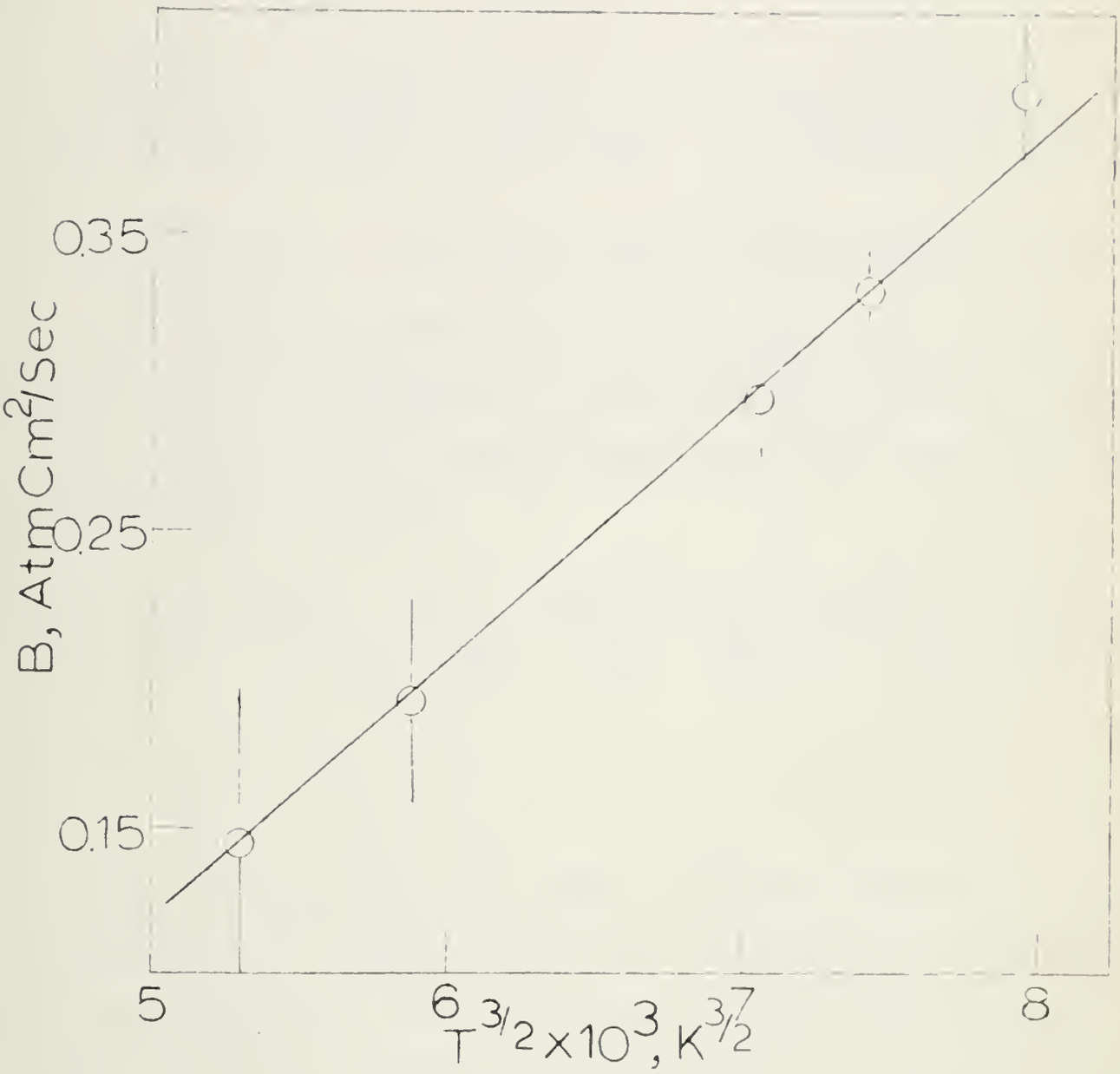
0.35
0.25
0.15
B, Atm Cm²/Sec
5
6
7
8
T^3/2 x 10^3, K^3/2

$$H_{H_2} - H_{N_2} = \frac{1}{u}\left(B_{H_2} - B_{N_2}\right) \qquad \text{(xLiv)}$$

in which the subscripts refer to the carrier gas used. According to this equation a plot of $H_{H_2} - H_{N_2}$ against 1/u should be a straight line of slope $B_{H_2} - B_{N_2}$. They obtained curved lines. If the proposed equation (xxxviii) is used, then equation (xLv) results for the difference in plate heights resulting from the use of two different carrier gases under the same conditions of pressure and velocity.

$$H_{H_2} - H_{N_2} = \frac{1}{u}\left(B_{H_2} - B_{N_2}\right) + u\left(E_{H_2} - E_{N_2}\right) + \overline{P}u\left(F'_{H_2} - F'_{N_2}\right) \qquad \text{(xLv)}$$

It can be seen from this equation that the difference in plate height does not result solely from differences in the longitudinal diffusion coefficients but also from differences in the resistances to mass transfer at the interface and in the gas phase. The resulting graph of $H_{H_2} - H_{N_2}$ vs 1/u would be curved as predicted by equation (xxxviii) and as reported by Bohemen and Purnell.

D Resistance to Mass Transfer in the Liquid Phase and the Gas-Liquid Interface: The C and E Term

Resistance to mass transfer in the liquid phase and at the gas-liquid interface are functions of the amount of liquid phase present. Hence they are discussed together.

In the general discussion it has been shown in Figures 7 and 9 that the intercept of C' vs $\bar{F}$ relations depend on the per cent liquid phase and the nature of the carrier gas. Figure 16 shows the intercepts as a function of the ratio of weight of liquid phase to weight of support with hydrogen as carrier gas. This figure has a small positive intercept on the C + E coordinate. This indicates that C and E are not related to the amount of liquid phase in the same sense. Martin (23) has shown that in the vicinity of 2 per cent of liquid there is an abrupt change in the rate of change of surface area with variation in per cent liquid. The variation of surface area with per cent liquid phase reported by Martin for the supports chromosorb and chromosorb W are shown in Figure 17. Since the interface term depends on surface area of liquid and since the surface area increases markedly in the 0 to 2 per cent region, the interface term E will change markedly in this region. Hence, Figure 16 should tend to have a positive intercept as shown, if the values of C + E with 4 to 30 per cent liquid are extrapolated back to zero per cent. It would be expected that if values of C + E for the 0 to 2 per cent range

Figure 16

Relation Between the Sum of the Interfacial and Liquid Phase Resistances to Mass Transfer, C + E, and the Ratio of Di-n-decylphthalate to Support, S/f, at 44°C with Hydrogen Carrier Gas and n-Pentane as Solute.

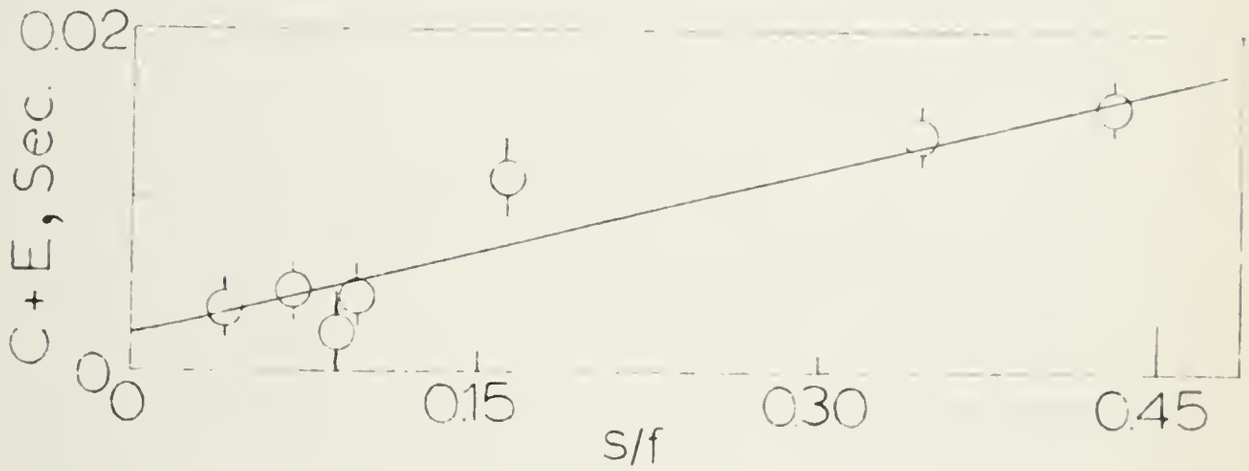
0.02
0
C + E, Sec.
0
0.15
0.30
0.45
s/f

Figure 17

Effect of Amount of Liquid Phase on Apparent Surface Area of the Liquid Phase, β,β' Thiodipropionitrile, on Chromosorb (Columnpak), and chromosorb W. (Martin (23)).

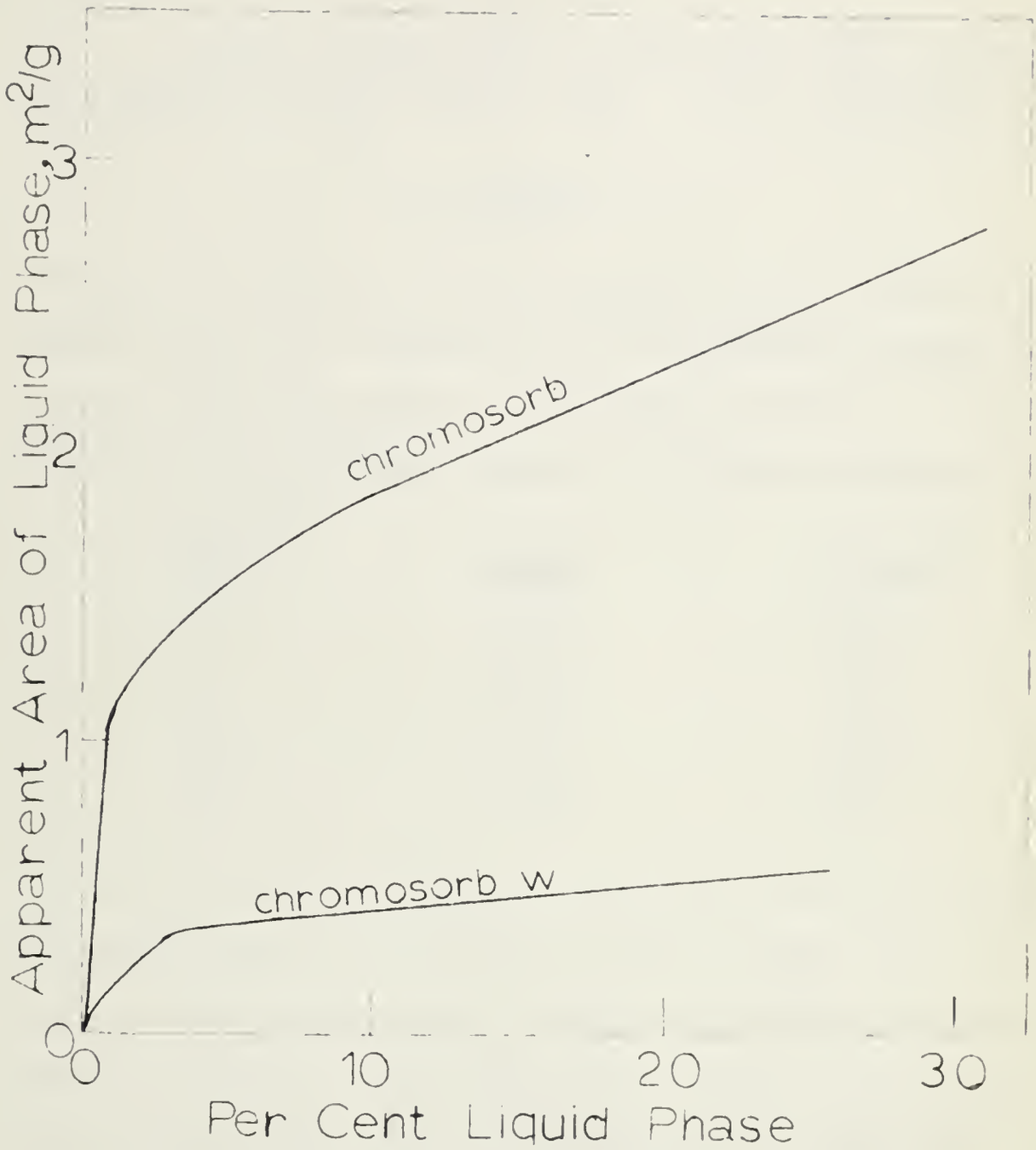
Apparent Area of Liquid Phase, m²/g
3
2
1
0
chromosorb
chromosorb w
0
10
20
30
Per Cent Liquid Phase

were extrapolated to zero then the plot would pass through the origin.

Table 3 shows that C + E increases with an increase in polarizability of the carrier gas. If this variation was due

TABLE 3

The Relation Between the Polarizability of the Carrier Gases and the Sum of the Coefficients of Resistance to Mass Transfer In the Liquid Phase and the Gas-Liquid Interface, C + E, for 6.7% Di-n-decylphthalate Column at 44°C and n-Pentane as Solute.

Carrier Gas	C + E Seconds	$\alpha \times 10^{25}$
H_2	0.0040	8.1
N_2	0.0098	17.4
CH_4	0.0115	25.8
CO_2	0.0205	26.5

to a modification of the nature of the liquid phase due to a change of the carrier gas, a change in distribution coefficient would be observed. The modification of the liquid phase would have to be brought about by differences in solubility of the carrier gases in the liquid phase. This in turn could bring about differences in solubility of the solute in the liquid phase with a consequent change in the distribution coefficient. Table 4 shows that no variation in the distribution coefficient

was observed with the various gases.

TABLE 4

Effect of Carrier Gas on the Distribution Coefficient in Gas-Liquid Chromatography Using 6.7% Di-n-decylphthalate Column at 44°C with n-Pentane as Solute.

Gas	Distribution Coefficient
H_2	135
N_2	135
CH_4	135
CO_2	135

Hence the variations obtained inthe sum of the resistances to mass transfer in the liquid phase and at the gas-liquid interface with different carrier gases are associated with a variation in the nature of the interface and not due to a modification of the liquid phase by the carrier gas.

It has been pointed out in the theoretical section that a plot of the coefficient of the combined resistances to mass transfer, C', against the reciprocal of the factor $\left(\frac{1}{M_1} + \frac{1}{M_2}\right)^{\frac{1}{2}} \Big/ \left(V_1^{\ 1/3} + V_2^{\ 1/3}\right)^2$, (D_g'), should intercept the C' coordinate at a value corresponding to the coefficient of resistance to mass transfer in the liquid phase. The combined

coefficient of resistance to mass transfer, C', is given by the sum of the coefficients for resistance to mass transfer in the liquid phase (C), resistance to mass transfer at the gas-liquid interface (E) and resistance to mass transfer in the gas phase at the prevailing pressure ($F'\bar{P}$). Hence, if F' is removed from C' then C E is obtained. Thus if C + E is plotted against the reciprocal of $\left(\frac{1}{M_1} + \frac{1}{M_2}\right)^{\frac{1}{2}} \Big/ \left(V_1^{1/3} + V_2^{1/3}\right)^2$ then this relation also should have an intercept on the C + E coordinate at a value corresponding to the resistance to mass transfer in the liquid phase C. This latter plot is given in Figure 18 for a 6.7 per cent di-n-decylphthalate column at 44°C. From such plots E is obtained from the slope. Knowing the value of E for one column it is possible to calculate the value of E and C for another column with the same substrate and a different percentage of liquid with two other pieces of information. These are the value of C + E for one carrier gas with this column and the ratio of surface areas of the liquid in the two columns.

The apparent area of the liquid phase has been plotted in Figure 17 as a function of per cent liquid (23). One can make estimates of the change in E with amount of liquid phase by means of this figure. Thus since E is a function of the surface area of liquid, the ratio of two areas obtained from Figure 17 gives the ratio of the corresponding E values. If one value of E is known the other can then be obtained by

Figure 18

Relation Between the Sum of the Coefficients of the Interfacial and Liquid Phase Resistances to Mass Transfer, C + E, and the Molecular Factors of Carrier Gas and n-Pentane Solute, $\left(V_1^{1/3} + V_2^{1/3}\right)^2 \Big/ \left(\frac{1}{M_1} + \frac{1}{M_2}\right)^{\frac{1}{2}}$.

● 30% di-n-decylphthalate column

◑ 14% di-n-decylphthalate column

○ 6.7% di-n-decylphthalate column

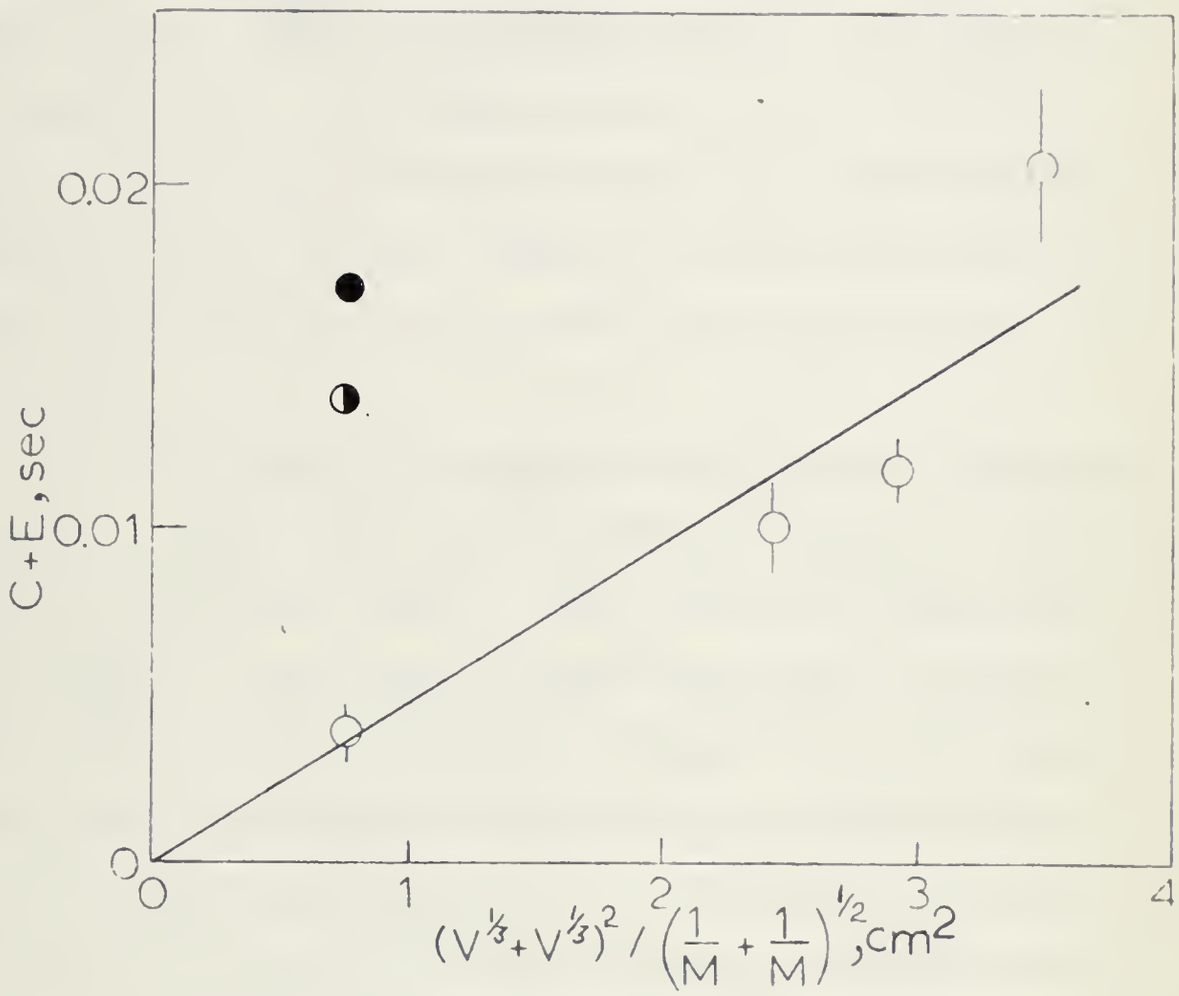
0.02
0.01
0
C+E, sec
0
1
2
3
4
$(V^{1/3}+V^{1/3})^2 / \left(\frac{1}{M}+\frac{1}{M}\right)^{1/2}$, cm^2

constructing a line of slope E through a value of C + E for a particular carrier gas. The coefficient C is given by the intercept with the C + E coordinate. It can be seen in Figure 17 that liquid surface area increases slightly with increasing liquid phase over the range studied. Hence, E should increase only slightly with increasing proportion of liquid in the data presented here. Two extra values of C + E for 14 and 30 per cent columns are included in Figure 18. Lines drawn through these points of slopes slightly greater than the one for 6.7 per cent would give C by their intercept with the C + E coordinate.

It should be kept in mind that the data presented in Figure 17 would give only approximate values of C and E. In order to determine true C and E values by this method the areas in Figure 17 must represent the true areas of the liquid phase. The true and apparent areas of liquid are not necessarily the same since the apparent area is equal to the surface area of the uncoated support minus the surface area of support after addition of liquid. The true area is dependent on how the liquid is retained in the pores and on the surface of the support particles.

The temperature dependence of resistance to mass transfer in the liquid phase is complex as the distribution coefficient and diffusivity are both affected. Fryer (40) has shown that the distribution coefficient factor $K'/(I+K')^2$ increases with temperature to a maximum where $K' + I$ and then falls. The temperature corresponding to the maximum is above that which

is normally used and therefore this factor may be considered as increasing with increasing temperature. Diffusivity in the liquid phase increases with temperature and hence tends to decrease the contribution of C to HETP. It would be expected that an increase in temperature would decrease the bonding forces between the liquid phase and the carrier gas molecules. Hence it is expected that E would decrease with increasing temperature. The decrease in E and increase of D_l with increasing temperature would perhaps result in a decrease of the sum C + E with increasing temperature.

The effect of temperature on the sum of the resistances to mass transfer at the gas-liquid interface and resistance to mass transfer in the liquid phase, C + E, is presented in Figure 19. It is seen that over the range of 24°C to 123°C there is a decrease in the sum C + E with an increase in temperature. Dewet and Pretorius (41) have found a similar relation. However, Dewet and Pretorius made no allowance for resistance to mass transfer in the gas phase. Fortunately, they considered data at low flow rates and with columns having relatively large amounts of liquid where the resistance to mass transfer in the gas phase would be small compared to the resistance to mass transfer in the liquid phase. Hence, the variation of resistance to mass transfer in the gas phase with temperature from their data would be insignificant compared to C + E. Their relation therefore agrees with that reported in this thesis. The effect of temperature on resistance to mass transfer in the gas phase is discussed in the next section.

Figure 19

Effect of Temperature on the Interface Resistance Plus Liquid Phase Resistance to Mass Transfer with 25% Di-n-decylphthalate Column and Hydrogen as Carrier Gas and n-Pentane as Solute.

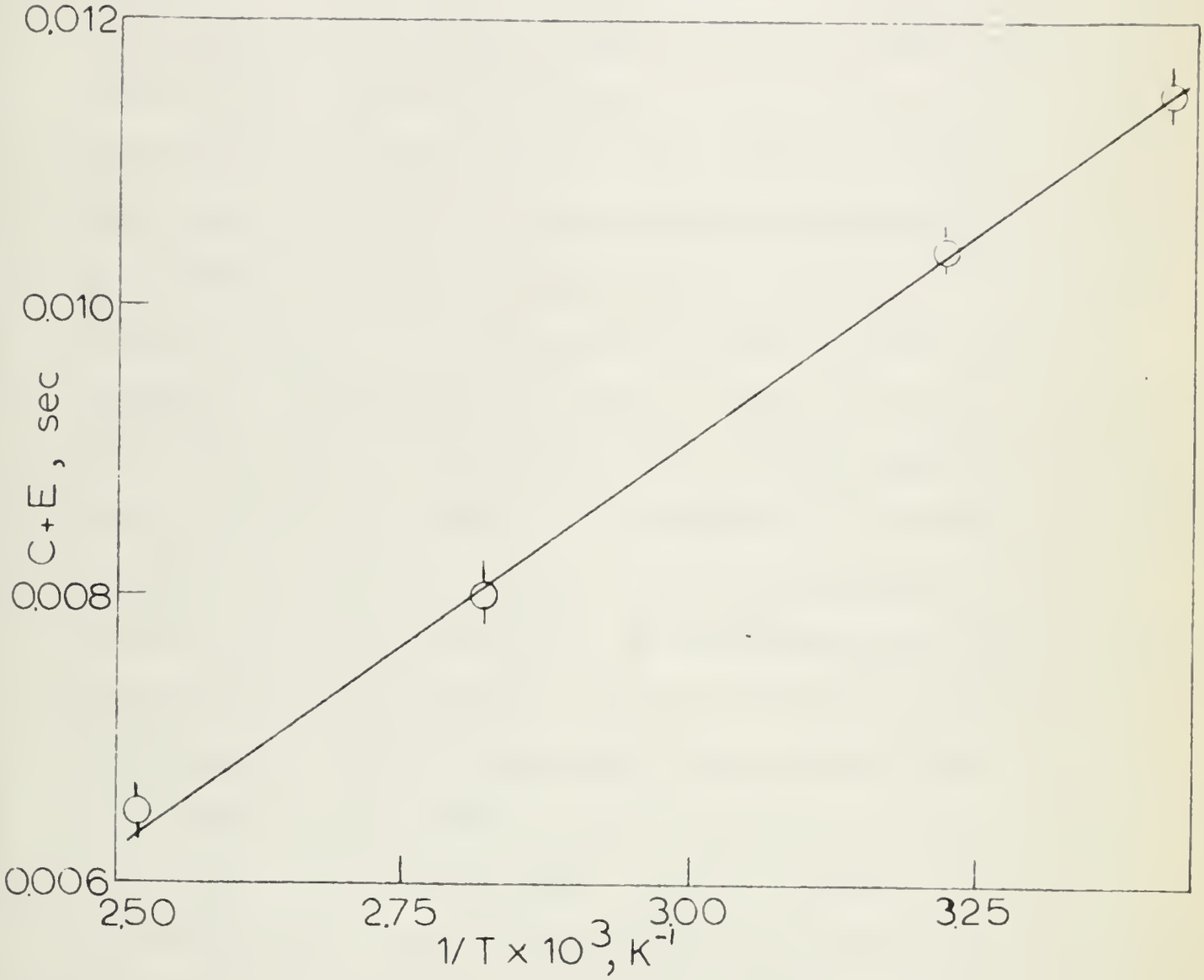
0.012
0.010
0.008
0.006
C+E, sec
2.50
2.75
3.00
3.25
1/T x 10^3, K^-1

E. Resistance to Mass Transfer in the Gas Phase: The F' Term

Resistance to mass transfer in the gas phase is reflected in the F' term of equation (xLiii). Van Deemter (12) assumed this term to be insignificant on the ground that the ratio of the diffusion time in the gas phase to the diffusion time in the liquid phase is only 10^{-5} to 10^{-7}. Hence, any appreciable resistance to mass transfer should be associated with the liquid phase. Such an assumption is erroneous as has been shown in Figure 9 in the general discussion. Figure 9 shows a variation in resistance to mass transfer with a variation in pressure and nature of the carrier gas. Even with a gas such as hydrogen, resistance to mass transfer in the gas phase can be appreciable. The existence of resistance to mass transfer in the gas phase has been experimentally shown very recently by Kieselbach (26). He considered resistance to mass transfer in the gas in the pores of the support particles as well as in the mobile gas phase. He concluded from his data that there is resistance to mass transfer in the gas phase. Furthermore, Kieselbach (26) obtained a variation in the F' term with liquid concentration which he interpreted as being due to a variation in the effective diffusional path length, d_m, and correspondingly influenced the value of F'. In Figure 8, F' is given as a function of the ratio of weight of liquid to weight of support. It can be seen there is no variation in F' with a variation in liquid concentration with a ten-fold

change of liquid phase. This is expected if the liquid phase is in the pores of the support. Furthermore, the thickness of liquid phase outside of the pores would be small relative to the size of the mobile gas channels. Hence, a change in liquid phase thickness over the range of percentage studied would bring about a relatively small change in size of the gas channels.

The effect of carrier gas on the combined resistance to mass transfer in the gas phase is depicted in Figure 20. As expected, the figure shows that resistance to mass transfer in the gas phase is inversely proportional to diffusivity. The large errors in the value of F' shown in this figure are due to the method of solution, i.e. any error in determining C' of equation (xxv) will be magnified in F' since F' is a second derivative.

The validity of incorporating velocity profile effects into the resistance to mass transfer in the gas phase term F' as suggested by Jones (13) is difficult to prove. The combined resistance to mass transfer in the gas phase term is considered to be made up of three terms, involving resistance to mass transfer associated with the mobile gas phase and the relatively non-mobile or stagnant phase as given by equation (xxix). If F' is considered to be made up of three terms related to velocity profile, then F' should depend upon viscosity of the carrier gas. If the thickness of these two gas phases is independent of the carrier gas then the concentrations at a cross section of the

Figure 20

Relation Between the Coefficient of Resistance to Mass Transfer in the Gas Phase, F', and the Diffusivity Function of the Carrier Gas and Solute with a 6.7% Di-n-decylphthalate Column at 44°C.

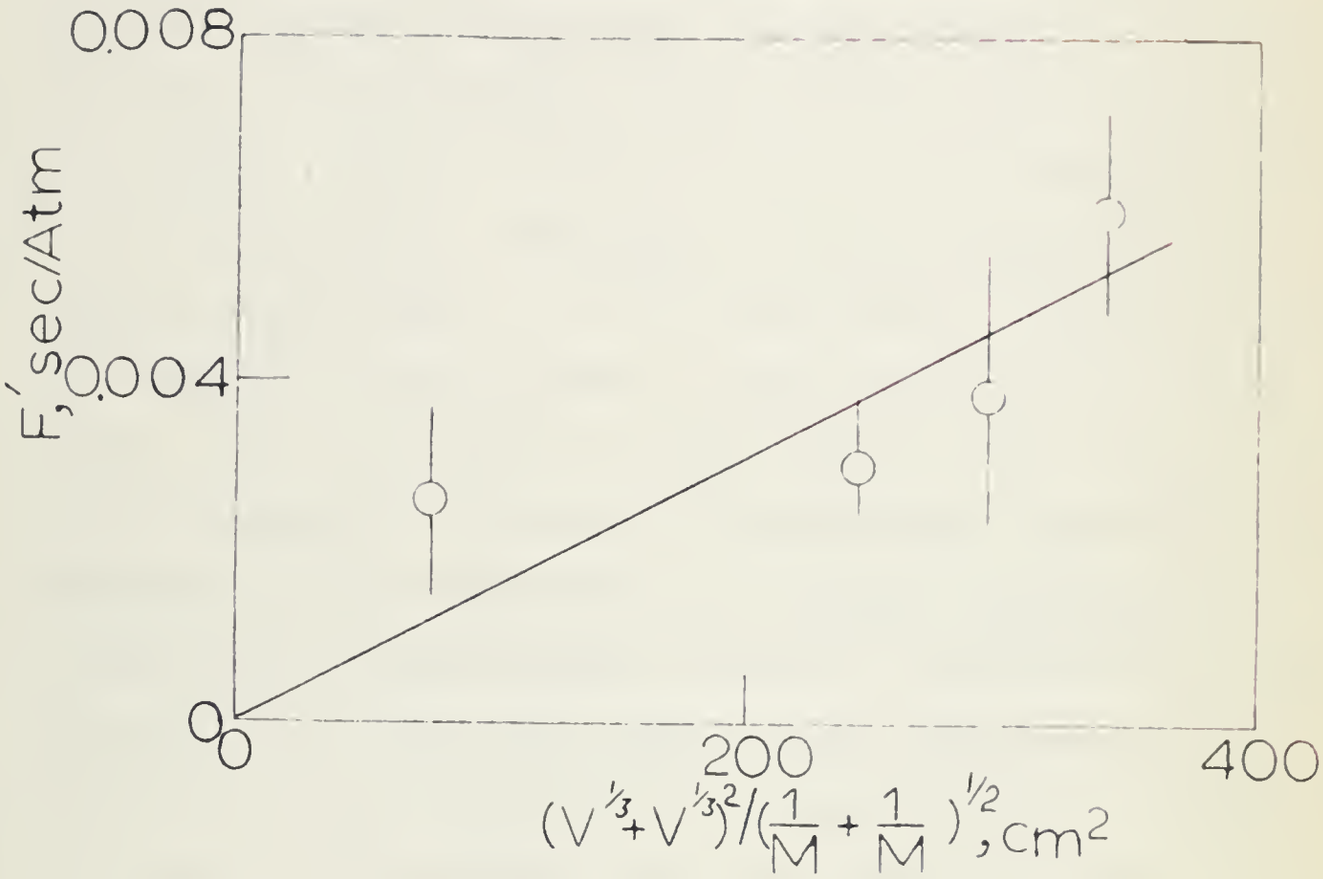
0.008
0.004
0
F', sec/Atm
0
200
400
$(V^{1/3}+V^{1/3})^2/(\frac{1}{M}+\frac{1}{M})^{1/2}$, cm²

column will be dependent on the viscosity of the carrier gas. Since the velocity at any point in a moving gas stream relative to the velocity perpendicular to the centre of the stream is inversely proportional to gas viscosity, it follows that with a high viscosity gas the central portion will move more rapidly relative to the portion near the walls than with a low viscosity gas. Therefore, F' will be larger with the higher viscosity gas. If on the other hand a certain velocity is considered as the boundary of the stagnant and the mobile phases, then the thickness of the stagnant phase will increase with an increase in viscosity of carrier gas. Therefore the resistance to mass transfer in the stagnant gas phase will increase with a corresponding decrease in resistance to mass transfer in the mobile gas phase. Since the effect of viscosity on the velocity profile of these two terms is unknown it is possible to determine the contribution of each.

The variation of F' with carrier gas viscosity is shown in Figure 21. It is apparent from this figure that viscosity is a variable in determining HETP in gas-liquid chromatography. Since F' increases with viscosity it would indicate that either resistances in both the stagnant and moving gas phases increase with viscosity of carrier gas or that one increases more rapidly than the other decreases.

The idea of division of the carrier gas portion of the column into two phases can be carried further. Thus we

can visualize a large number of small divisions or even more realistically consider the gas phase as one term in which allowance is made for the continuous variation in velocity by means of viscosity. Hence, the resistence to mass transfer in the gas phase could possibly best be accounted for in one single term.

The effect of temperature on resistance to mass transfer in the gas phase, F', is readily seen from a consideration of the coefficients $\frac{K'^2}{(1 + K')^2} \frac{d^2_m}{D_g}$ of equation (v). Any change of temperature will have little effect on $\frac{K'^2}{(1 + K')^2}$ as the values of K' are usually large so that $\frac{K'^2}{(1 + K')^2}$ will usually be about one. Hence, any change in temperature will affect the F' term primarily through its effect on D_g. Since D_g is a function of temperature to the three-halves power then F' should be inversely proportional to the temperature to the three-halves power. In Figure 22 it is shown that the experimental data agree with the expectation.

Bohemen and Purnell (21) have pointed out that resistance to mass transfer is a function of support particle size. They pointed out that the more uniform the particle size the greater is the column efficiency. This enhanced efficiency is brought about by the effect of particle size on channel size. With a wide range of particle sizes the channels formed by the large particles are filled with the

Figure 21

Relation Between the Combined Resistance to Mass Transfer in the Gas Phase (F') and viscosity of carrier gas (η). with a 6.7% Di-n-decylphthalate Column at 44°C.

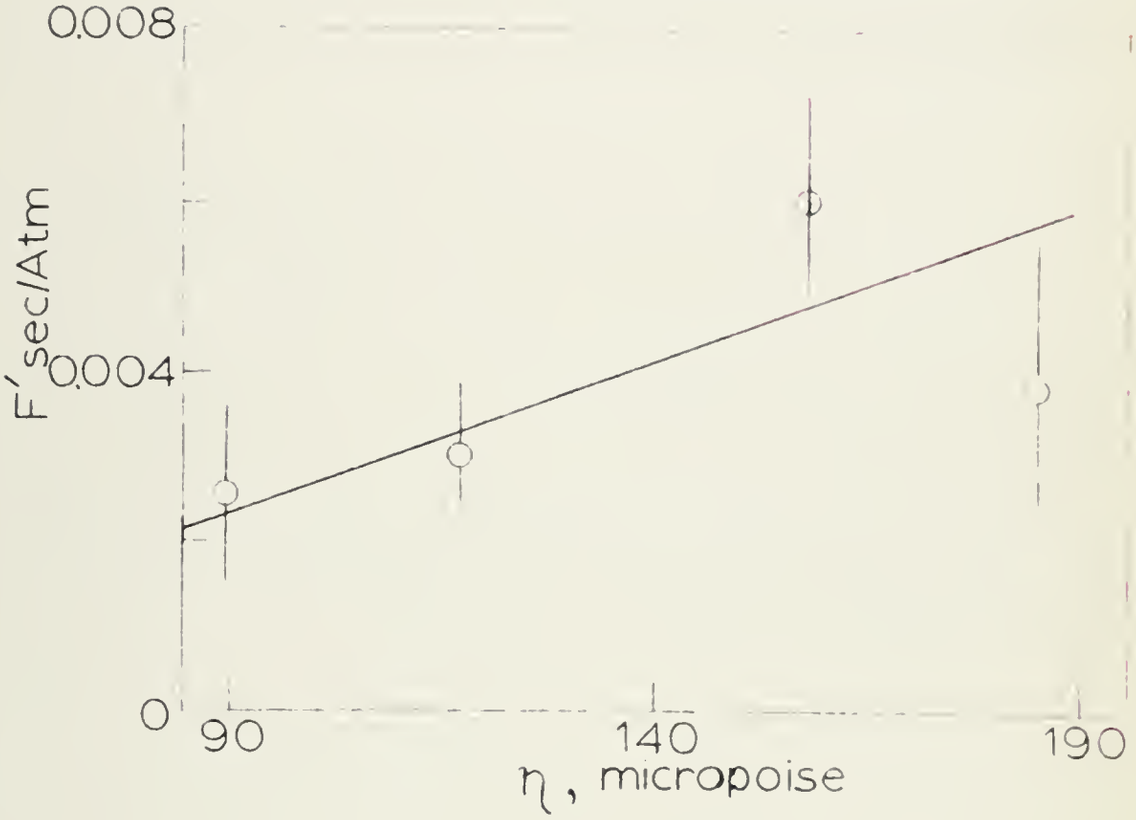
0.008
0.004
0
F′ sec/Atm
90
140
190
η, micropoise

Figure 22

Effect of Temperature on Combined Resistance to Mass Transfer in the Gas Phase (F') with 25% Di-n-decylphthalate Column and Hydrogen Carrier.

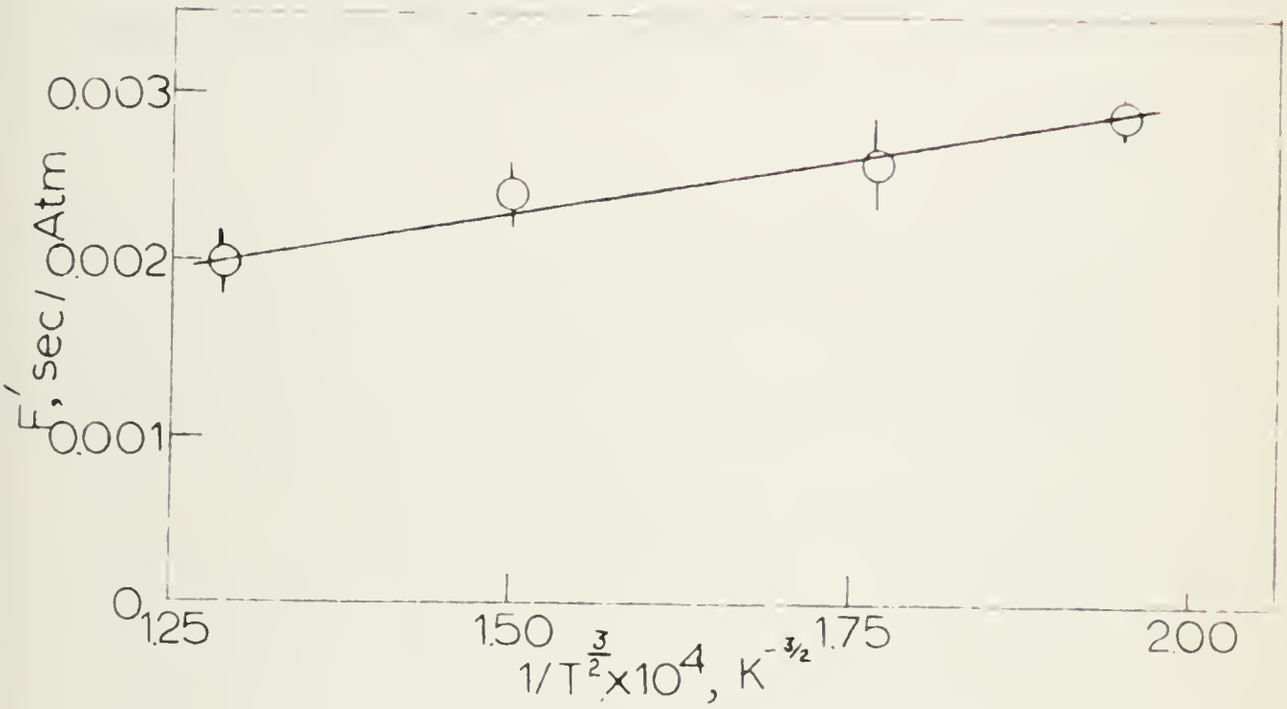
0.003
0.002
0.001
0
F', sec / Atm
1.25
1.50
1.75
2.00
1/T^{3/2} x 10^4, K^{-3/2}

small particles creating smaller effective channels. Small channels are also brought about by using small support particles. In both cases the effect is the same, that is, an increase in pressure for a given flow rate with a corresponding increase in resistance to mass transfer in the gas phase. Thus the enhanced efficiency brought about by uniform particle size of support can be understood.

F. Summary

It has been concluded in the foregoing sections that a simplified rate equation relating HETP with linear velocity and pressure in gas-liquid chromatography is of the form

$$H = A + \frac{B}{\overline{P}u} + Cu + Eu + F'\overline{P}u \qquad (x \llcorner vi)$$

This equation contains two of the terms proposed by Khan (16) in addition to those proposed by van Deemter et al (12). These two terms are the E and F' terms accounting for resistance to mass transfer at the gas-liquid interface and in the mobile gas phase respectively.

Confirmation of the gas-liquid interface resistance to mass transfer term has been obtained from the pressure independent variation in resistance to mass transfer with a variation in carrier gas. The necessity of including this term has also been substantiated by showing that carrier gas does not affect the distribution coefficient and that this term can be related to the polarizability of the carrier gas.

The evidence for a term accounting for resistance to mass transfer in the gas phase consists of variations in the combined resistance to mass transfer term which are pressure dependent and also depend on the nature of the carrier gas. It has been shown that the gas phase term F' is related

to the reciprocal of the diffusivity of solute in the carrier gases. The components of F' have not been conclusively defined although the effect of velocity profile has been indicated by relating F' to carrier gas viscosity. As the velocity profile is continuous across the flowing gas channels the total effect of the gas phase could possibly best be accounted for in one single term as in the equation given.

The validity of the proposed equation is substantiated by virtue of being able to account for phenomena observed by other workers as well as the phenomena observed in the data of this thesis. Thus by means of this equation the observation of negative eddy diffusion values, curvature in $H_{H_2} - H_{N_2}$ vs $\frac{1}{u}$ relations and the change in slope of H vs u relations in the range of velocities where resistance to mass transfer is important, by Bohemen and Purnell (21) are explicable. These variations can be accounted for by the increased resistance to mass transfer in the gas phase with increasing pressure. The effect of increasing pressure and resistance to mass transfer in the gas phase was not considered by these workers.

It has also been shown that stagnant gas in the pores of the packing has no effect on the eddy diffusion term or on HETP in general. This conclusion is based on the observation that eddy diffusion is independent of pressure and nature of the carrier gas and that the gas phase resistance

term is independent of the per cent liquid phase.

The values of the coefficient for a 6.7% di-n-decylphthalate column at 44°C are given in the following equation for n-pentane solute and hydrogen as carrier gas.

$$H = 0.11 + \frac{0.34}{\overline{P}u} + 0.001u + 0.004u + 0.003\overline{P}u \qquad \text{(xLvii)}$$

It can be seen from the relative size of these coefficients that gas phase resistance cannot be ignored. It is also evident that the gas-liquid interface term is of sufficient value to have a marked effect on HETP with carrier gas variation as well as per cent substrate variation. The value of C + E for the 30 per cent liquid phase column with hydrogen as carrier gas was 0.015. Half of this value is due to the interface resistance to mass transfer. Hence, even with high per cent liquid phase the interface term is an appreciable portion of resistance to mass transfer.

Each term of the proposed equation has been examined for temperature effects. These studies yield an equation of the form

$$H = A + \frac{B''T^{3/2}}{\overline{P}u} + \frac{C''u}{T} + \frac{E''u}{T} + \frac{F''\,\overline{P}u}{T^{3/2}} \qquad \text{(xLviii)}$$

where $B'' = \frac{B}{T^{3/2}}$, $C'' = CT$ and $E'' = ET$ and $F'' = F'T^{3/2}$. In these relations the temperature is expressed in degrees absolute and the coefficients A, B, C, E and F' are as previously defined. The variation in efficiency with temperature is thus seen to be due to competition between the variation in the longitudinal diffusion term and the resistance to mass transfer terms. It is expected, because of the relative sizes of the longitudinal diffusion term and the sum of the resistance to mass transfer terms, that longitudinal diffusion has the greatest effect. Hence, the poor separations at high temperatures is understandable. The effect of temperature on HETP is predominantly influenced by longitudinal diffusion in the gas phase from 4.3 to 30 per cent liquid phase.

IV. BIBLIOGRAPHY

1. M. Tswett, Ber. deut. botan. Ges. 24, 316, 384 (1906).
2. R. Kuhn, O. Winterstein and E. Lederer, Hoppe-Seyler's Z. Physiol. Chem. 197, 141 (1931).
3. N. C. Turner, Petroleum Refiner 22, 140 (1943).
4. A. J. P. Martin and R. L. M. Synge, Biochem. J. 35, 1358 (1941).
5. A. T. James and A. J. P. Martin, Biochem. J. 50, 679 (1952).
6. C. B. Euston and A. J. Martin, C. and EN 39, 46 (1961).
7. C. Phillips, "Gas Chromatography", Butterworths Scientific Publication, London, 1956.
8. A. I. M. Keulemans, "Gas Chromatography", Reinhold Publishing Corp., New York, 1957.
9. R. L. Pecsok, "Principles and Practice of Gas Chromatography", John Wiley, New York, 1959.
10. R. Kaiser, "Gas-Chromatographie ", Akadermische Verlagsgesellschaft Geist und Portig K.- G., Leipzig, 1960.
11. E. Boyer, "Gas Chromatography", Elsevier Publishing Co., Amsterdam, 1961.
12. J. J. van Deemter, F. J. Zuiderweg and A. Klinkenberg, Chem. Eng. Sci. 5, 271 (1956).
13. W. L. Jones, Anal. Chem. 33, 829 (1961).
14. J. C. Giddings, Nature, 184, 357 (1959).
15. J. C. Giddings, S. L. Seagar, L. R. Stucki and G. H. Stewart, Anal. Chem. 32. 867 (1960).

16. M. A. Khan, Nature 186, 800 (1960).

17. W. W. Brandt, Anal. Chem., 33, 23A July (1961).

18. W. J. Moore, "Physical Chemistry" p. 175, 2nd Edition, Prentice-Hall, Inc., 1955.

19. H. S. Taylor and S. Glasstone, "Treatise on Physical Chemistry Vol. II, 294, D. van Nostrand Co. Inc., New York, 1951.

20. R. C. Reid and T. K. Sherwood, "The Properties of Gases and Liquids", p. 268, McGraw-Hill Book Co. Inc., New York, 1958.

21. J. Bohemen and J. H. Purnell, "Gas Chromatography", p. 6, Edited by D. H. Desty, Academic Press, Inc., 1958.

22. E. R. Gilliland, Ind. Eng. Chem. 26, 681 (1934).

23. R. L. Martin, Anal. Chem. 33, 347 (1961).

24. H. S. Taylor and S. Glasstone, "Treatise on Physical Chemistry" Vol II, p. 297, D. van Nostrand Co. Inc., New York, 1951 .

25. R. Kieselbach, Anal. Chem. 32, 880 (1960).

26. R. Kieselbach, Anal. Chem. 33, 23 (1961).

27. "International Critical Tables" Vol. V, p.1, Editor-in-Chief, E. W. Washburn, McGraw-Hill Book Co., 1929.

28. C. P. Smythe, "Dielectric Behavior and Structure", p. 415, McGraw-Hill Book Co. Inc., New York, 1955.

29. O. A. Houghen and K. M. Watson, "Chemical Process Principles", Part III, p. 988, 2nd Edition, John Wiley and Sons, Inc., New York, 1954.

30. J. W. Mellor, "A Comprehensive Treatise on Inorganic and Theoretical Chemistry", VII, 916, Longman, Green and Co. Ltd., 1927.

31. J. W. Johnson, Jr. and F. H. Stross, Anal. Chem. 31, 357 (1959).

32. N. H. Ray, J. App. Chem. 4, 82 (1954).

33. D. H. Litchenfels, S. A. Fleck, F. H. Burrow and N. D. Coggeshell, Anal. Chem. 28, 1376 (1956).

34. R. E. Davis and R. A. Schreiber, "Advances in Gas Chromatography", D-91 Joint Symposium, New York, Sept., 1957.

35. R. J. Kokes, H. Tobin and Emmett, P. H., J. Am. Chem. Soc. 77, 5860 (1955).

36. W. E. Harris and W. H. McFadden, Anal. Chem. 31, 114 (1959).

37. R. L. Martin, Anal Chem. 32, 336 (1960)

38. E. R. Adlard and B.T. Whitham,"International Gas Chromatography Symposium" 243, Michigan State University, 1961.

39. Dewet, W. J. and Pretorius, V., Anal. Chem. 30, 325 (1958).

40. Fryer, J. F., "Resolution in Programmed Temperature Gas Chromatography", p. 16, Thesis, University of Alberta.

APPENDIX I

Calculations

Graphical methods of solution were used throughout this thesis to determine the various coefficients. The following is an example. The data in Table 5 is for a 25% di-n-decylphthalate column with hydrogen carrier and n-pentane as solute at 44°C. HETP (H) values in centimeters were calculated using equation (x L ix). In this equation L is the

$$H = \frac{L}{N} \qquad (x\ L\ ix)$$

length of column in centimeters and N is the number of theoretical plates calculated by equation (ii). To calculate N by equation (ii), V_R and W were expressed in minutes. Average pressures, $\overline{P}$, were calculated using equation (xxxvi) for inlet to outlet pressure ratios greater than 1.5. For smaller ratios the approximate equation (xxxvii) was used since no appreciable error is involved. Linear velocity of carrier gas was calculated from the retention time of the air peak and column length by equation (L). In this equation t_a is

$$u = \frac{L}{t_a} \qquad (L)$$

the retention time of air in seconds and L is the length of column in centimeters. This relation is based on the assumption that air is not retained by the liquid phase. In the

TABLE 5

HETP - Velocity-Pressure Data for 25% W/W Di-n-decylphthalate Column with Hydrogen Carrier and n-Pentane Solute at 44°C.

Peak	V_R min	W min	P_i atm	P_o atm	$\bar{P}$ atm	u cm/sec	H cm	H-B/$\bar{P}$u cm
Air	0.105		4.62	3.18	3.90	40.7		
n-pentane	1.205	0.285					0.894	0.892
Air	0.105					40.7		
n-pentane	1.200	0.270					0.811	0.811
Air	0.195		4.28	3.49	3.89	21.9		
n-pentane	2.132	0.430					0.654	0.649
Air	0.185					23.1		
n-pentane	2.110	0.415					0.620	0.615
Air	0.682		3.99	3.78	3.89	6.27		
n-pentane	7.755	0.872					0.202	0.186
Air	0.689					6.21		
n-pentane	7.745	0.882					0.208	0.192
Air	0.105		3.82	2.39	3.16	40.7		
n-pentane	1.240	0.295					0.906	0.906
Air	0.105					40.7		
n-pentane	1.240	0.300					0.938	0.938
Air	0.165		3.54	2.68	3.11	25.9		
n-pentane	1.970	0.370					0.562	0.557
Air	0.161					26.6		
n-pentane	1.955	0.370					0.575	0.570
Air	0.308		3.37	2.89	3.13	13.9		
n-pentane	3.511	0.535					0.372	0.363
Air	0.315					13.6		
n-pentane	3.490	0.515					0.348	0.339
Air	0.120		2.88	1.60	2.28	35.6		
n-pentane	1.268	0.270					0.726	0.721
Air	0.120					35.6		
n-pentane	1.275	0.265					0.692	0.687

TABLE 5

(continued)

Peak	V_R min	W min	P_i atm	P_o atm	$\overline{P}$ atm	u cm/sec	H cm	H-B/$\overline{P}$u cm
Air	0.145		2.76	1.60	2.21	29.5		
n-pentane	1.535	0.310					0.654	0.649
Air	0.145					29.5		
n-pentane	1.545	0.300					0.611	0.606
Air	0.470		2.38	2.04	2.21	9.10		
n-pentane	5.482	0.700					0.210	0.191
Air	0.465					9.20		
n-pentane	5.480	0.645					0.220	0.201
Air	0.240		2.54	1.93	1.84	17.8		
n-pentane	2.705	0.415					0.377	0.364
Air	0.245					17.5		
n-pentane	2.720	0.430					0.400	0.386
Air	0.155		2.04	1.14	1.59	27.6		
n-pentane	1.825	0.330					0.524	0.516
Air	0.160					26.7		
n-pentane	1.825	0.300					0.432	0.424
Air	0.230		1.90	1.28	1.59	18.6		
n-pentane	2.610	0.400					0.476	0.362
Air	0.235					18.2		
n-pentane	2.610	0.391					0.360	0.346
Air	0.380		1.76	1.38	1.57	11.3		
n-pentane	4.270	0.530					0.246	0.224
Air	0.375					11.4		
n-pentane	4.255	0.525					0.244	0.222

case of nitrogen as carrier gas, helium was used to give a peak corresponding to an air peak with other carrier gases.

The data in Table 5 were used to evaluate the coefficients of the various resistance to mass transfer terms. Before evaluation of the coefficient of the combined resistance to mass transfer, C', it was necessary to remove the effect of longitudinal diffusion in the gas phase. This was done to obtain straight line relationships of HETP and velocity. The values of the eddy diffusion term are given by the intercept of these lines with the HETP coordinate. Resistance to mass transfer in the gas phase, F', and the sum of the resistances to mass transfer in the liquid phase and at the gas-liquid interface were obtained from plots of C' vs $\overline{P}$.

Values of the coefficient of the longitudinal diffusion term, (B), were found by determining the slope of H vs $1/\overline{P}u$ plots. The slope of the best straight line representing these points was taken as the value of B. The probable error in these values were determined in the same manner as described for determining the probable error in C'. Figure 23 is a plot of H vs $1/\overline{P}u$ for a 30% di-n-decylphthalate column with hydrogen carrier and n-pentane as solute. The data for this figure are taken from Table 10.

In Table 5 the value of B at 44°C was calculated from the value of B at 126°C by means of relation (Li). The

Figure 23

Relation of HETP to the Reciprocal of the Product of Velocity and Average Column Pressure for a 30% W/W Di-n-decylphthalate Column at 126°C with Hydrogen As Carrier Gas and n-Pentane as Solute.

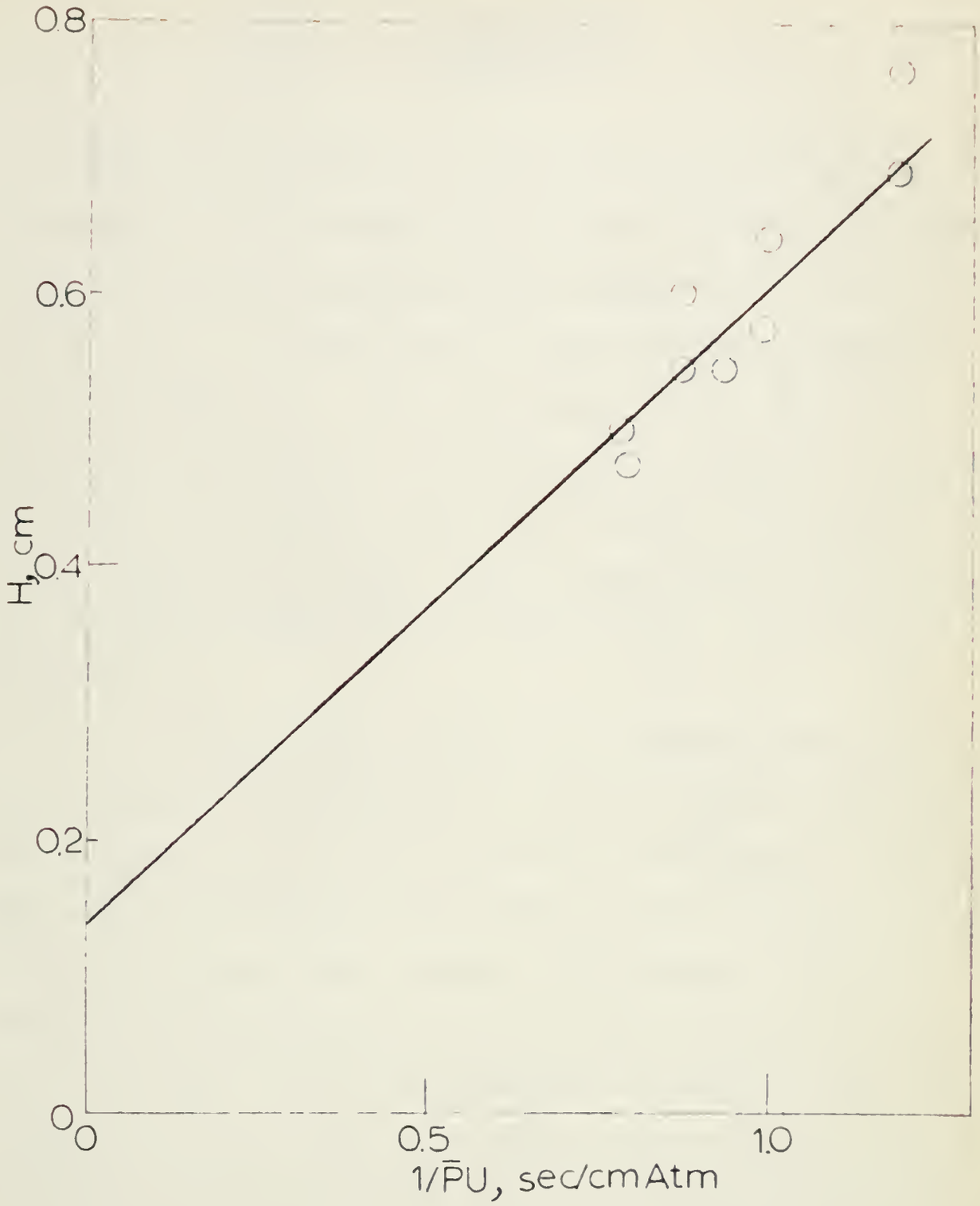
0.8
0.6
0.4
0.2
0
H, cm
0
0.5
1.0
1/P̄U, sec/cm Atm

value of B

$$\frac{B_{126°C}}{B_{44°C}} = \frac{(126+273)^{3/2}}{(44+273)^{3/2}} \qquad \text{(Li)}$$

at 126°C was determined by the method given in the following paragraph. Relation (Li) follows from the Gilliland equation (xxxiv) relating diffusivity and temperature. The calculated value of B at 44°C was used in constructing the nomograph given in Figure 24. This nomograph relates $\frac{B}{\overline{P}u}$ to $\overline{P}u$. Hence from the product of $\overline{P}u$ the value of $\frac{B}{\overline{P}u}$ can be obtained directly. The value of HETP due to eddy diffusion and combined resistance to mass transfer was given by the difference in the measured HETP and the value of $\frac{B}{\overline{P}u}$, i.e. H- $\frac{B}{\overline{P}u}$ of Table 5.

It has been pointed out by Johnson and Stross (31) that detector volume can have a marked effect on peak widths. The relative size of this effect was evaluated by determining the effective volume of the detector and comparing it with the gas volume of the columns. The detector volume was determined by measuring the retention volume of an air peak from the inlet side of the apparatus through a steel capillary column of known volume (0.33 cm^3) to the detector. The detector volume (0.87 cm^3) was given by the difference of the retention volume and volume of the capillary tube. Comparing the effective volume of the detector with the

Figure 24

Nomograph Relating the Longitudinal Diffusion Contribution to HETP to the Product of Pressure and Velocities of n-Pentane with Hydrogen as Carrier Gas at 44°C.

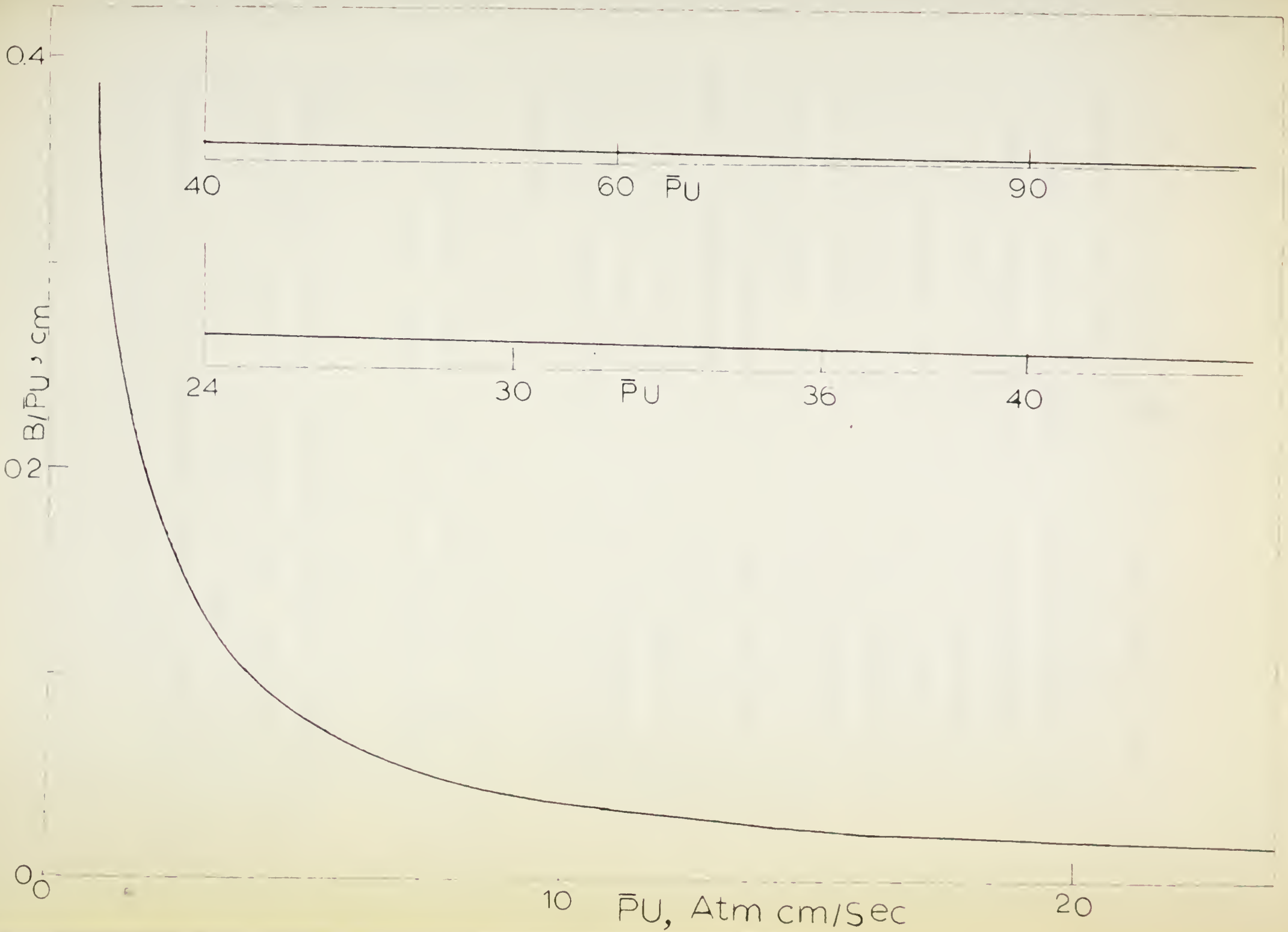
0.4
0.2
0
B/PU, cm
40
60
PU
90
24
30
PU
36
40
0
10
PU, Atm cm/sec
20

volumes of the columns (Ca 14 cm^3) shows that the effective detector volume accounts for approximately 6% of the total gas volume. Since the detector volume contributes to HETP by means of longitudinal diffusion in the gas phase, i.e. the B term of the proposed equation, then the effect of detector volume can be estimated from the diffusivity of solute in the carrier gas. The Gilliland equation (xxxiv) gives 0.317 cm^2/sec as the diffusivity of n-pentane in hydrogen at 150°C. Thus at a linear velocity of 10 cm/sec, 1 atmosphere pressure and 150°C the total contribution to HETP by longitudinal diffusion is 0.032 cm. Six per cent of this is due to the detector volume, i.e. 0.002 cm. Since this is within the limit of variation of the measured HETP values, the effect of detector volume has been considered negligible.

The values of the eddy diffusion term, A, were given by the intercept with the HETP coordinate of $H - \frac{B}{\bar{P}u}$ vs u and H vs $\frac{1}{\bar{P}u}$ plots. Examples of values obtained are given in Figures 11, 12 and 13. It has been shown in the section "Results and Discussion" that eddy diffusion is independent of temperature, pressure and carrier gas. Hence for any one column A is constant. The median of a group of A values determined by the above-mentioned method thus provides a fixed point involving graphs of H vs u or H vs $\frac{1}{\bar{P}u}$.

The combined resistance to mass transfer coefficients C', were obtained from plots of $H - \frac{B}{\overline{P}u}$ vs u. These relations are given in Figure 25. The median of the A values for this column is the fixed point on the H coordinate. The coefficients C' for the average pressures are given by the slopes of the lines of Figure 25. The probable errors in the coefficients of this figure were estimated by the slopes of lines which differed as much as possible from the chosen lines and which still could represent the data reasonably well. There probable errors are indicated in Figure 26 by the length of a bar drawn through the values of C'.

The value of the coefficient of the resistance to mass transfer in the gas phase was obtained from the slope of the plot of C' vs $\overline{P}$ in Figure 26. The error was estimated in the same manner used for estimating error in C'.

Figure 25

Relation Between HETP Corrected for Longitudinal Diffusion and Linear Gas Velocity for 25% Di-n-decylphthalate Column at 44°C and Hydrogen Carrier Gas at Various Average Pressures.

1. ● 3.89 atm.
2. ◑ 3.13 atm.
3. ◓ 2.21 atm.
4. ◒ 1.84 atm.
5. ○ 1.59 atm.

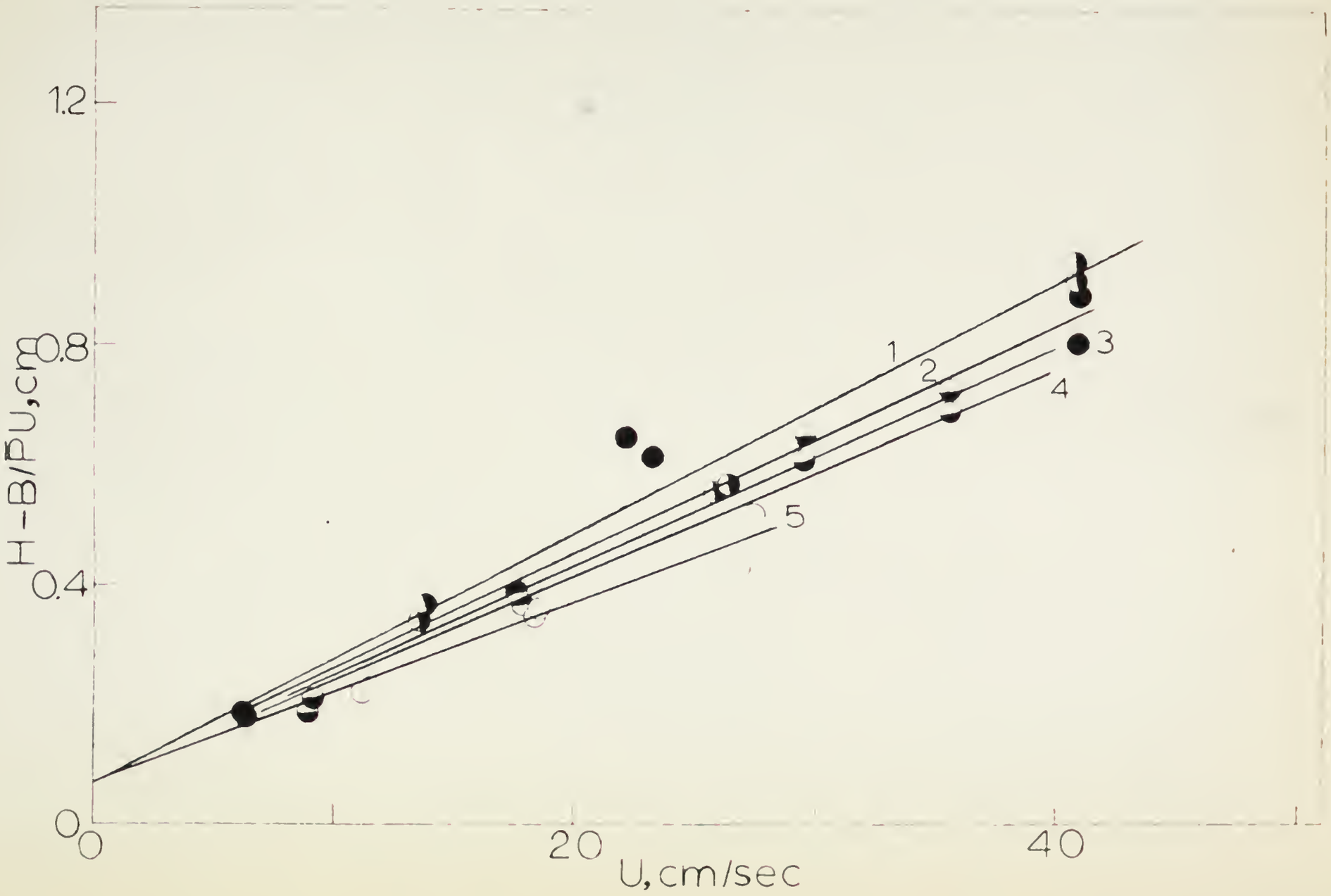
1.2
0.8
0.4
0
H - B/PU, cm
0
20
40
U, cm/sec
1
2
3
4
5

Figure 26

Relation Between the Combined Resistance to Mass Transfer Term (C') and Average Column Pressures for 25% Di-n-decylphthalate Column at 44°C and Hydrogen Carrier Gas and n-Pentane as Solute.

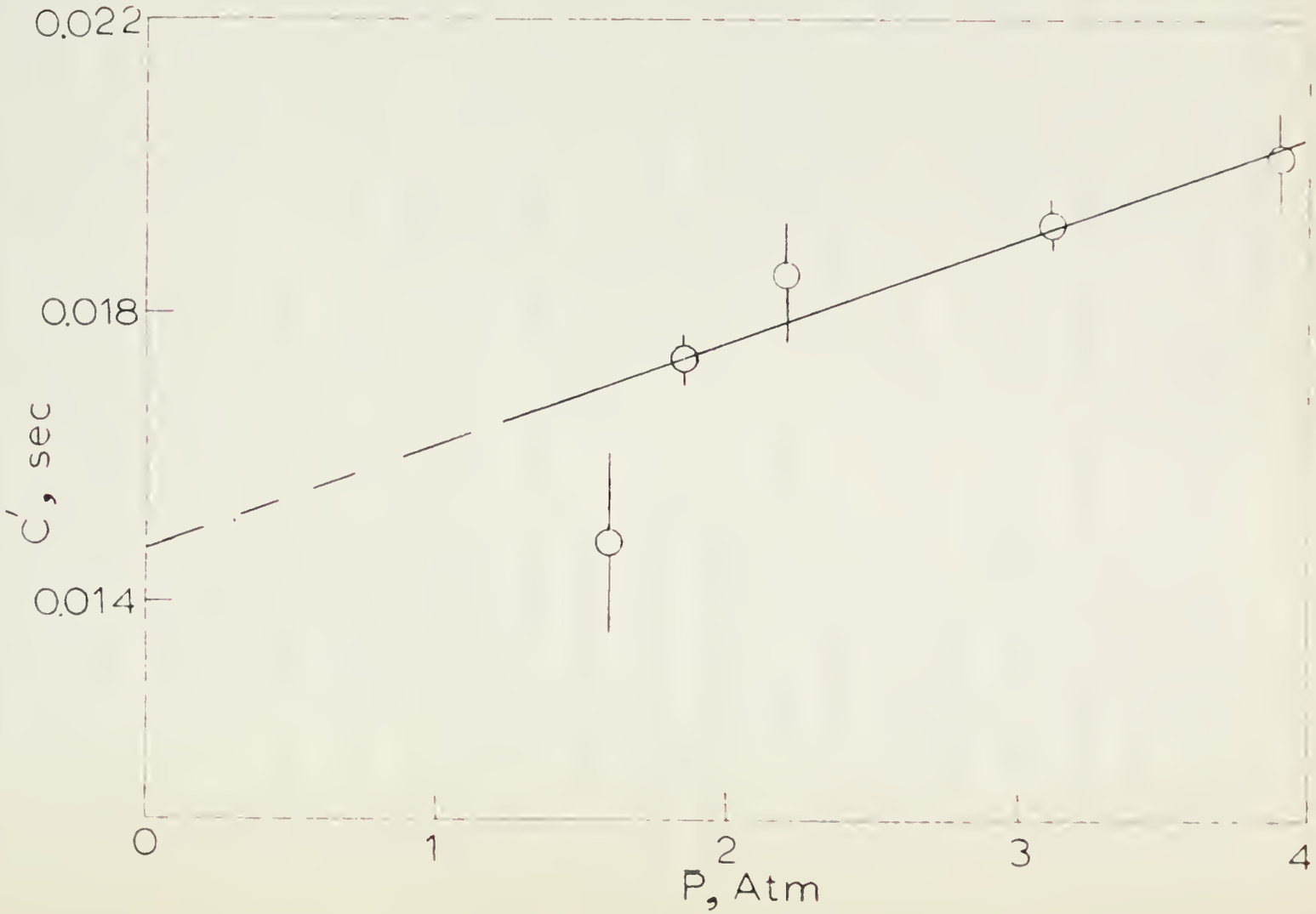
0.022
0.018
0.014
C', sec
0
1
2
3
4
P, Atm

VI. APPENDIX II

Subtractive Techniques

Since 1955 there has been active development of techniques for the separation of materials having similar boiling points and chemical characteristics which are not ordinarily separable by gas chromatography. Use of a combination of gas-solid and gas-liquid chromatography for the analysis of low boiling hydrocarbons was suggested by Ray (32). He used activated charcoal for the separation of hydrogen, carbon monoxide, acetylene, ethylene and ethane and a dinonylphthalate column was used for the separation of propane and butanes. Litchenfels et al (33) described an apparatus consisting of two columns in series arranged so that the first or stripping column could be back flushed. Since a detector was not included between the two columns, the apparatus was limited to the analysis of only that part of the sample which passed through both columns. Davis and Schreiber (34) improved Litchenfel's apparatus by providing a detector for each of the two columns. A sample consisting of materials with a range of boiling points was introduced into the first column which was operated at conditions such that the higher boiling point components in the sample were separated. The low boiling point components entered the second column essentially unresolved. Immediately after these components enter the second column the flow of carrier gas was diverted

to exclude the high boiling point fraction. The two columns were then operated separately. Since the instrumentation associated with this kind of gas-liquid chromatography is quite complex, further development along these lines will be principally of value for routine industrial control analysis.

Kokes, Tobin and Emmett (35) in 1955 used a catalytic reactor at the top of a chromatographic column of dioctylphthalate on celite. On passing a 50/50 mixture of ethane and propane in a current of hydrogen over a cracking catalyst at 400°C, the recorder indicated that some of the ethane formed C_4, C_5 and C_9 products. They pointed out that numerous applications of such techniques should be possible.

Harris and McFadden (36)described a method for the gas chromatographic determination of 2-bromobutane and 1-bromo-2-methylpropane in mixtures of alkylbromides. In their studies they used a short reactor tube packed with silver nitrate on firebrick to remove 2-bromobutane. The reaction is specific for secondary and tertiary bromides. They used a short reactor tube of sulphuric acid on firebrick to remove the alkenes formed by the reaction of alkylbromides with the solid silver nitrate.

The study described in this appendix was undertaken to evaluate the selectivity of various subtractive reagents. Sulphuric and phosphoric acids as subtractive reagents in gas chromatography streams are described in the sections which follow.

Experimental

The chromatographic analyses were performed with a Burrell Corp. Kromo-Tog K2. Nitrogen was used as a carrier gas. The analyzing column was 4 mm X 1 m glass tubing wound with a heating coil. The reactor columns were made of 4 mm X 15 cm glass tubing connected to the leading end of the analyzing column. The analyzing column was packed with Apiezon L (28.6%) on firebrick. The packing for the reactor columns consisted of 28.6% acid on firebrick. The temperature of the reactor columns were varied by a small electric furnace connected to a powerstat. Fisher columnpak, 30-60 mesh, was used as the support. All compounds were used as received from Eastman Chemicals, Rochester, N. Y.

Results and Discussion

A. Sulphuric Acid as a Reagent for Selective Reactivity

A series of alcohols, aldehydes, ketones, ethers, esters, alkenes and alkanes were passed through the analyzing column and then through the reactor column plus the analyzing column. All retention times were noted and the chromatograms compared. It was found that sulphuric acid allowed only the alkanes to pass. The compounds tested ranged in chain length from C_2 to C_{13}.

The temperature of the reactor column, shown in Table 6 has no effect on the retention time of the alkanes.

TABLE 6

Effect of Temperature of Reaction Column on Retention Time With a Reactor Column 7 cm in Length.

	Retention Time in Minutes			
Reactor Temperature	25°	40°	75°	135°
Compound				
Pentane	0.22	0.19	0.20	0.20
Hexane	0.31	0.31	0.30	0.30
Heptane	0.56	0.53	0.52	0.54
Octane	1.03	1.03	0.97	0.99

Above 135°C the recorder becomes erratic due to the deterioration of the silicone seals by the sulphuric acid. Table 7 shows that reactor column lengths down to 2 cm can be used effectively. One reactor column can be used for over one hundred determinations of twenty microlitres of sample without any change in the efficiency of the sulphuric acid solvent in the removal of all other substances.

Figure 27 contains two chromatograms of a mixture of alkanes with other substances, one without the sulphuric

TABLE 7

Effect of Sulphuric Acid Reactor Column Length at 40°C on Retention Time.

	Retention Time in Minutes	
Length	2 cm	7 cm
Compound		
n-Pentane	0.19	0.19
n-Hexane	0.31	0.31
n-Heptane	0.53	0.53
octane	1.00	1.03

acid reactor , A, and one with the sulphuric acid reactor, B. It is obvious from the figure that the sulphuric acid column has eliminated those substances with retention times the same as some of the alkanes and has made the analysis for the alkanes easier.

Phosphoric Acid as a Reagent for Selective Reactivity

Phosphoric acid was studied with the same compounds as used with sulphuric acid. Phosphoric acid eliminates aldehydes, ketones and alcohols up to and including C_{13} compounds.

Figure 27

Gas Chromatographs of a Mixture of n-Hexane, n-Heptane, n-Octane, 2,4-Dimethylpentane, Cyclohexane, Cyclohexene, Ethanol, Propanol, Butanol, 2-Butanone, 3-Pentanone, 2-Heptanone, 3-Heptanone and 4-Heptane without a Sulphuric Reactor Column (A) and with a Sulphuric Acid Reactor Column (B).

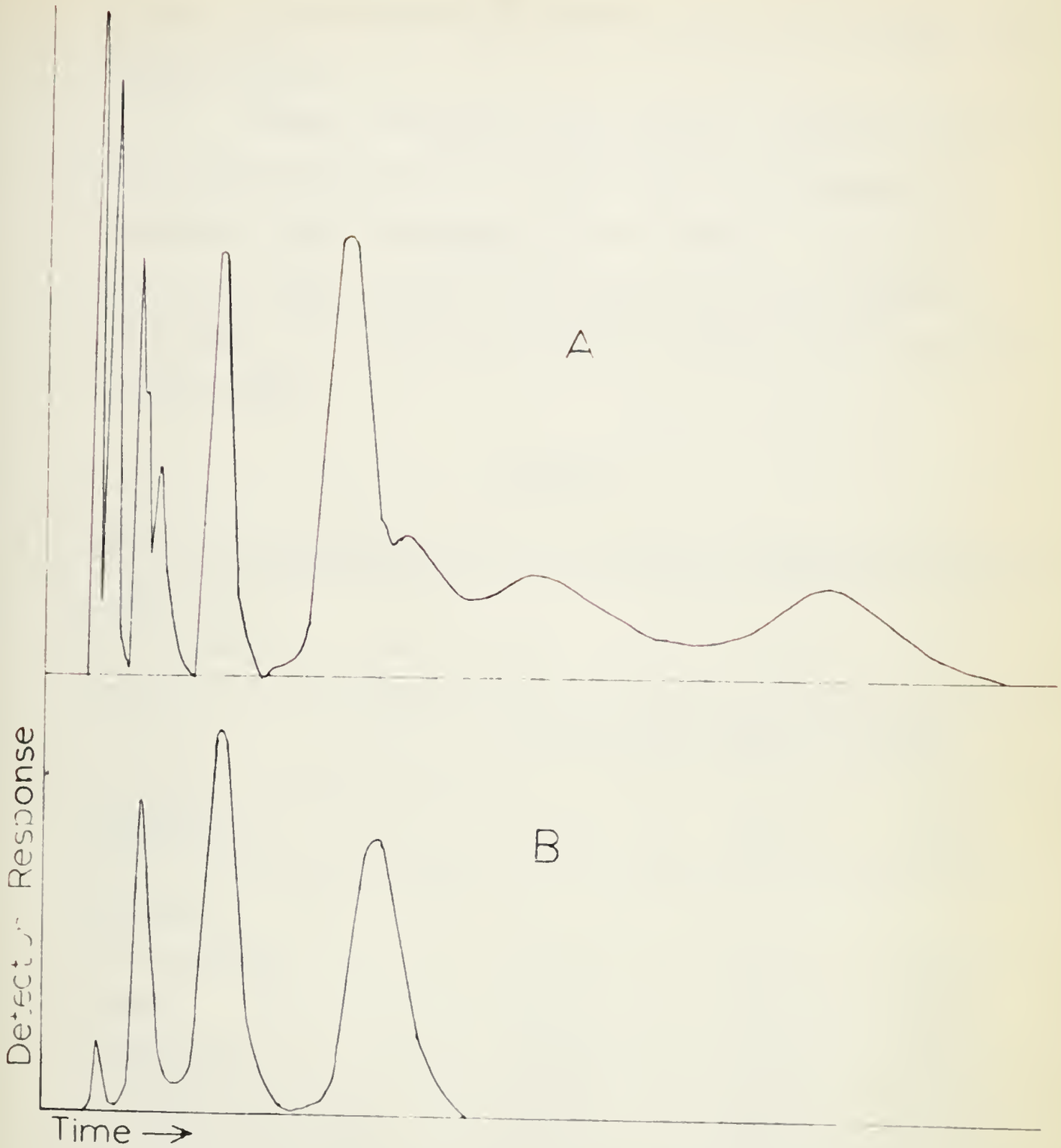
A
B
Detector Response
Time →

Alkanes, alkenes and esters readily pass the phosphoric acid reactor column.

Table 8 indicates that reactor temperatures up to about 75°C can be used. At the higher temperatures the phosphoric acid deteriorates quite rapidly. At 75°C a column has been used for two weeks without any change in efficiency. At 140°C the column is useable only for about one-half hour.

TABLE 8

Effect of Temperature of an 8 cm Reactor Column on Retention Time.

	Retention Times in Minutes		
Reactor Temperature	30°C	44°C	75°C
Compound			
Cyclohexene	3.31	3.00	3.13
Octane	5.75	5.50	5.00
p-Xylene	9.75	9.37	9.00
n-Butyl-n-Butyrate	13.13	12.85	12.00

The effect of length of reaction zone retention time is illustrated in Table 9 from which it is seen that length of reaction zone has little effect on the retention times of the alkanes, alkenes and esters.

TABLE 9

Effect of Reactor Length on Retention Time at 67°C

	Retention Time in Minutes				
Reactor Length cm	2.0	5.5	9.5	24.9	96.5
Compounds					
Cyclohexene	3.00	3.00	3.00	2.80	3.10
Octane	5.25	5.00	5.25	5.13	5.50
p-Xylene	9.00	9.37	9.00	8.87	9.25
n-Butyl-n-butyrate	12.00	12.00	12.00	12.00	12.50

Figures 28, 29 and 30 show the chromatograms resulting from a mixture of alcohols and ketones in the presence of alkenes (C and D), alkanes (E and F) and propionates (G and H) with and without the short reactors of phosphoric acid. The chromatograms D, F and H clearly show the absence of the peaks due to alcohols and ketones. Since

the retention times of the alkenes, alkanes and propionates did not change, they can be determined by conventional techniques.

Since the termination of work in this area of gas-liquid chromatography other subtractive reagents have been reported. The 1961 Spring edition of "The Perkin-Elmer Instrument News" (V.12 No.3) that Trotman-Dickenson has applied the following four reagents successfully.

For olefins: Ethylene glycol 20g., mercuric acetate 9g., mercuric nitrate 3g.

For acetylene: Tetramethyldiamino-diphenylmethane-dinonylphthalate, or N, N-dimethyl-p-toluidine.

For iodine: Sodium thiosulphate mixed with firebrick and heated so that it dissolves in its water of crystallization.

For aldehydes: A mull of sodium bisulphite in ethylene glycol.

Others (37,38) have used 5A molecular sieves to separate n-parafins from branched chain hydrocarbons.

Figure 28

Gas Chromatographs of a Mixture of Pentene-1, Pentene-2, Ethanol, n-Propanol, n-Butanol, 2-Butanone, 3-Pentanone, 2-Heptanone, 3-Heptanone and 4-Heptanone without a Phosphoric Acid Reactor Column (C) and with a Phosphoric Acid Reactor Column (D). Marker, n-octane.

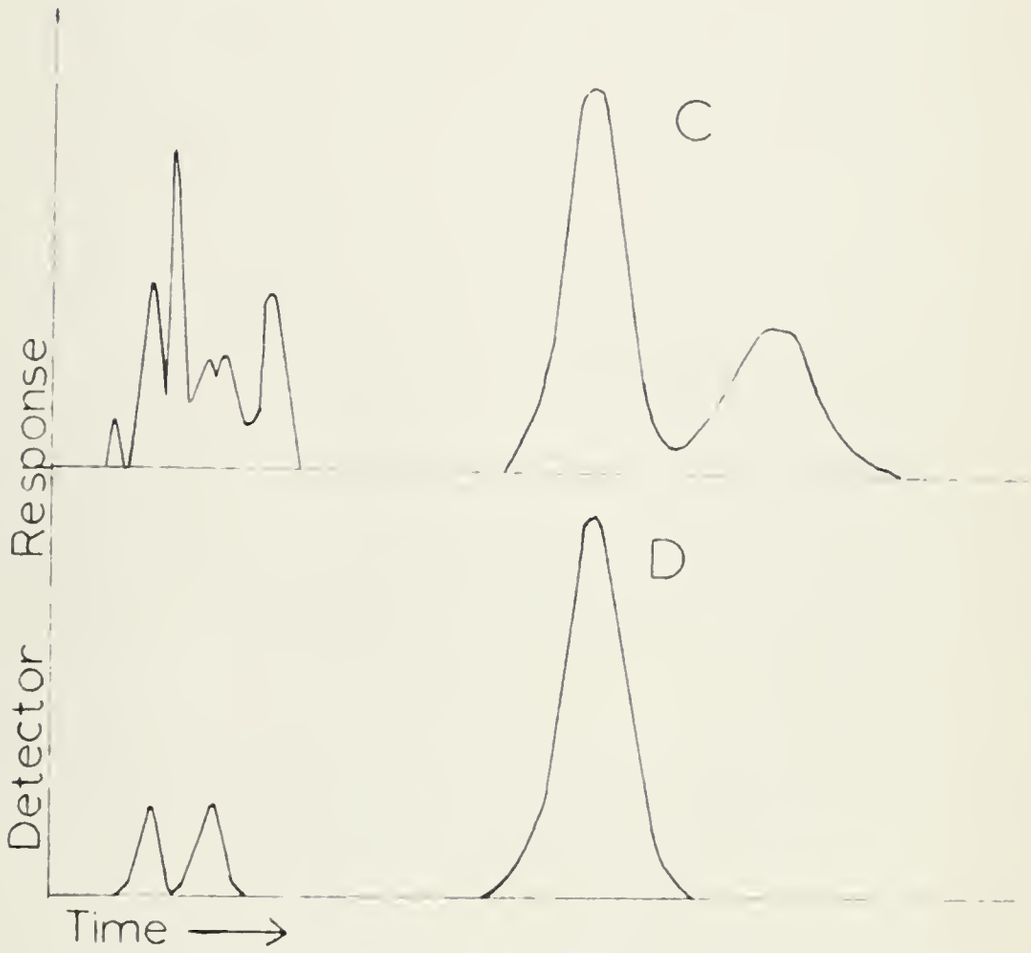
C
D
Detector Response
Time

Figure 29

Gas Chromatographs of a Mixture of n-Hexane, 2,4-Dimethylpentane, n-Heptane, Cyclohexane, Octane, Ethanol, Propanol, Butanol, 2-Butanone, 3-Pentanone, 2-Heptanone, 3-Heptanone, and 4-Heptanone without a Phosphoric Acid Reactor Column (E) and with a Phosphoric Acid Reactor Column (F).

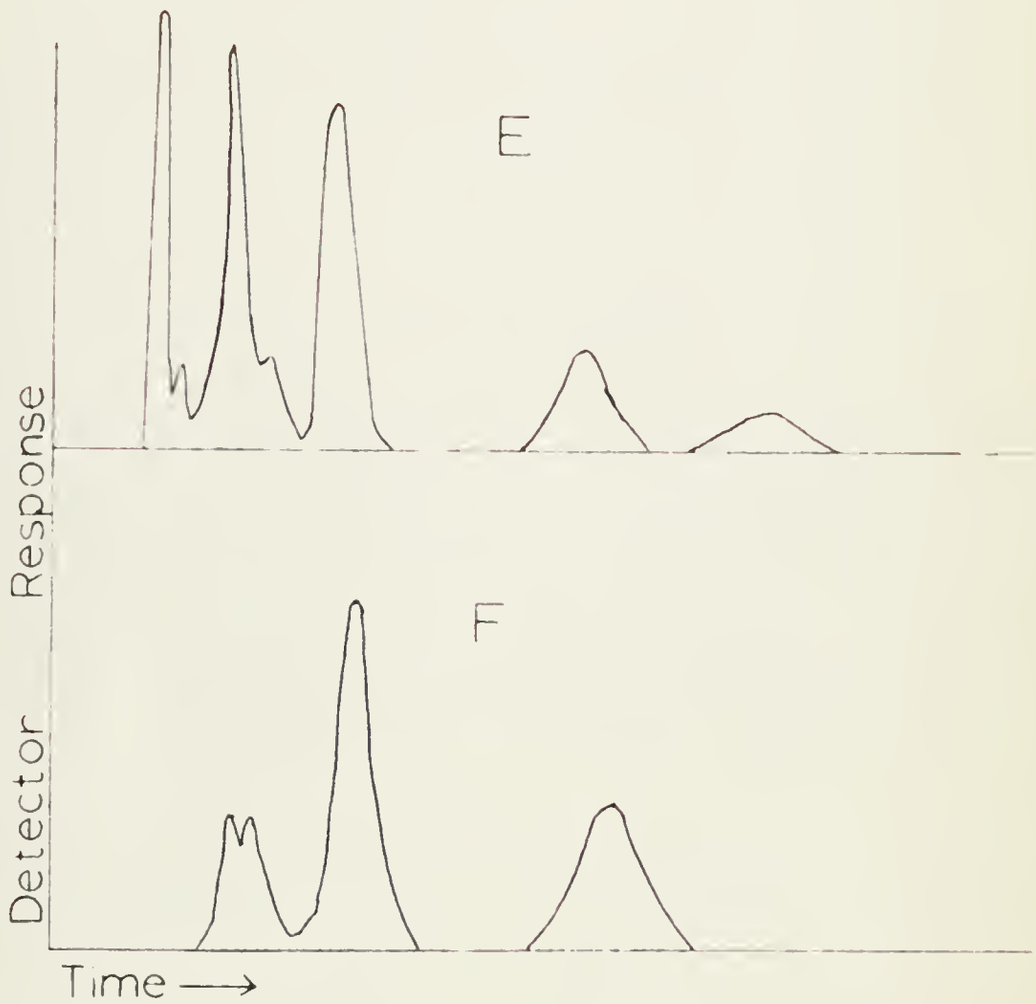
E
F
Detector Response
Time →

Figure 30

Gas Chromatographs of a Mixture of Methyl, Ethyl, n-Propyl, n-Butylpropionate, Ethanol, Propanol, Butanol, 2-Butanone, 3-Pentanone, 2-Heptanone, 3-Heptanone and 4-Heptanone without a Phosphoric Acid Column (G) and with a Phosphoric Acid Column (H). Marker, n-octane.

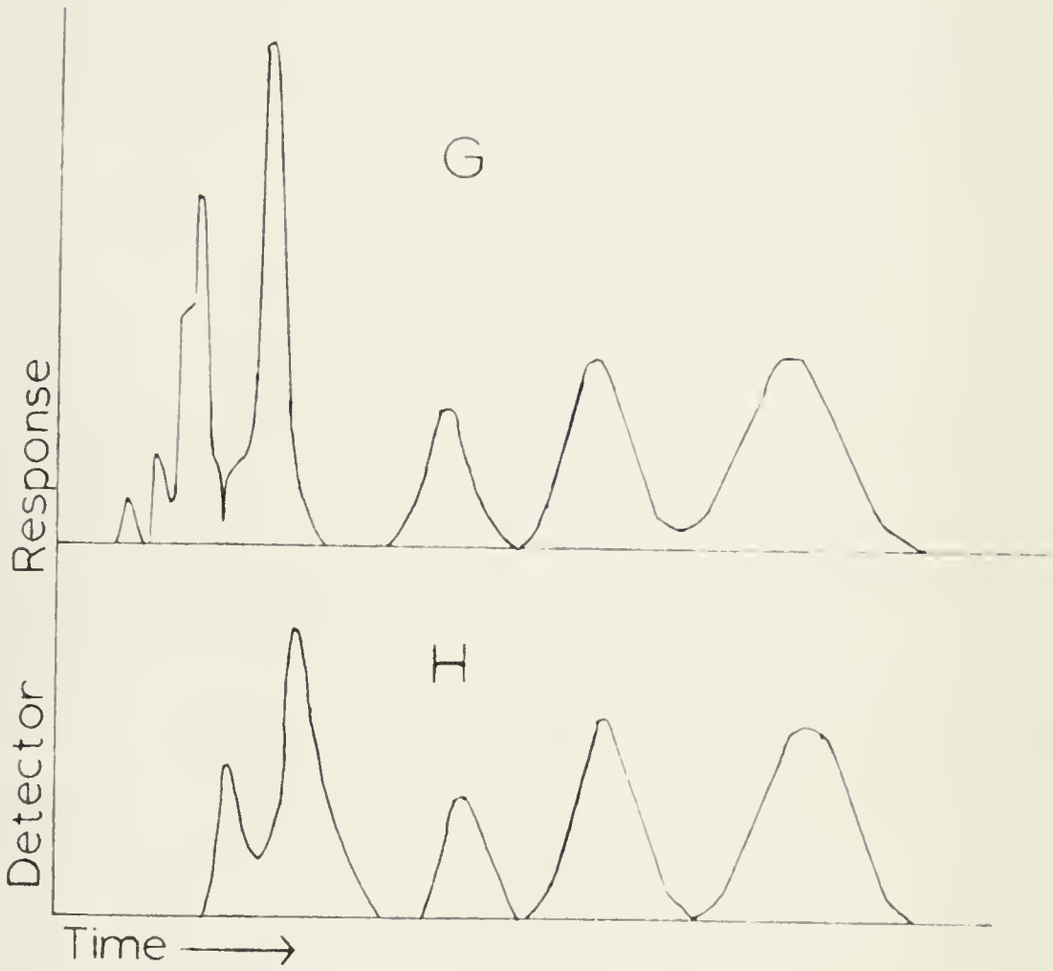
G
Response
H
Detector
Time

VII. APPENDIX III

Tables of HETP - Velocity-Pressure Data

TABLE 10

HETP - Velocity-Pressure Data for 30% w/w Di-n-Decylphthalate Column with Hydrogen Carrier Gas and n-Pentane Solute at 126°C.

$\bar{P}$ Atm.	u cm/sec	H cm
0.94	0.88	0.690
0.94	0.88	0.768
0.95	1.13	0.578
0.95	1.13	0.547
0.96	1.06	0.579
0.96	1.04	0.644
0.96	1.21	0.547
0.96	1.21	0.607
0.97	1.30	0.478
0.97	1.32	0.501
0.98	1.98	0.458
0.98	2.05	0.416
1.05	3.51	0.295
1.05	3.45	0.276
1.06	3.97	0.277
1.06	3.99	0.286
1.13	5.94	0.262
1.13	5.91	0.271

TABLE 10

(continued)

$\overline{P}$ Atm.	u cm/sec	H cm
1.36	9.15	0.279
1.36	9.24	0.363
1.36	9.24	0.311
1.41	12.0	0.323
1.41	12.1	0.335
1.41	12.1	0.333
1.39	11.0	0.328
1.39	11.5	0.389
1.28	8.67	0.319
1.28	8.67	0.303
1.51	14.2	0.362
1.51	13.9	0.383

TABLE 11

HETP - Velocity-Pressure Data for 30% w/w Di-n-decylphthalate Column with Helium Carrier Gas and n-Pentane Solute at 126°C.

$\overline{P}$ Atm.	u cm/sec	H cm
0.965	0.584	0.936
0.965	0.584	0.910
0.971	0.661	0.730
0.971	0.677	0.740
0.977	0.926	0.593
0.985	1.020	0.551
1.003	1.209	0.472
1.003	1.182	0.464
1.058	1.742	0.358
1.058	1.765	0.392
1.058	1.712	0.381
1.087	2.155	0.286
1.087	2.155	0.325
1.087	2.155	0.335
1.194	3.470	0.307
1.194	3.440	0.312
1.272	4.250	0.280
1.409	5.52	0.361
1.409	5.35	0.364

TABLE 11

(continued)

$\bar{P}$ Atm.	u cm/sec	H cm
1.483	6.49	0.262
1.483	6.35	0.274
1.707	8.58	0.299
1.707	8.51	0.304
1.823	9.34	0.347
1.823	9.45	0.319
1.779	9.56	0.281

TABLE 12

HETP - Velocity-Pressure Data for 30% w/w Di-n-decylphthalate Column with Methane Carrier Gas and n-Pentane Solute at 126°C.

$\overline{P}$ Atm.	u cm/sec	H cm
0.96	0.53	0.431
0.96	0.53	0.451
0.96	0.62	0.391
0.97	0.80	0.315
0.97	0.80	0.317
0.98	1.20	0.255
0.99	1.23	0.258
0.99	1.23	0.241
1.00	1.42	0.232
1.00	1.44	0.253
1.00	1.46	0.284
1.01	1.58	0.238
1.01	1.61	0.269
1.01	1.63	0.238
1.01	1.72	0.269
1.01	1.72	0.280
1.10	3.68	0.254
1.10	3.65	0.269

TABLE 12

(continued)

$\overline{P}$ Atm.	u cm/sec	H cm
1.21	5.35	0.313
1.21	5.39	0.308
1.21	5.35	0.328
1.25	6.16	0.357
1.25	6.25	0.358
1.25	6.20	0.403
1.26	6.30	0.333
1.26	6.41	0.308
1.30	6.41	0.345
1.30	6.41	0.345
1.41	7.46	0.315
1.41	7.46	0.298
1.41	7.46	0.356
1.44	7.73	0.356
1.44	7.53	0.356
1.44	7.80	0.363
1.49	8.50	0.315
1.49	8.50	0.298
1.49	8.50	0.356

TABLE 12

(concluded)

$\bar{P}$ Atm.	u cm/sec	H cm
1.56	11.3	0.425
1.56	11.2	0.456
1.56	11.2	0.465
1.99	15.2	0.588
1.99	15.2	0.613
1.99	15.2	0.609

TABLE 13

HETP - Velocity-Pressure Data for 30% w/w Di-n-decylphthalate Column with Nitrogen Carrier Gas and n-Pentane Solute at 126°C.

$\overline{P}$ Atm.	u cm/sec	H cm
0.98	0.70	0.333
0.98	0.73	0.295
0.98	0.75	0.287
1.02	1.29	0.228
1.02	1.31	0.269
1.02	1.32	0.250
1.06	1.96	0.206
1.06	1.96	0.206
1.06	1.95	0.185
1.11	2.60	0.221
1.11	2.58	0.181
1.30	4.73	0.233
1.30	4.73	0.245
1.63	5.42	0.236
1.63	5.60	0.271
1.63	5.45	0.239
1.66	8.42	0.310
1.66	8.42	0.320
1.66	8.10	0.243
1.94	7.45	0.303
1.94	7.48	0.258
1.94	7.66	0.324

TABLE 14

HETP - Velocity-Pressure Data for 30% w/w Di-n-decylphthalate Column with Carbon-Dioxide Carrier Gas and n-Pentane Solute at 126°C.

$\bar{P}$ Atm.	u cm/sec	H cm
0.97	0.93	0.243
0.97	0.92	0.256
0.97	0.91	0.202
0.97	0.91	0.212
0.97	0.91	0.233
1.01	1.26	0.202
1.00	1.11	0.249
1.04	1.74	0.209
1.10	2.64	0.177
1.24	6.21	0.380
1.24	5.99	0.330
1.24	6.15	0.440
1.24	6.59	0.392
1.24	6.06	0.342
1.24	6.12	0.340
1.51	7.66	0.455
1.51	7.80	0.434
1.51	7.77	0.414
1.51	7.66	0.450

TABLE 14

(continued)

$\overline{P}$ Atm.	u cm/sec	H cm
1.67	9.78	0.522
1.67	9.67	0.604
1.67	9.34	0.530
1.67	9.62	0.578
1.67	9.62	0.558
1.75	10.1	0.595
1.87	11.5	0.645
1.87	12.0	0.620
1.87	11.7	0.600
1.87	11.7	0.580
1.92	10.8	0.898
1.92	13.5	0.684
1.92	12.0	0.613
1.92	12.0	0.442

TABLE 15

HETP - Velocity-Pressure Data for 30% w/w Di-n-decylphthalate Column with Freon 13B1 Carrier Gas and n-Pentane Solute at 126°C.

$\bar{P}$ Atm.	u cm/sec	H cm
0.98	0.78	0.228
0.98	0.99	0.286
0.99	0.93	0.243
1.06	1.96	0.318
1.06	1.96	0.279
1.07	2.23	0.243
1.07	2.23	0.239
1.07	2.23	0.249
1.19	3.61	0.305
1.19	3.60	0.336
1.19	3.61	0.296
1.32	4.30	0.339
1.32	4.34	0.364
1.32	4.31	0.359
1.39	5.99	0.433
1.39	5.99	0.435
1.39	5.91	0.336
1.39	6.00	0.374
1.54	7.56	0.623
1.54	7.56	0.576
1.54	7.56	0.736
1.67	8.50	0.544
1.67	8.50	0.570
1.67	8.50	0.615

TABLE 16

HETP - Velocity-Pressure Data for 30% w/w di-n-decylphthalate Column with Freon 114 Carrier Gas and n-Pentane Solute at 126°C.

$\bar{P}$ Atm.	u cm/sec	H cm
0.96	0.84	0.190
0.97	0.81	0.330
0.97	0.81	0.229
0.98	1.06	0.230
0.98	1.06	0.182
0.98	1.14	0.290
0.98	1.12	0.271
1.01	1.81	0.177
1.01	1.88	0.179
1.03	1.90	0.167
1.03	2.24	0.201
1.03	3.24	0.191
1.15	4.25	0.403
1.15	4.36	0.432
1.26	5.48	0.479
1.26	5.48	0.485
1.28	4.48	0.471

TABLE 17

HETP - Velocity-Pressure Data for 30% w/w Di-n-decylphthalate Column with Hydrogen Carrier Gas and n-Pentane Solute at 44°C.

$\bar{P}$ Atm.	u cm/sec	H cm	$H - \frac{B}{\bar{P}u}$ cm
1.26	22.5	0.588	0.577
	25.0	0.585	0.570
1.86	8.86	0.332	0.312
	9.24	0.339	0.320
	23.7	0.551	0.544
	23.7	0.635	0.628
	27.4	0.690	0.684
	27.4	0.723	0.719
2.09	9.44	0.602	0.586
	9.62	0.598	0.582
	12.5	0.690	0.678
	12.5	0.680	0.668
	15.7	0.795	0.785
	15.7	0.800	0.790
2.23	11.8	0.398	0.386
	11.8	0.400	0.388
	17.7	0.510	0.502
	17.7	0.554	0.546
	23.6	0.660	0.654
	25.0	0.629	0.623

TABLE 17

(continued)

$\bar{P}$ Atm.	u cm/sec	H cm	$H - \frac{B}{\bar{P}u}$ cm
2.75	10.7	0.398	0.387
	10.7	0.414	0.403
	23.6	0.609	0.604
	23.6	0.704	0.688
	32.7	0.830	0.828
	32.7	0.830	0.828
2.95	12.5	0.764	0.755
	13.3	0.716	0.708
	17.0	0.873	0.868
	17.0	0.888	0.883
	22.4	0.880	0.875
	22.4	0.850	0.845
3.32	21.2	0.730	0.726
	21.2	0.796	0.792
	35.4	1.03	1.03
	35.4	1.17	1.17
4.08	34.4	0.895	0.895
	34.4	0.965	0.965
	41.0	1.14	1.14
	43.0	1.05	1.05
	43.0	1.25	1.25

TABLE 18

HETP - Velocity-Pressure Data for 14% w/w Di-n-decylphthalate Column with Hydrogen Carrier Gas and n-Pentane Solute at 44°C.

$\bar{P}$ Atm.	u cm/sec	H cm	$H - \frac{B}{\bar{P}u}$ cm
1.63	9.75	0.448	0.428
	10.0	0.494	0.484
	14.1	0.488	0.474
	14.5	0.486	0.472
	21.6	0.533	0.524
	21.8	0.550	0.541
2.35	9.17	0.423	0.408
	9.27	0.424	0.409
	11.4	0.435	0.423
	11.5	0.424	0.412
	16.8	0.550	0.542
	17.3	0.519	0.511
	23.3	0.626	0.621
	24.6	0.699	0.694

TABLE 18

(continued)

$\bar{P}$ Atm.	u cm/sec	H cm	$H - \frac{B}{\bar{P}u}$ cm
3.39	9.85	0.435	0.425
	9.92	0.414	0.404
	13.6	0.506	0.499
	13.7	0.530	0.523
	22.4	0.593	0.591
	22.5	0.640	0.638
	33.2	0.728	0.728
	34.5	0.744	0.744
4.05	4.63	0.314	0.302
	4.64	0.344	0.332
	16.1	0.557	0.554
	16.3	0.575	0.572
	28.7	0.776	0.776
	29.7	0.768	0.768

TABLE 19

HETP - Velocity-Pressure Data for 11% w/w Di-n-decylphthalate Column with Hydrogen Carrier and n-Pentane Solute at 44°C.

$\bar{P}$ Atm.	u cm/sec	H cm	$H - \frac{B}{\bar{P}u}$ cm
1.70	8.92	0.168	0.146
	9.11	0.120	0.109
	9.25	0.106	0.095
	9.34	0.101	0.090
	15.4	0.146	0.134
	15.7	0.176	0.164
	17.1	0.194	0.180
	17.5	0.151	0.140
	27.4	0.206	0.199
	27.4	0.242	0.235
	27.6	0.194	0.187
	27.6	0.216	0.209
2.05	8.07	0.131	0.111
	8.10	0.131	0.111
	16.5	0.164	0.154
	16.8	0.199	0.189
	27.6	0.191	0.186
	27.6	0.216	0.211

TABLE 19

(continued)

$\bar{P}$ Atm.	u cm/sec	H cm	$H - \frac{B}{\bar{P}u}$ cm
2.29	10.9	0.138	0.125
	11.2	0.133	0.121
	20.8	0.217	0.210
	20.8	0.232	0.225
	31.0	0.405	0.403
	32.4	0.267	0.265
2.97	7.50	0.127	0.113
	7.50	0.123	0.109
	14.0	0.177	0.169
	14.0	0.236	0.228
	23.8	0.231	0.229
	24.5	0.394	0.397
	35.1	0.364	0.364
	35.7	0.288	0.288
3.95	10.4	0.170	0.162
	10.4	0.184	0.176
	23.8	0.274	0.273
	24.4	0.234	0.234
	38.9	0.594	0.594
	40.6	0.370	0.370

TABLE 20

HETP - Velocity-Pressure Data for 11% w/w Di-n-decylphthalate Column with Hydrogen Carrier Gas and n-Pentane Solute at 44°C.

$\overline{P}$ Atm.	u cm/sec	H cm	$H - \frac{B}{\overline{P}u}$ cm
1.66	12.9	0.159	0.144
	12.9	0.174	0.159
	21.4	0.202	0.193
	22.8	0.242	0.233
	29.5	0.262	0.255
	31.0	0.303	0.297
2.04	12.2	0.179	0.166
	12.2	0.122	0.109
	27.6	0.279	0.274
	27.6	0.313	0.308
	40.8	0.321	0.321
	41.6	0.300	0.300
2.76	6.32	0.152	0.133
	6.44	0.155	0.136
	17.2	0.202	0.195
	17.7	0.243	0.236
	35.0	0.381	0.381
	38.2	0.320	0.320
	50.3	0.492	0.492
	53.5	0.790	0.790

TABLE 20

(continued)

$\overline{P}$ Atm.	u cm/sec	H cm	$H - \frac{B}{\overline{P}u}$ cm
3.54	8.84	0.146	0.136
	8.96	0.148	0.138
	18.2	0.253	0.250
	18.5	0.257	0.254
	29.5	0.333	0.333
	30.6	0.279	0.279
	45.2	0.338	0.338
	50.3	0.601	0.601

TABLE 21

HETP - Velocity-Pressure Data for 6.7% w/w Di-n-decylphthalate Column with Hydrogen Carrier Gas and n-Pentane Solute at 44°C

$\overline{P}$ Atm.	u cm/sec	H cm	$H - \frac{B}{\overline{P}u}$ cm
1.53	9.73	0.184	0.162
	9.80	0.184	0.162
	14.8	0.232	0.218
	15.1	0.242	0.228
	24.5	0.471	0.462
	26.0	0.336	0.328
1.63	15.2	0.197	0.184
	15.6	0.197	0.184
	23.8	0.213	0.205
	23.8	0.213	0.205
	42.8	0.320	0.328
	53.5	0.420	0.420
	61.2	0.433	0.433

TABLE 21

(continued)

$\overline{P}$ Atm.	u cm/sec	H cm	$H - \frac{B}{\overline{P}u}$ cm
2.00	14.3	0.268	0.257
	14.7	0.272	0.261
	15.0	0.185	0.174
	22.4	0.464	0.457
	24.5	0.298	0.292
	30.6	0.508	0.504
	31.1	0.495	0.491
	33.0	0.554	0.551
	35.8	0.502	0.500
	37.2	0.634	0.633
	37.2	0.518	0.517
2.24	10.6	0.210	0.197
	10.8	0.219	0.206
	23.8	0.381	0.375
	23.8	0.381	0.375
	37.2	0.477	0.477
	39.0	0.546	0.546

TABLE 21

(continued)

$\overline{P}$ Atm.	u cm/sec	H cm	$H - \frac{B}{\overline{P}u}$ cm
2.46	13.2	0.287	0.277
	13.2	0.314	0.304
	19.5	0.473	0.466
	19.8	0.412	0.405
	24.5	0.438	0.434
	25.2	0.516	0.512
	33.0	0.620	0.620
2.71	21.4	0.338	0.333
	22.0	0.372	0.367
	25.9	0.409	0.407
	26.8	0.476	0.474
	33.9	0.480	0.480
	33.9	0.485	0.485
3.49	10.3	0.198	0.189
	10.7	0.191	0.182
	19.7	0.260	0.258
	19.7	0.276	0.274
	26.0	0.448	0.448

TABLE 21

(concluded)

$\bar{P}$ Atm.	u cm/sec	H cm	$H - \frac{B}{\bar{P}u}$ cm
4.01	6.26	0.197	0.184
	6.40	0.207	0.194
	17.0	0.392	0.390
	17.5	0.396	0.394
	27.1	0.519	0.519
	27.7	0.528	0.528

TABLE 22

HETP - Velocity-Pressure Data for 4.1% w/w Di-n-decylphthalate Column with Hydrogen Carrier Gas and n-Pentane Solute at 44°C.

$\bar{P}$ Atm.	u cm/sec	H cm	$H - \frac{B}{\bar{P}u}$ cm
1.77	6.89	0.166	0.139
	18.6	0.224	0.215
	19.5	0.239	0.230
	35.0	0.221	0.217
	35.0	0.220	0.216
2.27	8.03	0.114	0.096
	8.38	0.145	0.127
	19.0	0.182	0.174
	19.4	0.143	0.136
	31.7	0.260	0.257
	32.8	0.365	0.363
	38.9	0.418	0.418
	38.9	0.550	0.550
2.80	16.4	0.172	0.164
	16.6	0.191	0.183
	34.2	0.424	0.424
	34.2	0.418	0.418
	50.3	0.498	0.498
	53.4	0.511	0.511

TABLE 22

(continued)

$\bar{P}$ Atm.	u cm/sec	H cm	$H - \frac{B}{\bar{P}u}$ cm
3.61	18.6	0.181	0.179
	19.2	0.189	0.187
	37.1	0.470	0.470
	37.1	0.487	0.487
	50.4	0.438	0.438
	52.2	0.640	0.640

TABLE 23

HETP - Velocity-Pressure Data for 6.7% w/w Di-n-decylphthalate Column with Methane Carrier Gas and n-Pentane Solute at 44°C.

$\bar{P}$ Atm.	u cm/sec	H cm	$H - \frac{B}{\bar{P}u}$ cm
0.78	14.6	0.302	0.292
	15.1	0.296	0.287
1.30	10.7	0.288	0.280
	10.7	0.298	0.290
	15.6	0.379	0.374
	15.9	0.382	0.377
1.51	17.9	0.412	0.408
	18.5	0.411	0.407
1.75	9.44	0.311	0.304
	9.44	0.312	0.305
	17.25	0.457	0.453
	17.3	0.509	0.505
2.06	2.55	0.147	0.125
	2.86	0.141	0.121
	10.9	0.352	0.347
	11.2	0.345	0.340
	14.8	0.352	0.349
	15.6	0.421	0.418
	17.5	0.476	0.473
	17.9	0.499	0.496
	18.2	0.348	0.345
	18.5	0.294	0.291

TABLE 23

(continued)

$\bar{P}$ Atm.	u cm/sec	H cm	$H - \frac{B}{\bar{P}u}$ cm
2.30	5.88	0.227	0.219
	5.88	0.233	0.225
	12.8	0.373	0.369
	12.8	0.374	0.370
	20.4	0.582	0.580
	20.9	0.498	0.496
2.94	9.23	0.320	0.316
	9.23	0.346	0.342
	15.9	0.450	0.448
	15.9	0.453	0.451
	17.9	0.530	0.528
	18.7	0.577	0.575
	23.2	0.556	0.555
	23.9	0.675	0.674
3.50	6.40	0.246	0.241
	6.40	0.260	0.255
	10.1	0.325	0.322
	10.1	0.362	0.359
	14.7	0.451	0.449
	14.8	0.504	0.502
	19.5	0.630	0.629
	19.7	0.634	0.633
	25.5	0.683	0.683
	25.5	0.693	0.693

TABLE 24

HETP - Velocity-Pressure Data for 6.7% w/w Di-n-decylphthalate Column with Nitrogen Carrier Gas and n-Pentane Solute at 44°C.

$\overline{P}$ Atm.	u cm/sec	H cm	$H - \frac{B}{\overline{P}u}$ cm
1.65	8.08	0.248	0.241
	8.40	0.244	0.237
	13.0	0.283	0.278
	13.0	0.361	0.356
1.75	10.2	0.326	0.320
	10.5	0.287	0.281
	12.6	0.315	0.310
	12.6	0.373	0.368
	15.1	0.361	0.357
	15.1	0.408	0.404
2.38	13.8	0.392	0.389
	14.3	0.398	0.395
	17.1	0.502	0.499
	17.2	0.521	0.518
2.54	10.9	0.358	0.355
	11.9	0.504	0.501
	19.1	0.822	0.820
	20.0	0.583	0.581

TABLE 24

(continued)

$\bar{P}$ Atm.	u cm/sec	H cm	$H - \frac{B}{\bar{P}u}$ cm
2.96	11.9	0.540	0.537
	13.2	0.755	0.752
	14.1	0.357	0.355
	20.4	0.508	0.507
	20.4	0.362	0.361
	35.7	0.882	0.882
	37.3	0.636	0.636
	53.6	1.13	1.13
4.05	9.75	0.706	0.703
	17.6	1.20	1.20
	17.9	1.47	1.47

TABLE 25

HETP - Velocity-Pressure Data for 67% w/w Di-n-decylphthalate Column with Carbon Dioxide Carrier Gas and n-Pentane Solute at 44°C.

$\bar{P}$ Atm.	u cm/sec	H cm	$H - \frac{B}{\bar{P}u}$ cm
0.85	9.05	0.330	0.321
	9.05	0.380	0.371
2.38	8.50	0.457	0.454
	8.84	0.454	0.451
	12.3	0.628	0.626
	13.0	0.554	0.553
	16.5	0.680	0.680
	16.5	0.739	0.779
3.18	9.63	0.538	0.536
	10.6	0.473	0.471
	12.8	0.670	0.669
	12.9	0.594	0.593
	19.1	0.495	0.495
	19.1	0.742	0.742
3.59	7.10	0.470	0.468
	13.2	0.592	0.591
	17.2	0.880	0.880
	17.5	0.904	0.904
	21.6	0.808	0.808

TABLE 26

HETP - Velocity-Pressure Data for 30% w/w Di-n-decylphthalate Column with Helium Carrier Gas and n-Pentane Solute at 108°C.

$\bar{P}$ Atm.	u cm/sec	H cm
0.970	0.633	0.696
0.970	0.636	0.683
0.979	0.667	0.676
0.979	0.669	0.651
0.994	0.882	0.529
0.996	0.924	0.511
0.996	0.920	0.504
1.01	1.23	0.405
1.01	1.19	0.416
1.02	1.38	0.362
1.02	1.38	0.348
1.12	2.67	0.257
1.12	2.68	0.247
1.29	4.51	0.250
1.29	4.51	0.235
1.44	6.01	0.249
1.44	6.07	0.279

TABLE 26

(continued)

$\overline{P}$ Atm.	u cm/sec	H cm
1.60	7.73	0.282
1.60	7.87	0.290
1.69	8.50	0.303
1.69	8.50	0.283
1.93	9.66	0.346
1.93	9.66	0.364

TABLE 27

HETP - Velocity-Pressure Data for 40% w/w Di-n-decylphthalate Column with Helium Carrier Gas and n-Pentane Solute at 95°C.

$\bar{P}$ Atm.	u cm/sec	H cm
0.957	0.540	0.786
0.957	0.520	0.779
0.959	0.588	0.726
0.959	0.589	0.662
0.983	0.880	0.488
0.990	0.872	0.466
1.03	1.08	0.453
1.03	0.98	0.437
1.03	1.63	0.317
1.05	1.59	0.298
1.05	1.67	0.309
1.16	1.90	0.271
1.16	1.86	0.279
1.23	3.21	0.233
1.23	3.29	0.226
1.24	3.93	0.282
1.28	3.88	0.291
1.28	4.43	0.238
	4.42	0.238

TABLE 27

(continued)

$\overline{P}$ Atm.	u cm/sec	H cm
1.37	5.36	0.231
1.37	5.36	0.236
1.37	5.50	0.241
1.56	7.39	0.280
1.56	7.59	0.282
1.69	8.48	0.292
1.69	8.68	0.340
1.84	10.0	0.373
1.84	9.88	0.331

TABLE 28

HETP - Velocity-Pressure Data for 30% w/w Di-n-decylphthalate Column with Helium Carrier Gas and n-Pentane Solute at 53°C.

$\bar{P}$ Atm.	u cm/sec	H cm
0.977	0.834	0.520
0.978	0.982	0.379
0.978	1.01	0.342
1.06	2.09	0.225
1.06	2.09	0.232
1.01	1.32	0.281
1.01	2.31	0.295
1.01	1.21	0.188
1.04	1.86	0.224
1.04	1.82	0.222
1.21	3.90	0.215
1.29	3.76	0.228
1.27	4.52	0.241
1.27	4.62	0.254
1.39	6.03	0.275
1.39	5.90	0.276
1.49	7.15	0.319
1.49	6.96	0.327
1.63	8.35	0.359
1.63	8.46	0.364
1.76	9.78	0.399
1.76	9.60	0.375

TABLE 29

HETP - Velocity-Pressure Data for 30% w/w Di-n-decylphthalate Column with Helium Carrier Gas and n-Pentane Solute at 28°C.

$\bar{P}$ Atm.	u cm/sec	H cm
1.02	1.39	0.282
1.03	1.66	0.227
1.03	1.66	0.228
1.24	4.67	0.240
1.24	4.64	0.239
1.32	5.28	0.311
1.32	5.35	0.278
1.50	7.43	0.358
1.66	9.09	0.445
1.66	8.95	0.429
1.82	10.7	0.493
1.82	10.7	0.491
1.96	12.1	0.580
1.96	11.8	0.482

TABLE 30

HETP - Velocity-Pressure Data for 25% w/w Di-n-decylphthalate Column with Hydrogen Carrier Gas and n-Pentane Solute at 123°C.

$\bar{P}$ Atm.	u cm/sec	H cm	$H - \frac{B}{\bar{P}u}$ cm
1.61	4.40	0.284	0.243
	4.59	0.301	0.258
	10.7	0.294	0.266
	10.7	0.299	0.271
	16.1	0.253	0.235
	16.1	0.275	0.257
	23.7	0.351	0.340
	24.4	0.292	0.281
2.38	4.88	0.230	0.190
	5.05	0.254	0.216
	11.5	0.242	0.226
	11.7	0.241	0.225
	23.5	0.316	0.308
	23.5	0.374	0.366
	34.1	0.421	0.419
	34.1	0.434	0.432

TABLE 30

(continued)

$\overline{P}$ Atm.	u cm/sec	H cm	$H - \frac{B}{\overline{P}u}$ cm
3.15	8.21	0.212	0.194
	8.29	0.228	0.210
	21.4	0.353	0.348
	21.5	0.353	0.348
	32.8	0.490	0.488
	34.2	0.433	0.431
3.94	5.92	0.224	0.206
	18.5	0.327	0.322
	18.5	0.356	0.351
	36.2	0.522	0.522
	36.2	0.605	0.605

TABLE 31

HETP - Velocity-Pressure Data for 25% w/w Di-n-decylphthalate Column with Hydrogen Carrier Gas and n-Pentane Solute at 81°C.

$\bar{P}$ Atm.	u cm/sec	H cm	$H - \frac{B}{\bar{P}u}$ cm
1.70	8.30	0.196	0.170
	8.46	0.196	0.170
	15.0	0.244	0.229
	15.0	0.265	0.250
	28.10	0.413	0.406
	30.95	0.476	0.470
2.28	10.0	0.228	0.212
	10.3	0.222	0.206
	19.8	0.335	0.328
	20.8	0.352	0.345
	31.5	0.488	0.484
	35.0	0.456	0.453
2.88	11.2	0.285	0.275
	11.3	0.271	0.261
	21.3	0.360	0.355
	21.3	0.372	0.367
	35.5	0.619	0.618
	37.1	0.634	0.633

TABLE 31

(continued)

$\bar{P}$ Atm.	u cm/sec	H cm	$H - \frac{B}{\bar{P}u}$ cm
3.56	5.22	0.171	0.150
	5.26	0.171	0.150
	13.8	0.301	0.294
	14.0	0.332	0.325
	23.5	0.506	0.505
	23.7	0.445	0.444
	35.6	0.817	0.817
	37.1	0.699	0.699
4.06	5.94	0.193	0.178
	6.08	0.182	0.167
	19.0	0.430	0.427
	19.5	0.423	0.420
	32.9	0.608	0.608
	34.2	0.688	0.688

TABLE 32

HETP - Velocity-Pressure Data for 25% w/w Di-n-decylphthalate Column with Hydrogen Carrier Gas and n-Pentane Solute at 24°C.

$\bar{P}$ Atm.	u cm/sec	H cm	$H - \frac{B}{\bar{P}u}$ cm
1.75	6.80	0.195	0.167
	6.86	0.194	0.166
	18.4	0.401	0.391
	19.9	0.411	0.402
	28.1	0.624	0.618
	29.8	0.640	0.634
2.51	7.49	0.206	0.196
	7.49	0.223	0.205
	22.2	0.520	0.515
	22.7	0.584	0.579
	32.8	0.786	0.783
	36.2	0.755	0.753
3.22	6.54	0.210	0.194
	6.64	0.215	0.199
	17.4	0.451	0.445
	17.8	0.435	0.429
	34.1	0.815	0.814
	34.7	0.775	0.774
3.93	7.74	0.274	0.265

TABLE 32

(continued)

$\overline{P}$ Atm.	u cm/sec	H cm	$H - \frac{B}{\overline{P}u}$ cm
3.93	8.06	0.290	0.282
	23.1	0.700	0.698
	23.8	0.635	0.633
	40.7	0.991	0.991
	40.7	1.06	1.06